UNIVERSITÁ DEGLI STUDI DI BARI

“ALDO MORO”

Dipartimento di Scienze del Suolo, della Pianta e degli Alimenti
(Di.S.S.P.A.)

Dottorato di ricerca in Gestione Sostenibile del Territorio

CICLO XXXVII

Settore Scientifico Disciplinare AGR/05

TITOLO DELLA TESI

DISENTANGLING THE MECHANISMS UNDERLYING URBAN FORESTS AS NATURE-BASED SOLUTIONS ON URBAN HEAT ISLANDS

Dottorando: Dott.ssa. Yaxue Ren

Coordinatore: Prof. Francesco Gentile

Supervisore: Prof. Raffaele Lafortezza

Prof. Giovanni Sanesi

ESAME FINALE

Contents

1. Introduction 4

2. The unrelenting global expansion of the urban heat island over the last century 8

Abstract 9

2.1 Introduction 11

2.2 Materials and methods 14

2.2.1 Literature search 15

2.2.2 Semantic extraction 16

2.2.3 Data analysis 17

2.3 Results 19

2.3.1 The spatial distribution and growth ratio of cities in UHI-related research 19

2.3.2 The latitude and altitude distribution of cities in UHI-related research 25

2.3.3 The spatial locations (hotspots) across the globe where UHI-related research is concentrated in multiple cities 29

2.3.4 Economic, demographic and environmental drivers underlying hotspot/non-hotspot distribution in the European continent 30

2.4 Discussion and conclusions 33

Acknowledgments 37

References 37

3. Exploring the non-linear impacts of urban features on land surface temperature using Explainable Artificial Intelligence 44

Abstract 45

3.1 Introduction 45

3.2 Materials and methods 48

3.2.1 Study area 48

3.2.2 Data 49

3.2.3 Methodology 53

3.3 Results 55
3.3.1 Comparison between the random forest and multiple linear regression model 55
3.3.2 Distribution of urban features impacting LST in the study area 56
3.3.3 Non-linear interactions of impact features with LST and other features 58
3.3.4 Contribution of the most important features impacting LST in different thermal contexts 61
3.4 Discussion 62
3.4.1 Advantages of the XAI machine learning model 62
3.4.2 Relationship between LST and impact features 63
3.4.3 Study implications and policy recommendations 64
3.4.4 Uncertainties and limitations 64
3.5 Conclusions 65
Acknowledgments 66
References 66
4. Understanding the coupling effect of multiple urban features on Land Surface Temperature in Europe ... 71
Abstract 72
4.1 Introduction 73
4.2 Materials and Methods 75
4.2.1 Study Area 76
4.2.2 Data Collection 77
4.2.3 Data Processing 79
4.2.4 Random Forest and SHAP Value Analysis 81
4.2.5 Generalized Additive Model Analysis 82
4.3 Results 82
4.3.1 Combined effects of urban features on LST across macro-regions in Europe 82
4.3.2 Urban features contributing the most to warming and cooling effects 85
4.3.3 Non-linear impact of the most influencing features on LST 87
4.4 Discussion 96
4.5 Conclusion 98

References 98

5.Conclusion 103

Introduction

As rapid urbanization reshapes landscapes worldwide, cities increasingly face environmental challenges that threaten sustainability and climate resilience. One of the most pressing issues is the urban heat island (UHI) effect, where urban areas experience higher temperatures than their rural surroundings. This phenomenon is driven primarily by the replacement of natural landscapes with impervious surfaces like asphalt and concrete, which absorb and retain heat more effectively than vegetation (Oke, 1982; Grimmond, 2007). The resulting temperature differential intensifies global warming impacts at a local level, contributing to extreme heat events that adversely affect both environmental systems and public health (Santamouris, 2014).

UHI is more than just a temperature anomaly; it has wide-ranging consequences for urban life. Elevated temperatures in cities lead to increased energy demand for cooling, rising greenhouse gas emissions, and greater air pollution levels, which in turn place additional strain on infrastructure and public health systems (Arnfield, 2003; Santamouris et al., 2011). Vulnerable populations, particularly those in densely populated and low-income areas, face increased health risks, such as heat-related illnesses and respiratory issues, due to prolonged exposure to high temperatures (Harlan et al., 2006). As cities worldwide strive to mitigate climate impacts, understanding and addressing the UHI effect has become a critical focus for researchers and policymakers alike.

Over the past few decades, a growing body of research has explored the drivers of UHI and potential mitigation strategies. Studies have shown that specific urban features—such as land cover

type, building density, and vegetation—play essential roles in shaping the urban thermal environment (Stone & Rodgers, 2001; Zhou et al., 2014). Green spaces, tree cover, and water bodies have been widely recognized for their cooling potential; vegetation provides shade and enhances evapotranspiration, while water bodies help regulate local temperatures (Gill et al., 2007; Bowler et al., 2010). However, much of the existing literature has relied on linear models that may oversimplify the complex interactions between urban features and land surface temperature (LST). Nonlinear approaches are increasingly necessary to capture the full dynamics of UHI, as recent studies have suggested that the cooling effects of vegetation, for instance, may vary depending on regional climate and specific vegetation characteristics (Chen et al., 2024).

In addition to the need for nonlinear modeling, most UHI studies have been limited geographically, often focusing on single cities or small-scale analyses. UHI manifests differently across diverse climatic regions and urban forms, highlighting the need for broader, multi-regional studies that can identify both universal and location-specific drivers of urban temperatures (Schwarz et al., 2011; Peng et al., 2012). Such research is essential for understanding how urban characteristics interact with climatic conditions and for developing tailored solutions that address local variations in UHI effects.

This doctoral research seeks to fill these gaps by providing a multi-scale, integrative analysis of UHI and LST. Through three studies conducted at different scales and using various methodologies,

this thesis explores how UHI has evolved globally, the nonlinear impacts of urban features on LST, and the regional variations in UHI mechanisms. The first study offers a century-long perspective on UHI's global spread, highlighting the increasing number of cities affected and the role of urbanization in amplifying heat retention. The second study focuses on a single city, Beijing, using explainable artificial intelligence (XAI) to reveal nonlinear relationships between urban features and LST. The third study expands to 780 cities across eight European macro-regions, investigating how ecological and built features jointly impact LST and emphasizing the importance of region-specific urban planning.

In summary, this thesis provides a comprehensive examination of UHI, emphasizing the significance of nonlinear analysis and regional diversity in urban climate studies. By synthesizing findings across different scales and contexts, this research aims to contribute to a more nuanced understanding of UHI mechanisms and to offer actionable insights for urban planners and policymakers. Addressing UHI requires not only a deep understanding of urban and ecological interactions but also a commitment to integrating climate resilience into urban development practices worldwide.

References

Arnfield, A. J. (2003). Two decades of urban climate research: A review of turbulence, exchanges of energy and water, and the urban heat island. International Journal of Climatology, 23(1), 1-26. https://doi.org/10.1002/joc.859

Bowler, D. E., Buyung-Ali, L., Knight, T. M., & Pullin, A. S. (2010). Urban greening to cool towns

and cities: A systematic review of the empirical evidence. Landscape and Urban Planning, 97(3), 147-155. https://doi.org/10.1016/j.landurbplan.2010.05.006

Chen, Y., Zhang, R., Asadi Alekouei, S., & Amani-Beni, M. (2024). Nonlinear impacts of landscape and climatological interactions on urban thermal environment during a hot and rainy summer. Ecological Indicators, 157, 112551. https://doi.org/10.1016/j.ecolind.2024.112551

Gill, S. E., Handley, J. F., Ennos, A. R., & Pauleit, S. (2007). Adapting cities for climate change: The role of green infrastructure. Built Environment, 33(1), 115-133. https://doi.org/10.2148/benv.33.1.115

Grimmond, C. S. B. (2007). Urbanization and global environmental change: Local effects of urban warming. Geographical Journal, 173(1), 83-88. https://doi.org/10.1111/j.1475-4959.2007.232_3.x

Harlan, S. L., Brazel, A. J., Prashad, L., Stefanov, W. L., & Larsen, L. (2006). Neighborhood microclimates and vulnerability to heat stress. Social Science & Medicine, 63(11), 2847-2863. https://doi.org/10.1016/j.socscimed.2006.07.030

Oke, T. R. (1982). The energetic basis of the urban heat island. Quarterly Journal of the Royal Meteorological Society, 108(455), 1-24. https://doi.org/10.1002/qj.49710845502

Peng, S., Piao, S., Zeng, Z., Ciais, P., Zhou, L., Li, L. Z., ... & Myneni, R. B. (2012). Surface urban heat island across 419 global big cities. Environmental Science & Technology, 46(2), 696-703. https://doi.org/10.1021/es2030438

Santamouris, M. (2014). On the energy impact of urban heat island and global warming on buildings. Energy and Buildings, 82, 100-113. https://doi.org/10.1016/j.enbuild.2014.07.022

Santamouris, M., Cartalis, C., Synnefa, A., & Kolokotsa, D. (2014). On the impact of urban heat island and global warming on the power demand and electricity consumption of buildings—A review. Energy and Buildings, 98, 119-124. https://doi.org/10.1016/j.enbuild.2014.09.052

Schwarz, N., Lautenbach, S., & Seppelt, R. (2011). Exploring indicators for quantifying surface urban heat islands of European cities with MODIS land surface temperatures. Remote Sensing of Environment, 115(12), 3175-3186. https://doi.org/10.1016/j.rse.2011.07.003

Stone, B., & Rodgers, M. O. (2001). Urban form and thermal efficiency: How the design of cities influences the urban heat island effect. Journal of the American Planning Association, 67(2), 186-198. https://doi.org/10.1080/01944360108976228

Zhou, W., Huang, G., & Cadenasso, M. L. (2011). Does spatial configuration matter? Understanding the effects of land cover pattern on land surface temperature in urban landscapes. Landscape and Urban Planning, 102(1), 54-63. https://doi.org/10.1016/j.landurbplan.2011.03.009

The unrelenting global expansion of the urban heat island over the last century

Yaxue Ren[1], Raffaele Lafortezza[1,2*], Vincenzo Giannico[1], Giovanni Sanesi[1], Xinna Zhang[2], Chengyang Xu[2]

[1]Department of Soil, Plant and Food Sciences, University of Bari Aldo Moro, Via Amendola 165/A 70126 Bari, Italy

[2]The Key Laboratory for Silviculture and Conservation of Ministry of Education, Key Laboratory for Silviculture and Forest Ecosystem of State Forestry and Grassland Administration, Research Center for Urban Forestry, Beijing Forestry University, Beijing 100083, China

*Corresponding author:

Prof. Raffaele Lafortezza, PhD
Department of Soil, Plant and Food Sciences
University of Bari Aldo Moro
Via Amendola 165/A 70126 Bari, ITALY
E-mail: raffaele.lafortezza@uniba.it

Abstract

The past century has seen dramatic increases in global temperatures and mounting urbanization. As a result of these events, the urban heat island (UHI) effect has received growing attention in scientific research worldwide. A global search was initially conducted using a scientific literature database to collect all available relevant publications to understand how the UHI has been expanding worldwide and affecting more cities across different latitudes and altitudes. Subsequently, a semantic analysis was performed to extract city names. The literature search and analysis combined resulted in 6,078 publications in which UHI was investigated in 1,726 cities worldwide in the 1901 to 2022 time period. The cities were grouped into 'first appearance' and 'recurrent appearance'. Results show that UHI was studied in only 134 cities during the 90-year period from 1901 to 1992, with a remarkable growth over time in the number of cities where interest in UHI increased. Interestingly, the number of first appearances was always notably higher than the number of recurrent appearances. The Shannon evenness index was employed to identify the spatial locations (hotspots) across the globe where UHI-related research has been concentrated in multiple cities over the last 120 years. Finally, Europe was selected as a testbed for conducting an analysis to shed light on how economic, demographic, and environmental factors can impact UHI. Our study is unique for having demonstrated not only the rapid growth of cities affected by UHI globally but also the increasing and unrelenting expansion of UHI occurrences across different latitudes and altitudes over time. These novel findings will undoubtedly be of interest to scientists investigating the UHI phenomenon and its trends.

Stakeholders will acquire a broader perspective and deeper understanding of UHI in order to engage in more effective urban planning to offset and mitigate the phenomenon's adverse effects in the context of increasing climate change and urbanization.

Keywords: UHI; Latitude; Altitude; Literature database; Climate; Vegetation

1. Introduction

Dramatic global climate change and urbanization, which are regrettably advancing at a rapid pace, are among the most important global trends of the 21st century (Marcotullio et al., 2021). According to the Intergovernmental Panel on Climate Change (IPCC) assessment report, the global mean air and surface temperature have significantly increased over the last century, and by the end of the 21st century will have increased by 1°C to 3.7°C (IPCC, 2013). At the same time, the world is urbanizing rapidly, and people living in cities have outnumbered rural dwellers (Yang and Zhao 2022). More than half of the global population will be living in urban settlements by 2030 (United Nations 2018). The end result will be a higher rise of temperatures in built-up areas (Radhi, et al., 2013) compared to their suburban counterparts, which defines what is commonly known as the urban heat island (UHI) effect (EPA, 2022). Of these events, UHI has received growing attention in scientific research worldwide (Balany et al., 2020; Mohajerani et al., 2017; Peng et al., 2012; Radhi et al., 2013).

The largest number of contributions to UHI-related research come from meteorology atmospheric sciences and environmental sciences (Huang & Lu, 2018). With regard to meteorology atmospheric sciences, investigations of the urban climate date back to the early 19th century. Hundreds of studies on the “urban temperature effect” or “heat island effect” have been published in the academic literature (Stewart, 2019), since Howard (1833) first suggested that the temperature difference between London and its countryside was proportional to urban density and development. The continuous exploration and development of theories, methods, and techniques (e.g., Arnfield,

2003; Balchin & Pye, 1947; Huang & Ye, 2015; Oke, 1995; Schwarz et al., 2012; Stewart, 2011; Zhou et al., 2019) by scientists and scholars in urban climatology have allowed UHI to grow in popularity from its modest beginnings into a research topic of prominent academic interest. Its negative effects (Akbari et al., 2001; Donovan & Butry 2009; Hirano & Fujita 2012; Lowry, 1977), spatiotemporal patterns (Jin et al., 2015; Ren et al., 2007) and causes (Akbari et al., 2001; Doulos et al., 2004; Mohajerani et al., 2017; Rossi et al., 2014) have been extensively reported.

The majority of contributions to the environmental sciences, on the other hand, demonstrate that increasing vegetation and green spaces in cities have proven to be a way to address the root causes of the UHI issue (Gill et al., n.d.; Givoni, 1991; Norton et al., 2015; Peng et al., 2012; Shi et al., 2021). Scientists from specific disciplines, such as environmental management, landscape ecology, ecological restoration and urban forestry, have investigated the impact factors (Barbierato et al., 2019; Radhi et al., 2013; Ren et al., 2013; Zhou et al., 2014) and mitigation measures of UHI (Broadbent et al., 2018; Oliveira, 2011; Tan et al., 2010). It has also been suggested that controlling population size and GDP growth per capita may help to mitigate the UHI effect (Li et al., 2020). Correspondingly, most secondary sources (review articles) have not only focused on causes (Mohajerani et al., 2017; Ward et al., 2016) and mitigation measures (Aleksandrowicz et al., 2017; Balany et al., 2020; Bowler et al., 2010; Santamouris, 2013) but also on UHI evaluation methods (Neinavaz et al. 2021; Ward et al. 2016). In the early literature, the UHI was determined by measuring urban air temperature using

various methods, such as sensors mounted on bicycles (Budel & Wolf, 1933), motorcars (Fukui, 1941; Oke, 1976; Schmidt, 1927) and climate stations (Besson, 1931). Subsequently, the developments in remote sensing technology and spatial science have greatly incremented UHI research based on land surface temperature (e.g., Chen et al., 2022; Kong et al., 2014; Ren et al., 2013; Zhou et al., 2022), with an exponential growth trend beginning in 2005 (Zhou et al., 2019).

Viewed from another perspective, very few studies have dealt with the expansion of the UHI phenomenon. However, with the increased impact of climate change on cities (Gill et al., n.d.) and enhanced public awareness (Brondizio et al., 2021), various disciplines and interdisciplinary research areas focusing on climate change have been emerging (Lemos et al., 2019), thus expanding the UHI research trend. Oke (1982) had previously argued that there is a relative wealth of research on UHIs in temperate climates but a paucity of studies on heat islands in equatorial, tropical, subpolar and polar settlements. In contrast, 20 years later, Arnfield (2003) suggested that the areas studied for UHIs have included equatorial wet climates, tropical wet-dry and monsoonal climates, tropical highland climates, tropical deserts, subtropical climates and high latitude locations. Since then, another 20 years have passed and scientific research on the UHI effect continues to grow exponentially (e.g., Balany et al., 2020; Qi et al., 2019; Santamouris, 2013). However, this body of literature still does not provide evidence of UHI occurrence expanding to geographical regions worldwide.

The overarching goal of this study is to demonstrate how the UHI has been affecting an increasing amount of cities globally over a century and beyond (from here on referring to 120 years). The specific objectives of this study are to: (i) analyze the spatial distribution of cities where UHI has been investigated as well as the growth ratio of these cities over time; (ii) investigate the trend of UHI expansion in latitude and altitude; (iii) identify the spatial locations (i.e., hotspots) across the globe where UHI-related research is concentrated in multiple cities; and (iv) explore the economic, demographic and environmental drivers underlying the distribution of hotspots and non-hotspots with a focus on the European continent.

This singular study will greatly benefit urban planners and urban forestry research as well as offer scientists with important insights to deepen their understanding of the UHI phenomenon and its unrelenting and increasing worldwide trend. It will open the window of opportunity to policy makers and diverse stakeholders to engage in more skillful urban planning to offset and mitigate UHI's impacts on society and the environment at a time in history when global temperatures are dangerously increasing and the world's cities are rapidly urbanizing.

2. **Materials and methods**

To conduct our research, a large database (i.e., Scopus) of scientific literature focusing on the UHI phenomenon was accessed. For the purpose of including as many publications related to the UHI effect as possible in the study, (i) we used *climate* and *vegetation* as two main domains in the search

query (see Section 2.1); (ii) followed up the search by conducting a semantic extraction to restrict the publications to the urban area (see Section 2.2); and (iii) performed a subsequent data analysis with the extracted city information (Fig. 1) (see Section 2.3). Overall, the publications collected in this work focus on climate and vegetation in an urban context and will be referred to from here on as UHI-related research.

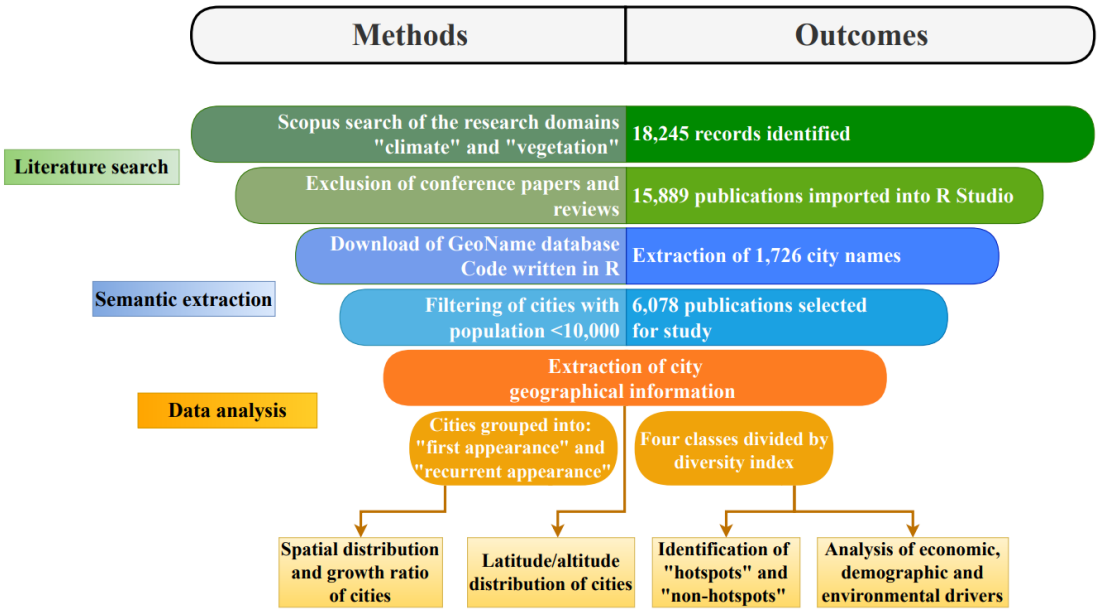

Fig. 1. Flowchart of the literature search and analytical process.

2.1 Literature search

To search publications in which UHI has been investigated at the global level, we performed a selection of keywords focusing on the two main research domains as follows (asterisks replace all possible characters at the end of a word):

- **Climate**: “urban heat island*” OR “UHI*” OR “land surface temperature” OR “microclimate”,

and

- **Vegetation**: “urban forest*” OR “green space” OR “green infrastructure” OR “vegetation” OR “tree*” OR “nature-based solution*” OR “canopy cover” OR “biomass".

2.2 Semantic extraction

An additional filtering step focusing on UHI-related research conducted in the urban area was performed by means of semantics. Firstly, BibTeX files were imported from the identified literature and downloaded from Scopus into an R statistical environment (Version 4.1.2). Secondly, the GeoNames (2009) database was downloaded, as it contains more than 25 million geographical names (cities, provinces, regions) and their respective latitude, longitude, and altitude. Thirdly, the code was written in R for the semantic analysis of publications to automatically extract city names from the title and abstract based on GeoNames. Cities with a population of less than 10,000 were filtered out to avoid incorrect matching with common names. For example, Shannon (Quebec, Canada) and William (California, USA) are names of cities with populations of 6,423 and 5,642, respectively, which more often refer to names of individuals.

In addition, a further analysis was conducted on abstract records. The analysis involved identifying the frequency of terms related to air temperature, local climate zone, land surface temperature, and land use. A Venn diagram was designed to represent the presence and intersection of terms found in each abstract. The same analysis was performed for four different timeframes to gain insight into the research history of each category. The analysis provides a comprehensive view of the research on

UHI and related parameters, and highlights the importance of considering multiple parameters in urban climate studies (see Supplementary Material, Fig. S1 and Table S1).

2.3. Data analysis

In our study, the probability density function (shown below) was used to standardize and compare the latitude and altitude distributions of cities between different timeframes,

$$F(x) = P\ (a \leq x \leq b) = \int_a^b f(x)dx = 1 \qquad \text{(Eq. 1)}$$

where probability (P) is the integration of the density function $f(x)$ from $x = a$ to $x = b$. The integer was set at 1 to compare multiple functions across time. The Shannon evenness index (Eq. 3), which is based on Shannon diversity (Shannon 1948) (Eq. 2), was used to analyze the spatial distribution of UHI-related research on a global scale over a period of 120 years. For the scope, we divided the globe into equal grids by overlapping a fishnet polygon (size 1x 1°) and calculated the evenness index for each grid. The formula is shown as follows:

$$H^{'} = -\sum_{i=1}^{S}(p_i \ln p_i) \qquad \text{(Eq. 2)}$$

where p_i and S are, respectively, the proportion of appearances belonging to the i-th city and the total number of cities within each cell of the grid for which UHI-related research has been conducted. The Shannon evenness index is defined as:

$$E = \frac{H^{'}}{H^{'}_{\max}} \qquad \text{(Eq. 3)}$$

where H' represents the number derived from the Shannon diversity index and H'_{max} is the maximum possible value of H'; E is constrained between 0 and 1.

To illustrate the behavior of the index included in our analysis, a schematic sample is given in Figure 2. Grids belonging to different classes with cities (indicated by black dots) and their respective appearances in the grid are shown on the right. For example, the grid in panel (b) contains 4 cities which appeared 8, 7, 3 and 2 times, respectively. Therefore, S is the total number of cities in the grid (N = 20), while p_i is the proportion of appearances belonging to the i-th city, which are respectively 0.4, 0.35, 0.15, 0.1, and H' is 1.249. The probability of H'_{max} in this grid, which is the equal number of appearances of the four cities, is 0.25 for all p, and H'_{max} is 1.386; thus, the Shannon evenness index equals 0.9.

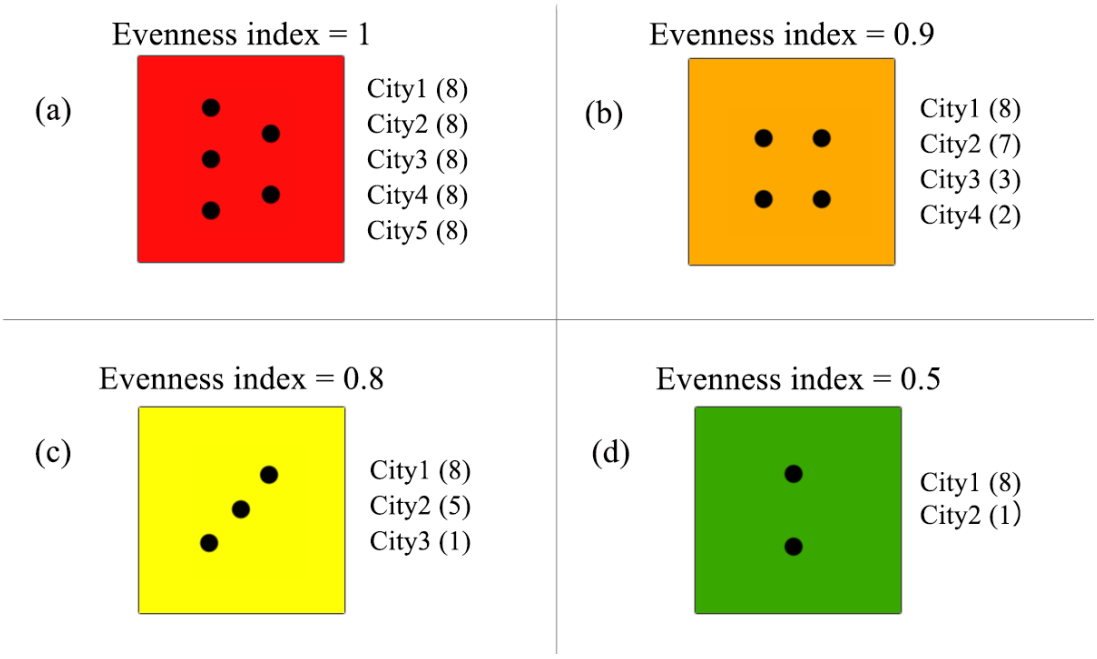

Fig. 2. Schematic sample of the Shannon evenness index grids of different classes: (a) 0.96-1; (b) 0.83-0.96; (c) 0.59-0.83; and (d) 0-0.59 extracted from the global map of Figure 8.

Finally, we explored the economic, demographic, and environmental drivers underlying the

distribution of hotspots and non-hotspots with a focus on the European continent for a specific timeframe: 2000-2021 (KC & Ruth, 2015).The selection of Europe and the above timeframe is motivated by the availability of consistent data, both spatially and temporally, for all cities in Europe. Gross Domestic Product (GDP) and population density data were retrieved from the Organisation for Economic Cooperation and Development (OECD) Regional Statistics Database (Anon, n.d.). Temperature data for summer (June, July and August) were sourced from WorldClim (www.worldclim.org).

3 Results

The Scopus search for scientific literature containing keywords from both domains – climate and vegetation – revealed 18,245 publications altogether from 1901 to 2022. Conference papers were excluded, which reduced the total number of publication records to 15,889 (most recent update: September 29, 2022). Subsequent to the semantic extraction strategy, 6,078 publications were finally included in our study for further analysis (Fig. 1). The statistics were visualized using Tableau (Version 2022.1) and the ggplots package (Wickham 2016) in R studio.

3.1 The spatial distribution and growth ratio of cities in UHI-related research

After running the code for semantics filtering, a total of 1,726 cities with 8,257 appearances in 6,078 publications were extracted in the last 120 years. The 120 years of research were divided into four

timeframes: 1901-1992; 1993-2002; 2003-2012; and 2013-2022 (1901-1992 constituted one timeframe due to the small amount of literature, while the others were grouped per decade). The appearance of each city is indicated by a dot on a map, while a further division of the cities into 'first appearance' and 'recurrent appearance' is represented by blue and orange dots, respectively (Fig. 3). In other words, the same city was identified as a first occurrence in the earliest timeframe that was extracted, and then as a reoccurrence if it was extracted in other timeframes. The results of a further analysis performed on abstract records are also shown on a map (Fig. 4), with the different colored dots representing the analysis conducted in that city for air temperature (AT), land surface temperature (LST), air temperature and land surface temperature (AT+LST), or other studies which did not mention AT or LST (Other). Results show a remarkable growth over time in the number of cities in which the UHI effect was studied (Figs. 3 and 4).

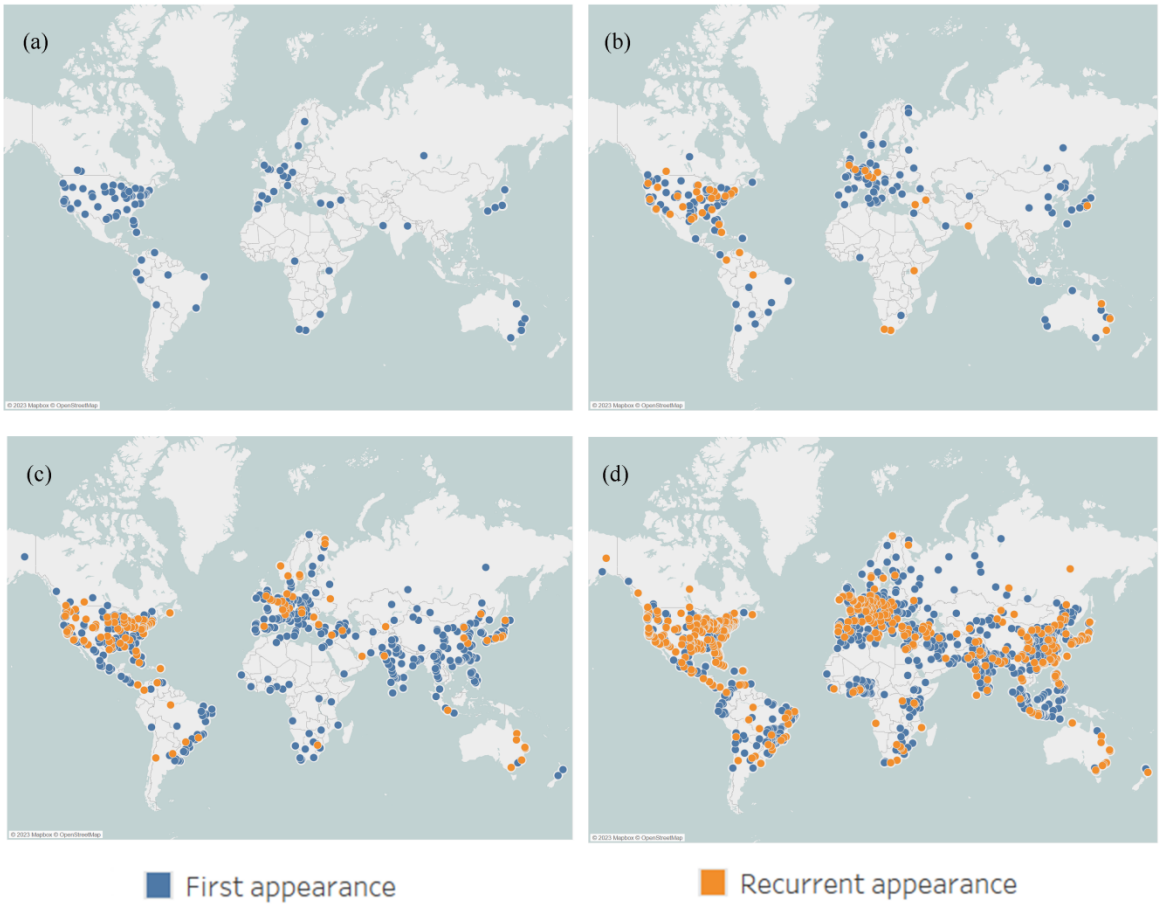

Fig. 3. Cities that appear in publications in which the UHI effect was studied. The blue and orange dots represent the first appearance of cities and the recurrent appearance of cities, respectively, for the timeframes (a) 1901-1992, (b) 1993-2002, (c) 2003-2012, and (d) 2013-2022.

Over the past century, new cities have been continuously included in research related to UHI worldwide, indicating that an increasing number of cities are affected by UHIs and, more specifically, that the UHI is becoming a growing phenomenon in the majority of cities where it has never occurred before. At the same time, the number of cities which have been repeatedly studied has also grown (see Fig. 3), although these (recurrent appearances) have been outnumbered by the new cities (first appearances). This secondary finding proves that the UHI effect has long captured the interest of scientists. Furthermore, research of the early timeframes (1901-2002) on the UHI specifically

investigating AT and LST shows that the number of appearances of both terms was more similar than in the latest timeframes (2003-2022), where scientists tended to focus on LST more frequently due to the global availability of thermal infrared satellite images.

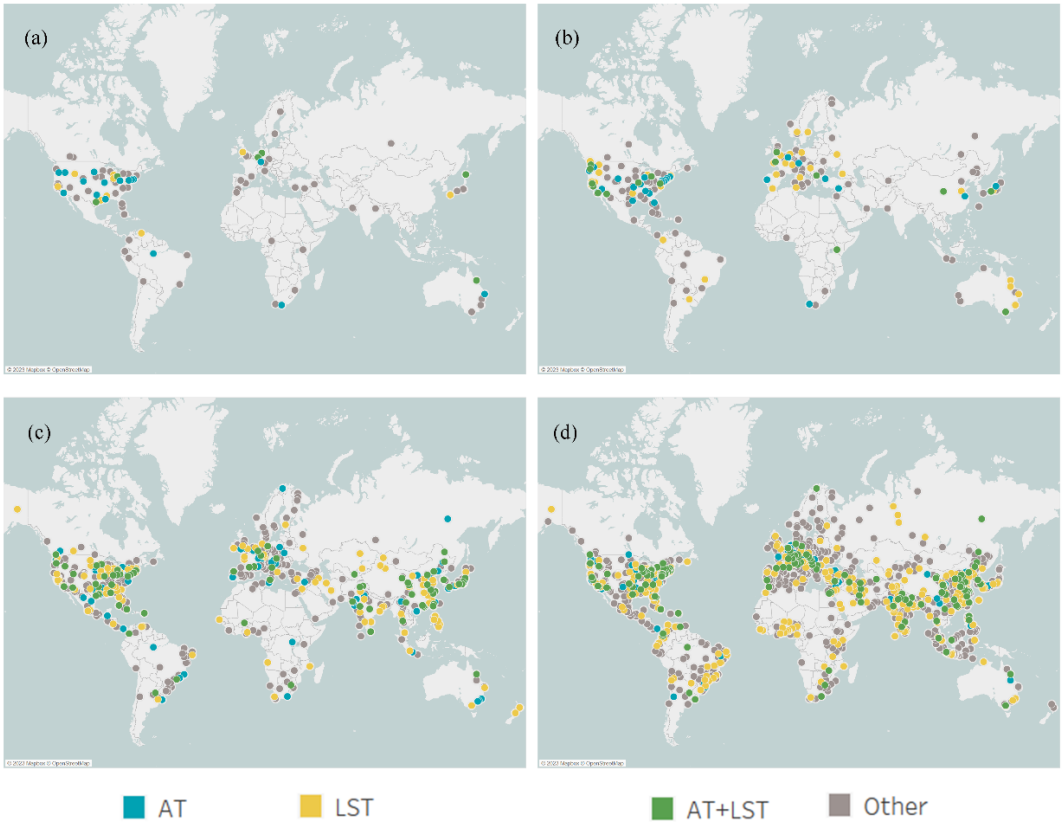

Fig. 4. Cities that appear in publications in which the UHI effect was studied. The sky-blue, yellow, green and gray dots represent the cities where the research included air temperature (AT), land surface temperature (LST), air temperature and land surface temperature (AT+LST), but not AT or LST (Other), respectively, for the timeframes (a) 1901-1992, (b) 1993-2002, (c) 2003-2012, and (d) 2013-2022.

After examining the spatial distribution of the cities studied in the UHI, we proceeded to explore the number of these cities and the proportion of their growth over time (Fig. 5). The results of our analysis show that the number of cities that appeared for the first time in publications was consistently

higher than the number of cities that appeared repeatedly (n = 187 vs. 49, 1993-2002 timeframe; n = 440 vs. 143, 2003-2012 timeframe; n = 965 vs. 431, 2013-2022 timeframe). The difference in this number was consistently more than double, except for the first timeframe where no cities were considered to be recurrent (n = 134 vs. 0, 1901-1992 timeframe). In the 2003-2012 and 2013-2022 timeframes, the percentage increase in recurring cities was even more striking, at 191.8% and 201.4%, respectively. At the same time, the growth ratio of first appearance cities never fell below 100%, except for the 1993-2002 timeframe, indicating that scientists have never lost interest in studying the UHI effect.

Meanwhile, the term LST was always used more often than the term AT, except in the first timeframe (Fig. 5), where scientists focused more on AT. Also, the growth ratio of LST appearance was constantly higher than the appearance of all other terms, except the last timeframe, which may be due to the rapid development of remote sensing technology and its application in the field of urban forestry. Although the number of studies investigating AT+LST was always the lowest, the results show that scientists have worked on combining AT and LST in conducting UHI research.

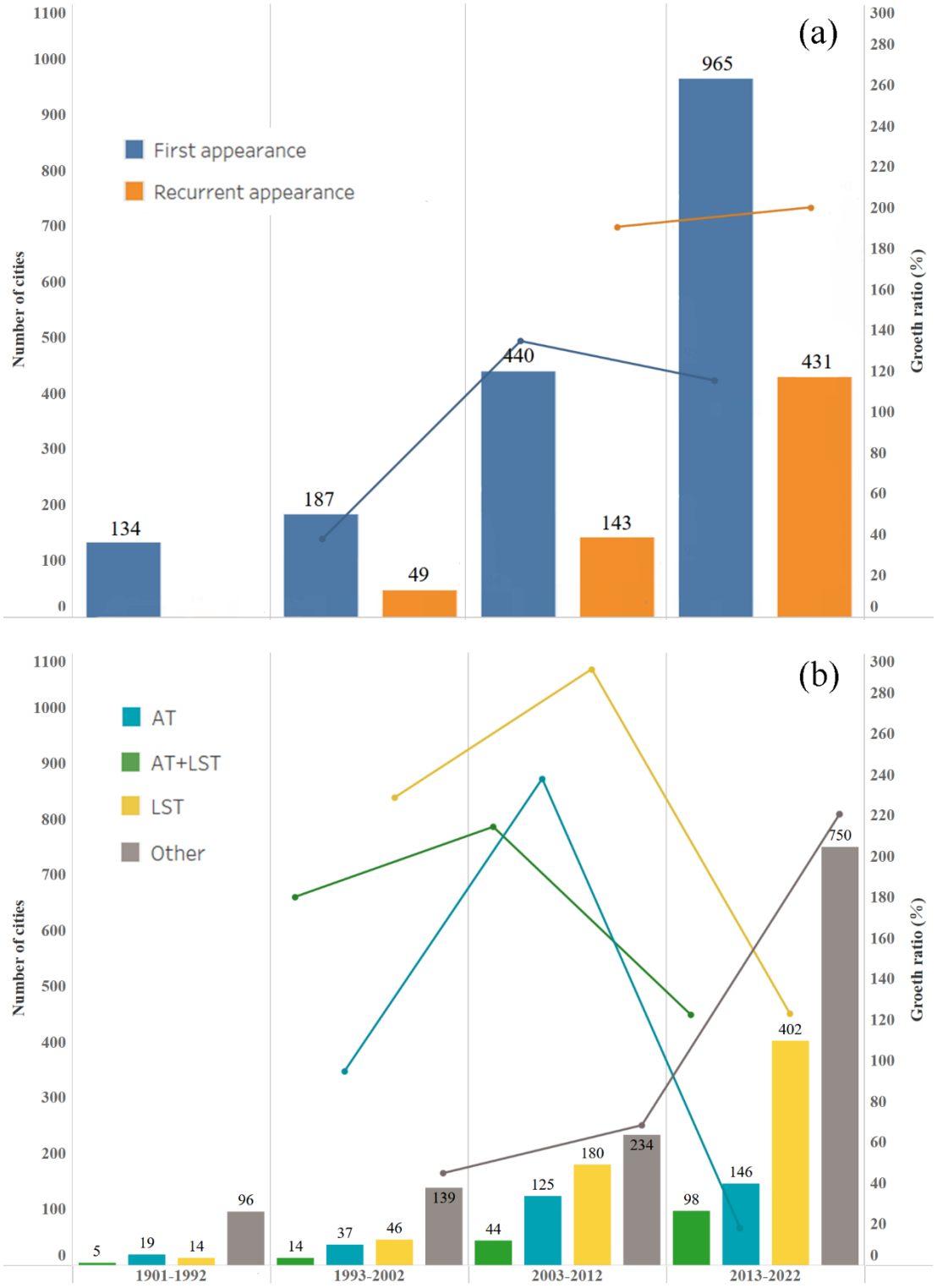

Fig. 5. Number and growth ratio of cities with different times of appearance (a) and different terms (b) in the four timeframes under study (1901-2022). AT, air temperature; LST, land surface temperature; AT+LST, air temperature and land surface temperature; and Other, other studies which did not mention AT or LST.

3.2 The latitude and altitude distribution of cities in UHI-related research

The latitudes of cities where scientists conducted UHI-related research during different timeframes were compared in a probability density diagram (Fig. 6). The density curve as a whole was negatively skewed, with skewness increasing over time (Table 1). This indicates that most of the cities extracted from the publications are distributed in the northern hemisphere and vary in decreasing latitude with time. The peaks of the density plot (Fig. 6) display where the values are concentrated over the intervals. The overall shape of the curve illustrates that the density distribution patterns of the latitudes of cities in the publications for all timeframes are single-peaked, concentrating around the 40° latitude. The standard deviation trended upward from 1901-1992 to 2013-2022 (Table 1), indicating that the latitudes of cities are gradually separating from the mean. This outcome implies that the latitudinal range of cities where scientists have conducted UHI-related research is expanding. The two curves representing the 1901-1992 and 1993-2002 timeframes, respectively, are the steepest. Over different timeframes, the height of the remaining curves decreased while their width increased, suggesting an increment in the differences in latitude between cities. In other words, more cities of different latitudes globally are being included in studies relating to UHI. Contrarily, the curve of the 2013-2022 timeframe is the lowest, implying that in the last decade the latitude range of cities has been the widest, and further confirming the above finding that at decreasing curve height a greater number of cities at different latitudes are being included in UHI-related research.

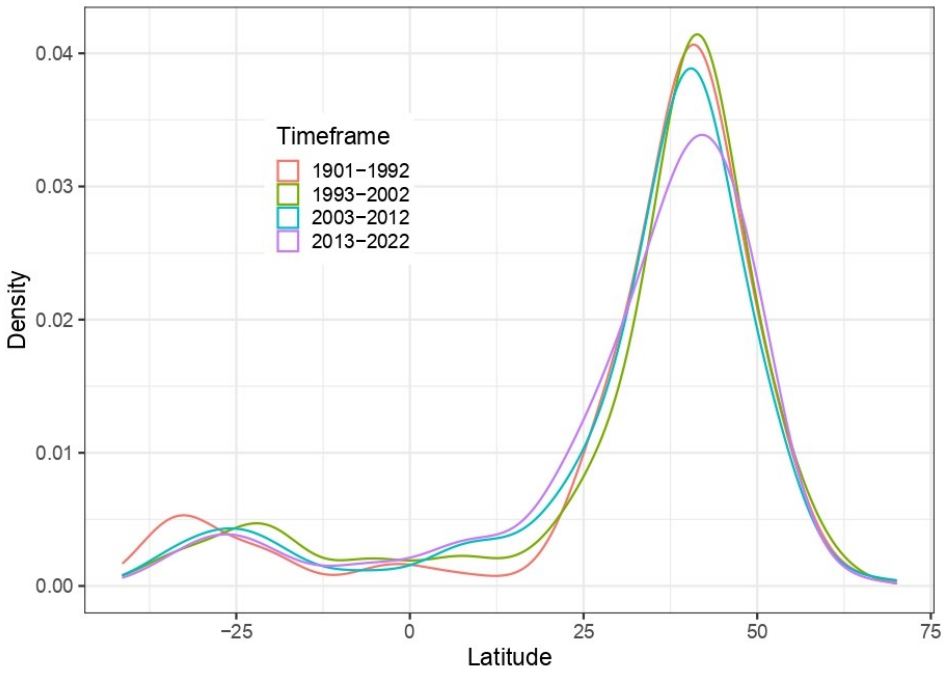

Fig. 6. Latitude distribution by timeframe of cities mentioned in UHI-related research.

Table 1. Metrics of the latitude probability distribution of cities in UHI-related research.

Timeframe	Mean	StdDev	Kurtosis	Skewness
1901-1992	32.02	23.09	2.81	-1.95
1993-2002	32.42	21.99	2.27	-1.79
2003-2012	31.69	21.51	2.50	-1.79
2013-2022	31.97	20.85	2.48	-1.75

The same increasing trend over time observed for latitude can be observed for altitude ranges (Fig. 7), except for the 1901-1992 timeframe, which is likely due to the long time span and small amount of data. The density curves were positively skewed overall, with most of the data concentrated in the lower altitude range and the skewness decreasing over time (Table 2). This indicates that the altitude of cities extracted from publications gradually extends to a higher range. The kurtosis of the

altitude distribution (Table 2) was always greater than the kurtosis of the latitude (Table 1), implying a greater degree of difference between the steepness of its distribution pattern and that of the Gaussian distribution. This is explained by the fact that most of the world's cities are concentrated at low altitudes and do not follow the Gaussian distribution. Our research on the UHI effect in the two timeframes of 2003-2012 and 2013-2022 involves cities in a wider altitude range (Fig. 7). In addition to the height concentration observed for the 0- to 500-m altitude range, some peaks can be noted at other altitudes. For example, peaks around 700 m depicted in red representing the 1901-1992 timeframe and in green representing the 1993-2002 timeframe (Fig. 6) are due to the fact that cities in this altitude range (600-700 m), exemplified by Madrid, appear 11 and 22 times, respectively, in publications related to the UHI. Cities at the same altitude were studied 56 and 163 times in the 2003-2012 and 2013-2022 timeframes, respectively, without showing significant peaks, which proves that there are more publications related to the UHI phenomenon in the last two decades.

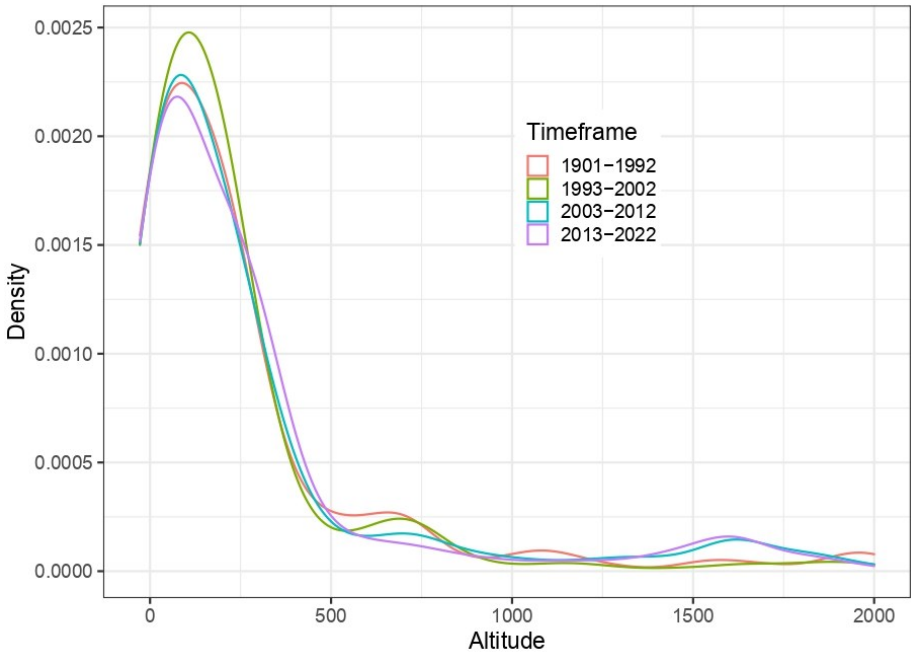

Fig. 7. Altitude distribution density by timeframe of cities mentioned in UHI-related research.

Table 2. Metrics of the altitude probability distribution of cities in UHI-related research.

Timeframe	Mean	StdDev	Kurtosis	Skewness
1901-1992	326.49	552.61	13.64	3.37
1993-2002	269.62	434.14	11.77	3.32
2003-2012	361.28	568.68	6.29	2.51
2013-2022	326.65	513.28	9.42	2.84

From 1901 to the present day, most studies in which the UHI has been investigated have focused on cities at latitudes between 30° and 50° and at altitudes below 500 m. One possible reason is that the world's population is mainly distributed at this latitude and altitude range (Cohen & Small, 1998; Bill Rankin, 2008). In the past, many cities did not face the challenges caused by climate change, thus the earlier studies focused on a narrower range of latitudes and altitudes. However, with the

current increasing UHI trend being associated with rapid climate change and urbanization, scientists have begun to conduct relevant studies in cities where these challenges had not been previously considered.

3.3 The spatial locations (hotspots) across the globe where UHI-related research is concentrated in multiple cities

All city data in the 1901-2022 time period were combined and the Shannon evenness index was calculated in grid units and displayed on a map (Fig. 8). The grids were divided into four quartile classes: 1st quartile 0-0.59; 2nd quartile 0.6-0.83; 3rd quartile 0.84-0.96; and 4th quartile 0.97-1.00, representing high-to-low evenness, while an additional gray grid represents 'no city studied'. The three continents – North America, Europe and Asia – containing the greatest number of hotspots (i.e., locations with an evenness index ≥0.59) were zoomed in to visualize the details.

The Shannon evenness index was used to measure the extent to which the number of cities in a region where UHI-related research was conducted was evenly distributed among those affected by UHI (cities subjected to at least one UHI study). The value of the index ranges from 0 to 1, with 0 indicating minimal diversity and 1 indicating maximal diversity. When UHI-related research in a region is concentrated in a single city, the value is 0, and when UHI-related research is conducted in all cities of our database and the number of studies is evenly distributed among them, the value is 1. Therefore, the hotspot locations are those having a higher concentration of UHI-related research

focusing on multiple cities rather than a single city. In other words, hotspot areas are likely to reflect the UHI characteristics of the entire region to a larger extent and the cities of the region studied are more evenly distributed.

As shown in Figure 8, most of the hotspots are concentrated in all three continents. Furthermore, the hotspots in North America are almost entirely in the United States. In Europe, most of the hotspots are concentrated in Western Europe, such as the United Kingdom, Spain and the Netherlands, while in Asia they are located in China, Japan, Indonesia and India.

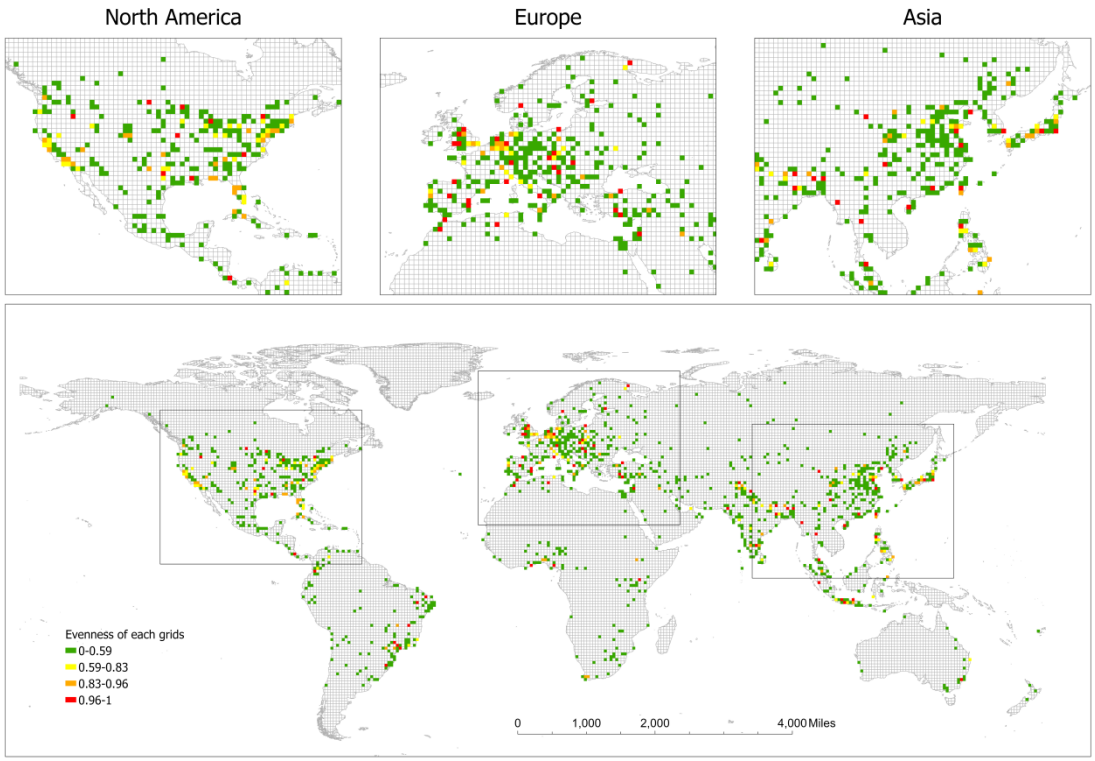

Fig. 8. Evenness of cities worldwide where UHI-related research was conducted from 1901 to 2022.

3.4 Economic, demographic and environmental drivers underlying hotspot/non-hotspot distribution in the European continent

A dynamic analysis of economic, demographic and environmental drivers underlying hotspot/non-

hotspot distribution was conducted using GDP, population density, and minimum and maximum summer temperatures as (surrogate) proxies. The analysis was conducted with a focus on the European continent beginning in 2001 (for GDP, population density and summer temperature) and ending in 2018 (for summer temperatures only) and in 2021 (for GDP and population density). Grids with an evenness index ≤0.59 (Fig. 8) were considered as non-hotspots and are represented by green lines (Fig. 9), while hotspots are represented by red lines (Fig. 9).

The results show a clear upward trend in GDP and population density for both hotspots and non-hotspots, with two exceptions. The negative growth in GDP and population in 2011 could relate to the impact of the European sovereign debt crisis, while that of 2021 might be due to the COVID-19 pandemic. However, hotspots demonstrated a consistently higher growth rate in comparison to non-hotspots. This trend may be attributed to the rapid economic expansion of hotspots, which tends to attract more population and resources, thereby exacerbating the UHI effect.

The analysis of summer temperature trends between hotspots and non-hotspots showed a surprisingly consistent pattern, with only minor differences observed. This finding suggests that the impact of changes in summer temperature on the extent of concentration of UHI-related research may not be relevant. However, even in 2004, the year with the highest rate of change, the summer temperature only changed by 2.1°; therefore, the temperature change over a 20-year period was not considered significant. When comparing GDP and population density with summer temperature, the

latter can be regarded as an insignificant driver.

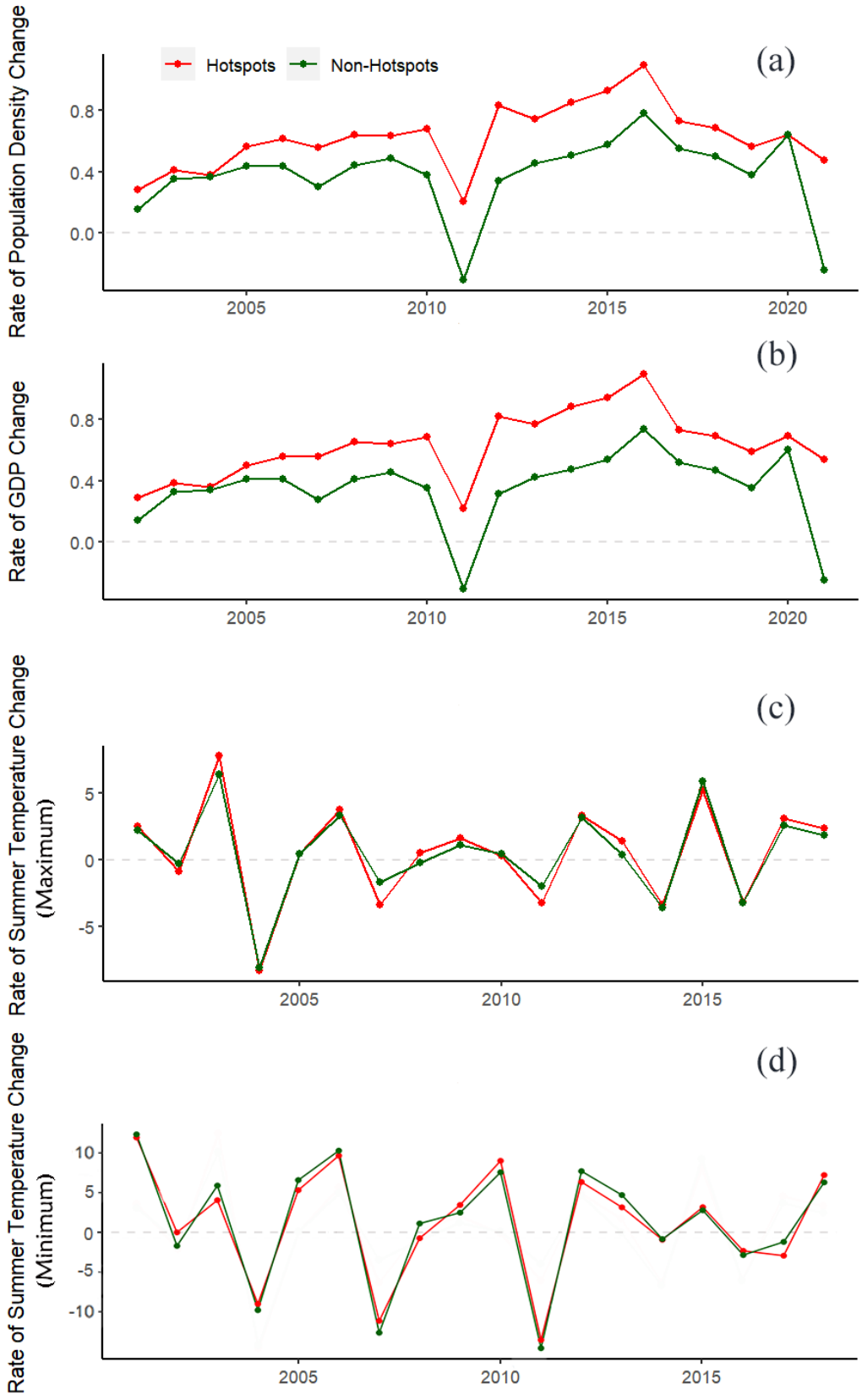

Fig. 9. Changes in gross domestic product (GDP), population density, and summer temperatures (minimum and maximum) in hotspots and non-hotspots over the last two decades beginning in 2001 (for GDP, population density and summer temperature) and ending in 2018 (for summer temperature) and in 2021 (for GDP and population density).

4. Discussion and conclusions

Previous studies on the UHI in relation to climate change, shedding light on its global phenomenology by analyzing thermal behavior aggregated at city scale or over seasonal or annual time periods (Mentaschi et al., 2022). For example, Zhang et al. (2010) assessed SUHI globally, while Clinton and Gong (2013) investigated urban areas with latitudes between 71° and -55° to characterize urban surface heat differences and identify urban environmental variables that are globally significant for diagnosing and predicting SUHI, but limited to one year: 2010. New research based on a global long-term dataset of daytime UHI delves into the space–time variability of urban–rural temperature differences, which is unprecedented at global scale (Mentaschi et al., 2022). Further study, proceeding from a literature review using data from 16 countries worldwide, analyzed UHI's global trend and provides insight on how it is linked with pollution (Ulpiani, 2021). The research we propose herein is rather based on an extensive and highly comprehensive global literature review and presents a unique aspect of the global UHI trend by focusing on its occurrences at different latitudes and altitudes over time. Our study results are solid and impressive. They not only confirm the rapid growth of

global research related to UHI over the last century and beyond, as represented by much of the collected literature (Aleksandrowicz et al., 2017; Deilami et al., 2018; Mohajerani et al., 2017), but also and perhaps more importantly demonstrate the unrelenting expansion of the UHI phenomenon to different geographical regions. Specifically, we have pioneered an analysis on the number of cities related to UHI research rather than concentrate on the number of publications as has been done in other review articles (Balany et al., 2020; Santamouris, 2013; Ward et al., 2016) to gain a more intuitive understanding of the worldwide expansion of UHI. Furthermore, the latitude and altitude of these cities were investigated to track the dynamic trend of UHI expansion, with most of the research at the beginning of the 20th century focusing on a latitude range from 25° to 50° and then expanding to lower and higher latitudes, as mentioned in other literature (Arnfield, 2003; Stewart, 2019). In this manner, our work has demonstrated how the UHI has affected an increasing number of cities across the globe during the course of 120 years.

In the time period (1901-2022) selected for our study, the results showed an increasing number of cities where UHI research was conducted (Figs. 3 and 4). While earlier studies were more often conducted for air temperature data collection, the later satellite era gave rise to more SUHI studies (Fig. 4). However, some geographical areas still exist where UHI has not been investigated (Fig. 3), perhaps because they are not affected by this phenomenon or as a result of lack of funding to conduct related research. Nevertheless, in recent decades the number of cities experiencing UHI has continued

to increase, suggesting that its expansion will not come to a halt, at least in the short term.

To explore the spatial locations that have attracted widespread scientific interest in UHI during the last century, we identified hotspots and non-hotspots at global scale based on a widely used diversity index – Shannon evenness. The focus on Europe served as an example to explore the economic, demographic, and environmental drivers underlying the distribution of hotspots and non-hotspots. Our analysis reveals that the growth of GDP and population density is positively associated with scientists' interest in the UHI phenomenon. However, we also found that the increase in summer temperature (both minimum and maximum) did not correspond to the expansion of the UHI effect, which is inconsistent with the results of other studies, such as that of Zhou (2014), who argued that climate has an overwhelming control on the spatial variability of UHI. One potential reason for this divergence of trends stems from the public perception that apparent temperature is influenced by humidity, wind, and radiation in addition to land surface temperature (Steadman, 1979). Another reason could be the limited resolution of the temperature data obtained from satellite images. In particular, the monthly temperature data from Worldclim have a resolution of only 21 km^2, and many of the urban biophysical elements that contribute to temperature variability are smaller than 60 m (Small, 2009). We intend to further investigate this aspect of the analysis, which is currently limited by lack of available data, by introducing other variables in order to acquire an in-depth understanding thereof. This research will likely point to important health and well-being implications of the UHI

effect for urban residents.

Although the concept of UHI was first introduced in 1958 (see Manley), the increase of higher temperatures in urban centers compared to suburban areas has been documented as early as 1833 (see Howard). For this reason, all relevant literature has been included and analyzed to the greatest extent possible to afford this study the most comprehensive perspective. Moreover, it is highly improbable for any database to contain all the early research because of the limits of technology. Some literature was not included in the Scopus database we employed, or if it was, no mention was found of cities being investigated for UHI, whether in the abstracts, keywords and titles, or references made to provinces and regions; therefore, this literature was not added to our study. Evidently, this could represent a study limitation, but we believe that for our intents and purposes the final database of 6,078 publications is highly satisfactory.

Our study points out that research gaps exist in some geographic regions, especially in the concentrated latitudinal and altitudinal range of UHI-related studies, and that further in-depth studies are warranted. Meanwhile, research on the UHI effect has become increasingly important and urgent due to the rapid advance in climate change and urbanization (Chapman et al., 2017; Grimmond, 2007; Ren, 2015), which necessitated an understanding of its history and trends. Hence, this work provides a broader perspective in time of UHI as a global phenomenon, which may enable scientists dedicated to urban forestry research and climate change to be more intuitive about UHI's impacts on current

society and the environment as well as its expanding trend. From their own perspective, policy makers and practitioners will be encouraged to become more vigilant in formulating appropriate mitigation and adaptation strategies. In point of fact, this study underscores the urgency of developing targeted mitigation and adaptation strategies to address the challenges posed by UHI and highlights the need for collaborative efforts among various stakeholders to achieve this goal.

Acknowledgments

This work was carried out under the research project "CLEARING HOUSE - Collaborative Learning in Research, Information-sharing and Governance on How Urban tree-based solutions support Sino-European urban futures", funded by the European Union's Horizon 2020 Research and Innovation Program (Grant Agreement No. 821242). The authors wish to thank Yole DeBellis for her contribution in reviewing this work.

References

Akbari, H., M. Pomerantz, and H. Taha. 2001. "Cool Surfaces and Shade Trees to Reduce Energy Use and Improve Air Quality in Urban Areas." *Solar Energy* 70(3):295–310. doi: 10.1016/S0038-092X(00)00089-X.

Aleksandrowicz, O., M. Vuckovic, K. Kiesel, and A. Mahdavi. 2017. "Current Trends in Urban Heat Island Mitigation Research: Observations Based on a Comprehensive Research Repository." *Urban Climate* 21:1–26. doi: 10.1016/j.uclim.2017.04.002.

Anon. n.d. "OECD Regional Statistics." Retrieved March 12, 2023 (https://www.oecd-ilibrary.org/urban-rural-and-regional-development/data/oecd-regional-statistics_region-data-en).

Arnfield, A. J. 2003. "Two Decades of Urban Climate Research: A Review of Turbulence,

Exchanges of Energy and Water, and the Urban Heat Island." *International Journal of Climatology* 23(1):1–26. doi: 10.1002/joc.859.

Balany, F., A. W. M. Ng, N. Muttil, S. Muthukumaran, and M. S. Wong. 2020. "Green Infrastructure as an Urban Heat Island Mitigation Strategy—a Review." *Water (Switzerland)* 12(12). doi: 10.3390/w12123577.

Balchin, W. G. V., and Norman Pye. 1947. "A Micro-Climatological Investigation of Bath and the Surrounding District." *Quarterly Journal of the Royal Meteorological Society* 73(317–318):297–323. doi: 10.1002/qj.49707331706.

Barbierato, Elena, Iacopo Bernetti, Irene Capecchi, and Claudio Saragosa. 2019. "Quantifying the Impact of Trees on Land Surface Temperature: A Downscaling Algorithm at City-Scale." *European Journal of Remote Sensing* 52:74–83. doi: 10.1080/22797254.2019.1646104.

Besson, L. 1931. "L'altération du climat d'une grande ville [Change of climate of a large town]." *Annales d'Hygiene Publique, Industrielle et Sociale* 9:405–38.

Bowler, Diana E., Lisette Buyung-Ali, Teri M. Knight, and Andrew S. Pullin. 2010. "Urban Greening to Cool Towns and Cities: A Systematic Review of the Empirical Evidence." *Landscape and Urban Planning* 97(3):147–55. doi: 10.1016/j.landurbplan.2010.05.006.

Broadbent, Ashley M., Andrew M. Coutts, Nigel J. Tapper, and Matthias Demuzere. 2018. "The Cooling Effect of Irrigation on Urban Microclimate during Heatwave Conditions." *Urban Climate* 23:309–29. doi: 10.1016/j.uclim.2017.05.002.

Brondizio, Eduardo S., Maria Carmen Lemos, Dabo Guan, Neil Jennings, Cheikh Mbow, Harini Nagendra, and Petra Tschakert. 2021. "Global Environmental Change: 30 Years of Interdisciplinary Research on the Human and Policy Dimensions of Environmental Change." *Global Environmental Change* 71:102416. doi: 10.1016/j.gloenvcha.2021.102416.

Budel, A., and J. Wolf. 1933. "Münchener Stadtklimatische Studien [Munich Town Climatic Studies]." *Zeitschrift Für Angewandte Meteorologie* 4–10.

Chapman, Sarah, James E. M. Watson, Alvaro Salazar, Marcus Thatcher, and Clive A. McAlpine. 2017. "The Impact of Urbanization and Climate Change on Urban Temperatures: A Systematic Review." *Landscape Ecology* 32(10):1921–35. doi: 10.1007/s10980-017-0561-4.

Chen, Yanhua, Wendy Y. Chen, Vincenzo Giannico, and Raffaele Lafortezza. 2022. "Modelling Inter-Pixel Spatial Variation of Surface Urban Heat Island Intensity." *Landscape Ecology* 37(8):2179–94. doi: 10.1007/s10980-022-01464-2.

Clinton, Nicholas, and Peng Gong. 2013. "MODIS Detected Surface Urban Heat Islands and Sinks: Global Locations and Controls." *Remote Sensing of Environment* 134:294–304. doi: 10.1016/j.rse.2013.03.008.

Cohen, Joel E., and Christopher Small. 1998. "Hypsographic Demography: The Distribution of Human Population by Altitude." *Proceedings of the National Academy of Sciences of the United States of America* 95(24):14009–14.

Deilami, Kaveh, Md Kamruzzaman, and Yan Liu. 2018. “Urban Heat Island Effect: A Systematic Review of Spatio-Temporal Factors, Data, Methods, and Mitigation Measures.” *International Journal of Applied Earth Observation and Geoinformation* 67:30–42. doi: 10.1016/j.jag.2017.12.009.

Donovan, Geoffrey H., and David T. Butry. 2009. “The Value of Shade: Estimating the Effect of Urban Trees on Summertime Electricity Use.” *Energy and Buildings* 41(6):662–68. doi: 10.1016/j.enbuild.2009.01.002.

Doulos, L., M. Santamouris, and I. Livada. 2004. “Passive Cooling of Outdoor Urban Spaces. The Role of Materials.” *Solar Energy* 77(2):231–49. doi: 10.1016/j.solener.2004.04.005.

Fukui, Eiichirô. 1941. “Horizontal Distribution of the Air Temperature in Greater Cities of Japan.” *Geographical Review of Japan* 17(5):354–72. doi: 10.4157/grj.17.354.

GeoNames. 2009. “GeoNames.”

Gill, S. E., J. F. Handley, A. R. Ennos, and S. Pauleit. n.d. “Adapting Cities for Climate Change: The Role of the Green Infrastructure.” *CLIMATE CHANGE AND CITIES* 33(1):19.

Givoni, B. 1991. “Impact of Planted Areas on Urban Environmental Quality: A Review.” *Atmospheric Environment. Part B. Urban Atmosphere* 25(3):289–99. doi: 10.1016/0957-1272(91)90001-U.

Grimmond, Sue. 2007. “Urbanization and Global Environmental Change: Local Effects of Urban Warming.” *Geographical Journal* 173:83–88. doi: 10.1111/j.1475-4959.2007.232_3.x.

Guo-Yu, Ren. 2015. “Urbanization as a Major Driver of Urban Climate Change.” *Advances in Climate Change Research* 6(1):1–6. doi: 10.1016/j.accre.2015.08.003.

Hirano, Y., and T. Fujita. 2012. “Evaluation of the Impact of the Urban Heat Island on Residential and Commercial Energy Consumption in Tokyo.” *Energy* 37(1):371–83. doi: 10.1016/j.energy.2011.11.018.

Howard, Luke. 1833. *The Climate of London: Deduced from Meteorological Observations Made in the Metropolis and at Various Places Around It*. Harvey and Darton, J. and A. Arch, Longman, Hatchard, S. Highley [and] R. Hunter.

Huang, Chudong, and Xinyue Ye. 2015. “Spatial Modeling of Urban Vegetation and Land Surface Temperature: A Case Study of Beijing.” *Sustainability* 7(7):9478–9504. doi: 10.3390/su7079478.

Huang, Qunfang, and Yuqi Lu. 2018. “Urban Heat Island Research from 1991 to 2015: A Bibliometric Analysis.” *Theoretical and Applied Climatology* 131(3):1055–67. doi: 10.1007/s00704-016-2025-1.

IPCC. 2013. *Climate Change 2013: The Physical Science Basis*.

Jin, Kai, Fei Wang, Deliang Chen, Qiao Jiao, Lei Xia, Luuk Fleskens, and Xingmin Mu. 2015. “Assessment of Urban Effect on Observed Warming Trends during 1955–2012 over China: A Case of 45 Cities.” *Climatic Change* 132(4):631–43.

KC, B., and M. Ruth. 2015. “Modeling of Urban Heat Island at Global Scale.” 2015:B32D-03.

Kong, F., H. Yin, P. James, L. R. Hutyra, and H. S. He. 2014. “Effects of Spatial Pattern of Greenspace on Urban Cooling in a Large Metropolitan Area of Eastern China.” *Landscape and Urban Planning* 128:35–47. doi: 10.1016/j.landurbplan.2014.04.018.

Lemos, Maria Carmen, Hallie Eakin, Lisa Dilling, and Jessica Worl. 2019. “Social Sciences, Weather, and Climate Change.” *Meteorological Monographs* 59(1):26.1-26.25. doi: 10.1175/AMSMONOGRAPHS-D-18-0011.1.

Li, Ying, Yanwei Sun, Jialin Li, and Chao Gao. 2020. “Socioeconomic Drivers of Urban Heat Island Effect: Empirical Evidence from Major Chinese Cities.” *Sustainable Cities and Society* 63:102425. doi: 10.1016/j.scs.2020.102425.

Lowry, William P. 1977. “Empirical Estimation of Urban Effects on Climate: A Problem Analysis.” *Journal of Applied Meteorology (1962-1982)* 16(2):129–35.

Manley, G. 1958. “On the Frequency of Snowfall in Metropolitan England.” *Quarterly Journal of the Royal Meteorological Society* 84(359):70–72. doi: 10.1002/qj.49708435910.

Marcotullio, Peter J., Carsten Keßler, and Balázs M. Fekete. 2021. “The Future Urban Heat-Wave Challenge in Africa: Exploratory Analysis.” *Global Environmental Change* 66:102190. doi: 10.1016/j.gloenvcha.2020.102190.

Mentaschi, Lorenzo, Grégory Duveiller, Grazia Zulian, Christina Corbane, Martino Pesaresi, Joachim Maes, Alessandro Stocchino, and Luc Feyen. 2022. “Global Long-Term Mapping of Surface Temperature Shows Intensified Intra-City Urban Heat Island Extremes.” *Global Environmental Change* 72:102441. doi: 10.1016/j.gloenvcha.2021.102441.

Mohajerani, Abbas, Jason Bakaric, and Tristan Jeffrey-Bailey. 2017. “The Urban Heat Island Effect, Its Causes, and Mitigation, with Reference to the Thermal Properties of Asphalt Concrete.” *Journal of Environmental Management* 197:522–38. doi: 10.1016/j.jenvman.2017.03.095.

Neinavaz, E., M. Schlerf, R. Darvishzadeh, M. Gerhards, and A. K. Skidmore. 2021. “Thermal Infrared Remote Sensing of Vegetation: Current Status and Perspectives.” *International Journal of Applied Earth Observation and Geoinformation* 102. doi: 10.1016/j.jag.2021.102415.

Norton, Briony A., Andrew M. Coutts, Stephen J. Livesley, Richard J. Harris, Annie M. Hunter, and Nicholas S. G. Williams. 2015. “Planning for Cooler Cities: A Framework to Prioritise Green Infrastructure to Mitigate High Temperatures in Urban Landscapes.” *Landscape and Urban Planning* 134:127–38. doi: 10.1016/j.landurbplan.2014.10.018.

Oke, T. R. 1976. “The Distinction between Canopy and Boundary-Layer Urban Heat Islands.” *Atmosphere* 14(4):268–77. doi: 10.1080/00046973.1976.9648422.

Oke, T. R. 1982. “The Energetic Basis of the Urban Heat Island.” *Quarterly Journal of the Royal Meteorological Society* 108(455):1–24. doi: 10.1002/qj.49710845502.

Oke, T. R. 1995. “Classics in Physical Geography Revisited: Sundborg, Å. 1951: Climatological

Studies in Uppsala with Special Regard to the Temperature Conditions in the Urban Area. Geographica 22." *Progress in Physical Geography: Earth and Environment* 19(1):107–13. doi: 10.1177/030913339501900105.

Oliveira, Sandra. 2011. "The Cooling Effect of Green Spaces as a Contribution to the Mitigation of Urban Heat: A Case Study in Lisbon." *Building and Environment* 9.

Peng, Shushi, Shilong Piao, Philippe Ciais, Pierre Friedlingstein, Catherine Ottle, Francois-Marie Breon, Huijuan Nan, Liming Zhou, and Ranga B. Myneni. 2012. "Surface Urban Heat Island Across 419 Global Big Cities." *Environmental Science & Technology* 46(2):696–703. doi: 10.1021/es2030438.

Qi, J. D., B. J. He, M. Wang, J. Zhu, and W. C. Fu. 2019. "Do Grey Infrastructures Always Elevate Urban Temperature? No, Utilizing Grey Infrastructures to Mitigate Urban Heat Island Effects." *Sustainable Cities and Society* 46. doi: 10.1016/j.scs.2018.12.020.

Radhi, Hassan, Fayze Fikry, and Stephen Sharples. 2013. "Impacts of Urbanisation on the Thermal Behaviour of New Built up Environments: A Scoping Study of the Urban Heat Island in Bahrain." *Landscape and Urban Planning* 113:47–61. doi: 10.1016/j.landurbplan.2013.01.013.

Ren, G. Y., Z. Y. Chu, Z. H. Chen, and Y. Y. Ren. 2007. "Implications of Temporal Change in Urban Heat Island Intensity Observed at Beijing and Wuhan Stations." *Geophysical Research Letters* 34(5). doi: 10.1029/2006GL027927.

Ren, Zhibin, Xingyuan He, Haifeng Zheng, Dan Zhang, Xingyang Yu, Guoqiang Shen, and Ruichao Guo. 2013. "Estimation of the Relationship between Urban Park Characteristics and Park Cool Island Intensity by Remote Sensing Data and Field Measurement." *Forests* 4(4):868–86. doi: 10.3390/f4040868.

Rossi, F., A. L. Pisello, A. Nicolini, M. Filipponi, and M. Palombo. 2014. "Analysis of Retro-Reflective Surfaces for Urban Heat Island Mitigation: A New Analytical Model." *Applied Energy* 114:621–31. doi: 10.1016/j.apenergy.2013.10.038.

Santamouris, M. 2013. "Using Cool Pavements as a Mitigation Strategy to Fight Urban Heat Island-A Review of the Actual Developments." *Renewable & Sustainable Energy Reviews* 26:224–40. doi: 10.1016/j.rser.2013.05.047.

Schmidt, W. 1927. "Die Verteilung der Minimumtemperaturen in der Frostnacht des 12.5.1927 im Gemeindegebiet von Wien." *Fortschr. Landwirtsch.* 2(21):681–86.

Schwarz, Nina, Uwe Schlink, Ulrich Franck, and Katrin Großmann. 2012. "Relationship of Land Surface and Air Temperatures and Its Implications for Quantifying Urban Heat Island Indicators—An Application for the City of Leipzig (Germany)." *Ecological Indicators* 18:693–704. doi: 10.1016/j.ecolind.2012.01.001.

Shannon, C. E. 1948. "A Mathematical Theory of Communication." *The Bell System Technical Journal* 27(3):379–423. doi: 10.1002/j.1538-7305.1948.tb01338.x.

Shi, Yi, Shuguang Liu, Wende Yan, Shuqing Zhao, Ying Ning, Xi Peng, Wei Chen, Liding Chen,

Xijun Hu, Bojie Fu, Robert Kennedy, Yihe Lv, Juyang Liao, Chunliang Peng, Isabel M. D. Rosa, David Roy, Shouyun Shen, Andy Smith, Cheng Wang, Zhao Wang, Li Xiao, Jingfeng Xiao, Lu Yang, Wenping Yuan, Min Yi, Hankui Zhang, Meifang Zhao, and Yu Zhu. 2021. "Influence of Landscape Features on Urban Land Surface Temperature: Scale and Neighborhood Effects." *Science of The Total Environment* 771:145381. doi: 10.1016/j.scitotenv.2021.145381.

Small, An Overview of Urban Spectral Diversity Christopher. 2009. "The Color of Cities." in *Global Mapping of Human Settlement*. CRC Press.

Steadman, R. G. 1979. "The Assessment of Sultriness. Part II: Effects of Wind, Extra Radiation and Barometric Pressure on Apparent Temperature." *Journal of Applied Meteorology* 18:874–85. doi: 10.1175/1520-0450(1979)018<0874:TAOSPI>2.0.CO;2.

Stewart, I. D. 2011. "A Systematic Review and Scientific Critique of Methodology in Modern Urban Heat Island Literature." *International Journal of Climatology* 31(2):200–217. doi: 10.1002/joc.2141.

Stewart, Iain D. 2019. "Why Should Urban Heat Island Researchers Study History?" *Urban Climate* 30:100484. doi: 10.1016/j.uclim.2019.100484.

Tan, Jianguo, Youfei Zheng, Xu Tang, Changyi Guo, Liping Li, Guixiang Song, Xinrong Zhen, Dong Yuan, Adam J. Kalkstein, Furong Li, and Heng Chen. 2010. "The Urban Heat Island and Its Impact on Heat Waves and Human Health in Shanghai." *International Journal of Biometeorology* 54(1):75–84. doi: 10.1007/s00484-009-0256-x.

Ulpiani, Giulia. 2021. "On the Linkage between Urban Heat Island and Urban Pollution Island: Three-Decade Literature Review towards a Conceptual Framework." *Science of The Total Environment* 751:141727. doi: 10.1016/j.scitotenv.2020.141727.

United Nations. 2018. *The World's Cities in 2018*. UN.

Ward, Kathrin, Steffen Lauf, Birgit Kleinschmit, and Wilfried Endlicher. 2016. "Heat Waves and Urban Heat Islands in Europe: A Review of Relevant Drivers." *Science of the Total Environment* 569:527–39. doi: 10.1016/j.scitotenv.2016.06.119.

Wickham, Hadley. 2016. *Ggplot2: Elegant Graphics for Data Analysis*. 2nd ed. 2016. Cham: Springer International Publishing : Imprint: Springer.

Yang, Chen, and Shuqing Zhao. 2022. "A Building Height Dataset across China in 2017 Estimated by the Spatially-Informed Approach." *Scientific Data* 9(1):76.

Zhou, D., S. Zhao, S. Liu, L. Zhang, and C. Zhu. 2014. "Surface Urban Heat Island in China's 32 Major Cities: Spatial Patterns and Drivers." *Remote Sensing of Environment* 152:51–61. doi: 10.1016/j.rse.2014.05.017.

Zhou, Decheng, Jingfeng Xiao, Stefania Bonafoni, Christian Berger, Kaveh Deilami, Yuyu Zhou, Steve Frolking, Rui Yao, Zhi Qiao, and Jose A. Sobrino. 2019. "Satellite Remote Sensing of Surface Urban Heat Islands: Progress, Challenges, and Perspectives." *Remote Sensing*

11(1):48. doi: 10.3390/rs11010048.

Zhou, Y., H. Zhao, S. Mao, G. Zhang, Y. Jin, Y. Luo, W. Huo, Z. Pan, P. An, and F. Lun. 2022. “Exploring Surface Urban Heat Island (SUHI) Intensity and Its Implications Based on Urban 3D Neighborhood Metrics: An Investigation of 57 Chinese Cities.” *Science of the Total Environment* 847. doi: 10.1016/j.scitotenv.2022.157662.

Exploring the non-linear impacts of urban features on land surface temperature using Explainable Artificial Intelligence

Fei Feng[1], Yaxue Ren[2], Chengyang Xu[1], Baoquan Jia[3], Shengbiao Wu[4],

Raffaele Lafortezza[2,1*]

1. Research Centre of Urban Forestry, Key Laboratory for Silviculture and Forest Ecosystem of State Forestry and Grassland Administration, Beijing Forestry University, Beijing 100083, China
2. Department of Soil, Plant and Food Sciences, University of Bari Aldo Moro, Via Amendola 165/A 70126 Bari, Italy
3. Research Institute of Forestry, Chinese Academy of Forestry, Beijing 100091, China
4. Future Urbanity & Sustainable Environment (FUSE) Lab, Division of Landscape Architecture, Department of Architecture, Faculty of Architecture, The University of Hong Kong, Hong Kong SAR

[*] Corresponding author:
Raffaele Lafortezza, PhD
Department of Soil, Plant and Food Sciences (Di.S.S.P.A.)
University of Bari Aldo Moro
Via Amendola 165/A 70126 Bari, Italy
E-mail: raffaele.lafortezza@uniba.it

Abstract

High land surface temperatures (LST) have emerged as crucial threats to urban ecosystems and sustainable urban development. To better understand and mitigate their impacts, it is essential to analyze the contributing urban features. Against this background, we developed a random forest model enhanced by Explainable Artificial Intelligence (XAI) to analyze the impact features of LST in Beijing, China. By applying the XAI method, our results suggest that the major impact features of LST in Beijing are elevation (44.19%), compactness of impervious surface (17.27%), Normalized Difference Vegetation Index (11.12%), proportion of impervious surface area (8.04%), and tree height (3.83%). Compactness of impervious surface exhibited an overall cooling effect, which became weaker at high values. LST increased with building height, and the trend became weaker as building height reached 5 m. The most important features impacting LST in the inner city are the proportion and height of buildings, whereas in the outer city these features are tree height and the compactness of impervious surfaces. The study applies XAI to explain the non-linear interactions between LST and urban features, offering innovative insights to policy-makers to develop sustainable urban planning strategies. Our findings suggest that increasing green spaces and water bodies as well as controlling building density and height can effectively mitigate heat in dense urban areas and enhance cooling effects.

Keywords: Urbanization impact, LST, Building structure, Urban vegetation, Urban climate research

1. Introduction

The rapid pace of urbanization has given rise to substantial alterations in land surface attributes, thereby disrupting the thermal equilibrium of urban structures and triggering a noticeable escalation

in temperatures within urban environments (Kalnay and Cai, 2003; Dadashpoor et al., 2019). As the primary sources of anthropogenic heat and greenhouse gas emissions (Zhou et al., 2023), compact urban environments are associated with high land surface temperature (LST) (Won and Jung, 2023). While many studies have explored the impact of environmental factors on LST (Estoque et al., 2017; Norton et al., 2015), gaps still exist in understanding these complex relationships. This comprehension is crucial for optimizing the urban structure and living environment.

Previous research has primarily focused on the impact that urban features exert on LST, including vegetation cover, water body size, land use, and artificial materials with high heat capacity and conductivity (e.g., concrete and waste heat emissions from different sources) (Chen et al., 2021; Ebrahimi et al., 2022; He et al., 2021). Further studies of urban features impacting LST have been conducted in Asia (Liu et al., 2021; Han et al., 2023; Zhang et al., 2023) Europe (Chen et al., 2022; Schwaab, 2022; Morrison et al., 2023), the Americas (Zhou et al., 2011; Zhang and Sun, 2019) and other global regions (Fahmy et al., 2023; Karami et al., 2023). A recent review (Kim and Brown, 2021) concludes that the primary factors influencing LST include meteorological elements and urban geometry aspects. These factors affect the urban thermal environment through processes of convection, conduction, and radiation. However, the interactions among these features have been relatively overlooked and are crucial for a comprehensive understanding of urban thermal dynamics.

Numerous models, including linear and non-linear models, have been employed in previous studies investigating LST. As in the studies by Logan et al. (2020) and Lu et al. (2023), linear regression models were used to analyze the relationship between LST and other variables. For example, from the negative correlation between NDVI and LST (Hong et al., 2007), the cooling effect of vegetation can be derived. However, these models often fall short in capturing the complex, non-linear relationships between LST and impact features. Conversely, non-linear models, including

machine learning algorithms, have demonstrated a remarkable ability to describe complex relationships(Li et al., 2023). These methods provide enhanced prediction capabilities, but are also prone to "black box" related issues which blur the understanding of their inner workings.

In response to these challenges, recent progress in Explainable Artificial Intelligence (XAI) has significantly facilitated the understanding of underlying physical mechanisms in AI-based models and provided global and fine-scale interpretation abilities of modeling behavior (Fleming et al., 2021; Gevaert, 2022; Gunning et al., 2019; McGovern et al., 2019). XAI introduces novel perspectives for the analysis of impact feature importance ranking and interpreting local effects, demonstrating its effectiveness in interpreting features of AI model (Fu et al., 2023). For instance, (Temenos et al., 2023) developed a convolutional neural network using Shapley additive explanation (SHAP) for land classification of remote sensing data and quantified the contributions of different spectral band values to the classification results. Huang et al. (2023) conducted a comparative analysis of different XAI models and found that SHAP explainable models outperformed other methods like LIME (local interpretable model-agnostic explanations) in predicting soil moisture based on the random forest model.

Nevertheless, a limited number of studies have reported the application of XAI techniques to investigate the relationship between LST and urban features (Kolevatova et al., 2021; Kim et al., 2023). Therefore, this study aimed to develop a machine learning model that employs XAI capability to quantify the contributions of different impact features to LST, using Beijing, China, as the site of analysis. The main objectives of this research are to: i) select the best model (between random forest and multiple linear regression) describing the impacts of urban features on LST; ii) to investigate the distribution of urban features impacting LST; iii) explain the non-linear interactions of each feature with LST and other features using the XAI method; and iv) analyze the contribution of the most

important features impacting LST in different thermal contexts.

This interdisciplinary study presents a novel approach for employing the XAI model as state-of-the-art technology to deepen our understanding of the mechanisms underlying the complex relationships between LST and urban features. This innovative methodology not only offers interpretable insights into how various urban elements contribute to LST variations but also underscores the necessity for systematic urban planning to mitigate the urban heat island effect. Applying our approach to Beijing's diverse urban landscape, this study fills a significant gap in urban climate research and sets a precedent for future studies to employ XAI in environmental science, enhancing both the precision and transparency of complex ecological models.

2. Materials and methods

2.1. Study area

As the world's largest developing country, China has experienced dramatic urban expansion since the reform of 1978 (Cai et al., 2020), and its capital city, Beijing, has ranked as one of the fastest growing in China, both economically and in size (Ding and Shi, 2013). Studying LST in Beijing helps to understand how urbanization impacts microclimates, which is crucial for urban planning and sustainable city development. Beijing is located on the northern edge of the North China Plain, with longitudes ranging from 115º25′ to 117º30′E and latitudes ranging from 39º28′ to 41º25′ N, near the Bohai Sea in the east, the Taihang Mountains in the west, and the Yanshan Mountains in the north. The landscape of Beijing is predominantly characterized by mountains and plains. The mountainous area is mainly distributed in the northwest, while the plain area is mostly distributed in the southeast, with an elevation generally 30 to 50 m above sea level. This latter area is also the most densely developed in Beijing, including the built-up areas of the city (**Fig. 1**).

The climate of Beijing is of the temperate, semi-humid continental monsoon type and features

four distinct seasons. The annual temperature is relatively moderate, with an average ranging from 10℃ to 12℃. The winter is cold and dry, with an average temperature of -4.7℃ in January, whereas the summer is hot and humid, registering an average temperature of 26℃ in July. The average annual precipitation level in Beijing is 626 mm, with approximately 80% concentrated in summer.

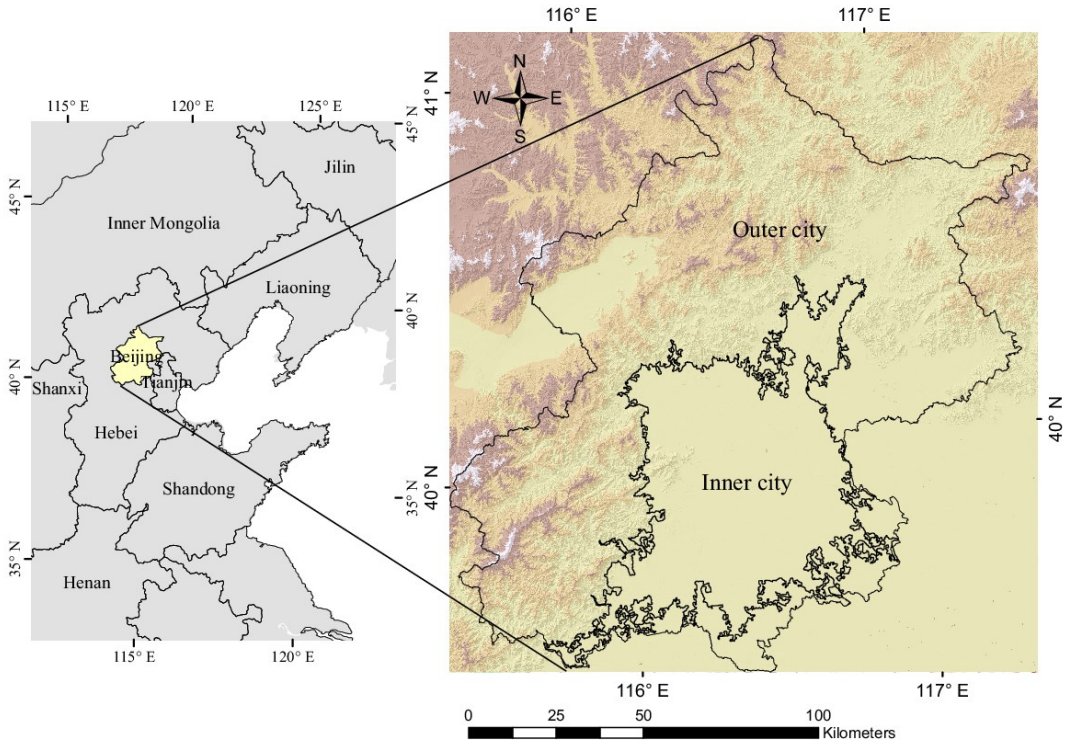

Fig. 1. Location map of the study area. The background map of Beijing (right) is a hillshade image generated from a digital elevation model.

2.2. Data

The boundaries of the city of Beijing were extracted using the 30-m global artificial impervious area (GAIA) and global urban boundary (GUB) (http://data.ess.tsinghua.edu.cn/gub.html) data (**Fig. 2a**). For a comprehensive analysis of LST impact features datasets for 2018 were used, including LST, DEM (digital elevation model), NDVI (Normalized Difference Vegetation Index), LC (land cover), TH (tree height), As_SoP (the proportion of area facing south on slopes) and BH (building height). The LST and NDVI data (**Fig. 2b, c**, respectively) from June to September in 2018 were derived from the Landsat 8 collection 2 dataset on Google Earth Engine, preprocessed to remove cloud-

contaminated pixels and corrected for atmospheric and geometric inconsistencies (Cook, 2014). DEM data (**Fig. 2d**) were derived from FABDEM (Copernicus digital elevation model, excluding forests and buildings), with buildings and forests removed using a machine learning model (Hawker et al., 2022), and were further used to calculate As_SoP. Land cover data (**Fig. 2e**) were obtained from the Landsat-based annual China land cover dataset (CLCD) and classified using the random forest model and spatial-temporal filtering method to enhance consistency (Yang and Huang, 2021). The Euclidean nearest-neighbor (ENN) distance data (**Fig. 2f**) were calculated using the Euclidean proximity index of impervious surfaces based on LC data. TH data (**Fig. 2g**) were extracted from the global forest height map, which was derived from the combination of the Global Ecosystem Dynamics Investigation (GEDI), a merged product of a regression tree ensemble model incorporating GEDI, LiDAR, and Landsat data, ensuring reliable forest height estimation (Potapov et al., 2021). BH data (**Fig. 2h**) were collected from the Global Human Settlement (GHS) dataset, processed through multi-scale convolutional, morphological, and textural transforms by merging ALOS World 3D, Shuttle Radar Topography Mission and Sentinel 2 composite data (Pesaresi et al., 2021), and validated against ground measurements in various cities to analyze 3D urban constructs. To integrate different data sources and conduct spatial analysis, all datasets were projected and resampled to ensure that they incorporated the same coordinate system and 30-m resolution.

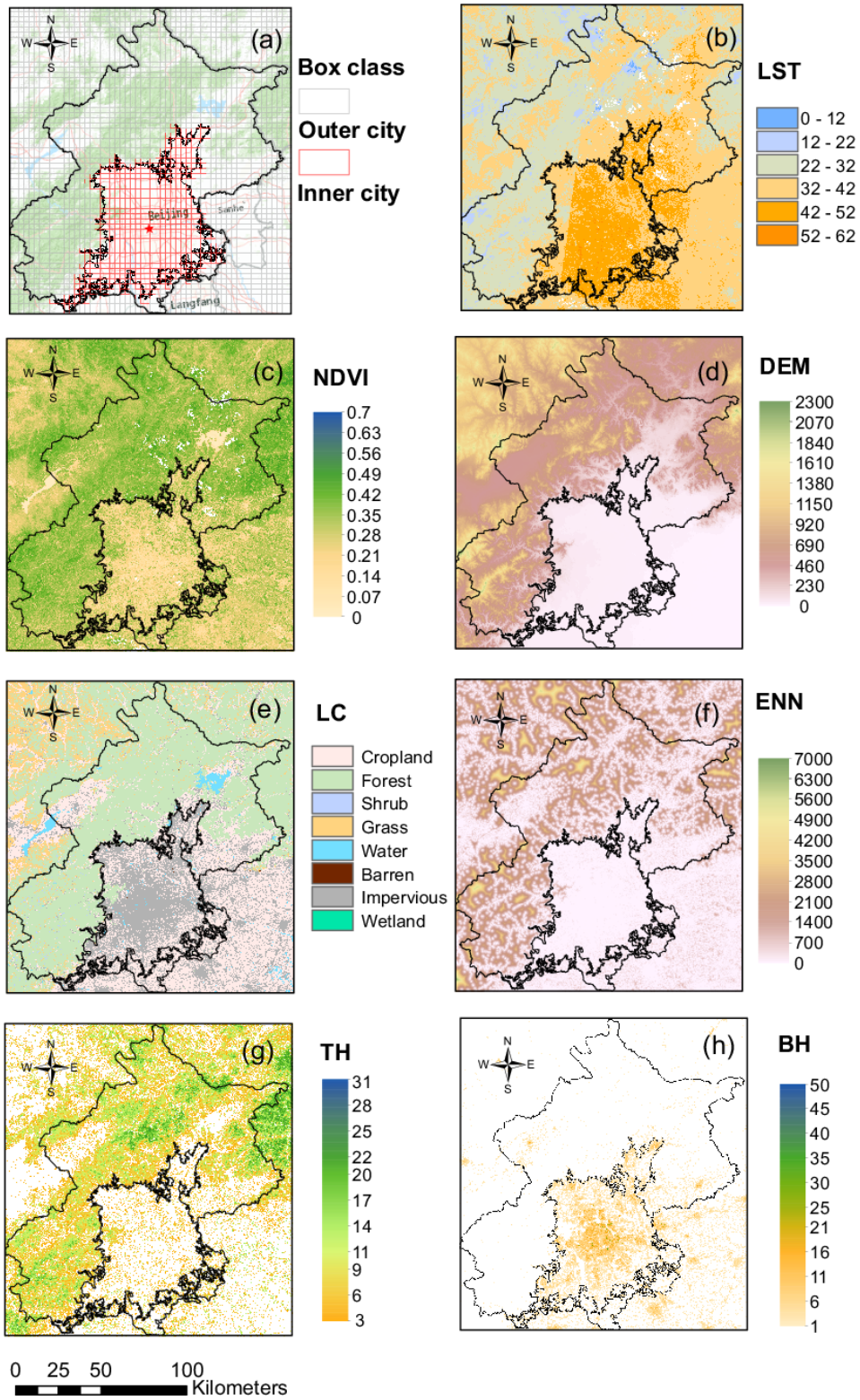

Fig. 2. Spatial distribution of the sample boxes LST, NDVI, DEM, LC, ENN, TH and BH in Beijing, China. (a) Boundary of inner and outer city. (b) LST, land surface temperature (unit: ℃); (c) NDVI, Normalized Difference Vegetation Index; (d) DEM, Digital Elevation Model (unit: m); (e) LC, land cover; (f) ENN, Euclidean nearest-neighbor (unit: m); (g) TH, tree height (unit: m); (h) BH, building height (unit: m).

Table 1. Summary of land surface temperature (LST) and impact feature datasets

Feature	Source	Spatial resolution	Types	References
LST	Landsat 8	100 m	Environmental	https://developers.google.com/earth-engine/datasets/catalog/LANDSAT_LC08_C02_T1_L2
WAT_P	CLCD	30 m	Environmental	https://zenodo.org/record/5816591
SHR_P	CLCD	30 m	Environmental	https://zenodo.org/record/5816591
GRA_P	CLCD	30 m	Environmental	https://zenodo.org/record/5816591
FOR_P	CLCD	30 m	Environmental	https://zenodo.org/record/5816591
CRO_P	CLCD	30 m	Environmental	https://zenodo.org/record/5816591
BAR_P	CLCD	30 m	Environmental	https://zenodo.org/record/5816591
NDVI	Landsat 8	30 m	Environmental	https://developers.google.com/earth-engine/datasets/catalog/LANDSAT_LC08_C02_T1_L2
TH	GEDI	30 m	Environmental	https://glad.umd.edu/dataset/gedi
DEM	FABDEM	30 m	Environmental	https://data.bris.ac.uk/data/dataset/25wfy0f9ukoge2gs7a5mqpq2j7
As_SoP	FABDEM	30 m	Environmental	Derived from DEM
IMP_P	CLCD	30 m	Anthropogenic	https://zenodo.org/record/5816592
ENN	CLCD	30 m	Anthropogenic	https://zenodo.org/record/5816591
BH	GHS	100 m	Anthropogenic	https://ghsl.jrc.ec.europa.eu/download.php?ds=builtH

WAT_P, proportion of water; SHR_P, proportion of shrub; GRA_P, proportion of grass; FOR_P, proportion of forest; CRO_P, proportion of cropland; BAR_P, proportion of barren; As_SoP, of area facing south on the slope; IMP_P, proportion of impervious; CLCD, China Land Cover Dataset; GEDI, Global Ecosystem Dynamics Investigation; FABDEM, digital elevation model excluding forests and buildings; GHS, Global Human Settlement. (See Fig. 2 for other acronyms of features)

2.3. Methodology

2.3.1 Random forest model

This study aims to quantify the contributions of different impact features to LST in both the inner city and outer city areas of Beijing by applying XAI in constructing a random forest (RF) model (**Fig. 3**). LST is the dependent variable, reflecting the key indicator of urban heat environment. Independent variables, including NDVI, LC, ENN, DEM, As_SoP, TH, and BH, were chosen due to their associations with regulating urban heat environment.

The main steps of the data analysis include: (1) Data collection and preprocessing: all data were uniformly projected and resampled to 30-m resolution; invalid values were removed. (2) Feature values extraction: A 3x3 km grid was created within the study area to extract the average values of influencing factors in each grid cell. (3) Model development: The RF model was used to predict LST and compared with traditional multiple linear regression (MLR) models. (4) Model results: The SHAP method was applied to explain the non-linear impacts of each feature in model predictions (**Fig. 3**).

Firstly, the 3x3 km grid was created using ArcGIS covering all the administrative boundaries of Beijing with individual boxes having a side length of 3 km. For each box the mean values were extracted for LST, NDVI, DEM, LC, ENN, TH, BH, and the proportion of each land use type. A total of 3416 sample boxes were detected in the entire study area, 674 of which were considered as inner city boxes and the remaining as outer city boxes.

Secondly, we built a RF model and a MLR model based on the impact feature data obtained above to compare their performances. MLR is a classical statistical method used to model the relationship between a dependent variable and multiple independent variables. The RF model was finally selected for its superior performance. Eighty percent of the dataset was employed as the training set, while 20% was randomly selected as validation data. To ensure the stability of the RF model, we conducted 100 cross-validation iterations to make it stable and defined hyperparametric grids for tuning. Specifically, GridSearchCV was used to optimize the maximum number of decision trees and the number of split features (optimized parameters: 500 estimators, max.10 features).

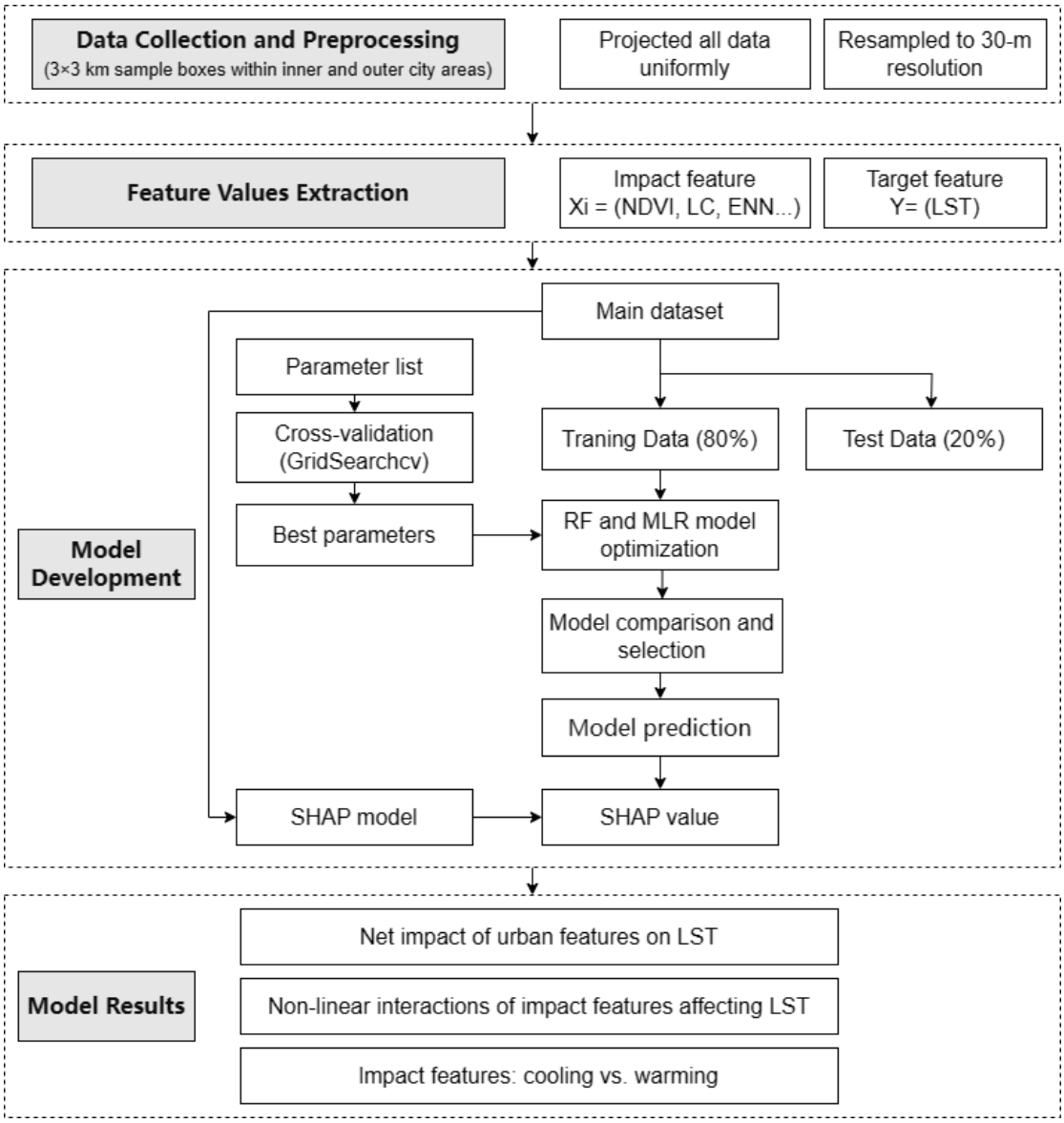

Fig. 3. Flowchart of the data analysis process.

2.3.2 SHAP interpretation for LST prediction

Although the RF model has advantages in processing high-dimensional data, reducing overfitting risks, evaluating feature importance, and parallel computing, its interpretability is far inferior to traditional MLR models, which are subject to AI black box problems of machine learning (McGovern et al., 2019). Therefore, the SHAP method was applied to solve this issue and visualize the non-linear impact between LST and impact features. The basic theory of SHAP, referred to as the Shapely value method proposed by Shapley (1952) , has been employed in the field of cooperative games with the aim to solve conflicts. The Shapley value is calculated based on the marginal contribution of the members to the alliance, which has the advantage that the benefits shared by the

members are equal to the average of the marginal benefits they create for their participating alliance. The specific formula is as follows:

$$\delta_i(v) = \sum_{K \epsilon N} \frac{[(|K|-1)!\,(n-|K|)!]}{n!} \times [v(K) - v(K(i))]$$

$$Zi = Z_b + h(x_{i1}) + h(x_{i2}) \ldots + h(x_{ij})$$

In a cooperative game system, the variable n represents the total number of players, and N is the set of members (1, 2, ..., n). K is a subset of N that consists of different players. The benefits of the alliance S are represented by $v(K)$, while $\delta_i(v)$ indicates the benefits obtained by player i in the alliance K. The number of players in the alliance K is denoted by $|K|$. $n!$ signifies the factorial of n. $S(i)$ represents the set obtained after removing player i from K. The marginal contribution of member i participating in different alliances, K, is expressed as $[v(K) - v(K(i))]$. The weight of the benefits created by member i in the entire alliance is denoted as $[(|K|-1)!(n-|K|)!]n!$. Zi represents the predicted value of the i-th sample. Z_b refers to the RF model's baseline, and $h(xij)$ represents the contribution of the j-th feature of the i-th sample to the final prediction of LST.

The SHAP value is an additional feature attribution method that interprets the predicted values of the model as the sum of attribution values for each input feature. Therefore, the positive or negative SHAP values (x_{ij}) express the specific impact of different features in the study area in the prediction of LST.

3. Results

3.1 Comparison between the random forest and multiple linear regression model

The relationship between LST and impact features was not a simple linear one, as can be seen in **Figure 4**. In the scatter plot, the x-axis represents the observed LST values, and the y-axis represents the LST predicted by the models. The high R^2 value of the RF model (0.89 vs 0.83) indicates that it could more precisely explain the relationship between LST and impact features. The RF model exhibited smaller RMSE (2.10 vs 2.65) and negative biases (-0.035 vs -0.056), indicating that it could predict LST more accurately. Taken together, the RF model was generally superior to the MLR model. Therefore, it was used in this study to capture the complexity of non-linear relationships

between LST and impact features given the ability to outperform other models.

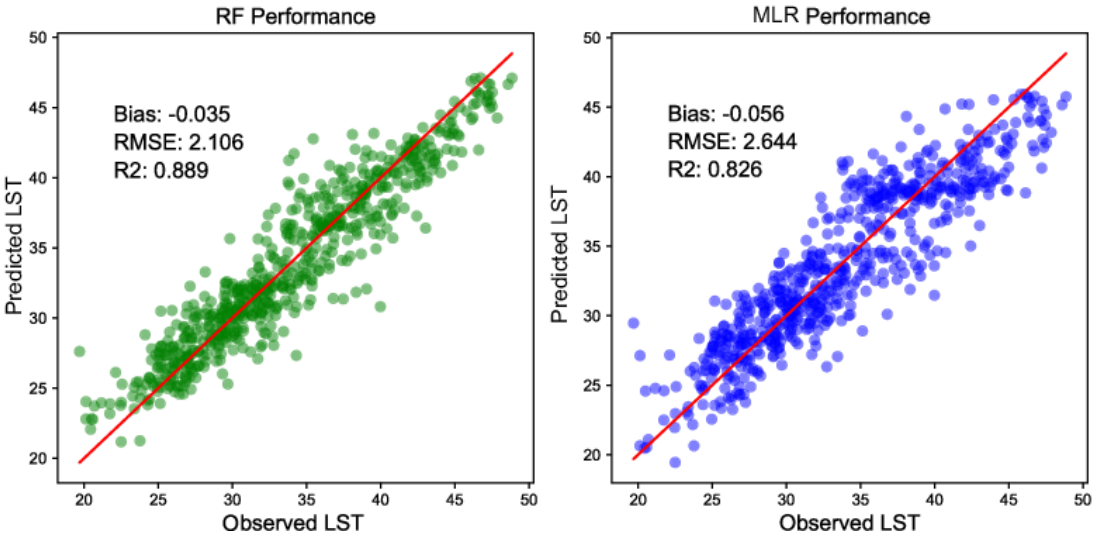

Fig. 4. Validation of the random forest (RF) model and multiple model linear regression (MLR). LST, land surface temperature; R^2, coefficient of determination; RMSE, root mean square error.

3.2 Distribution of urban features impacting LST in the study area

As shown in **Figure 5**, the features affecting LST were arranged according to importance in descending order from top to bottom. The y-axis shows the different impact features and the x-axis displays each sample's SHAP value, with red indicating a positive impact (warming) and blue a negative impact (cooling). For each feature, sample points were stacked vertically; the greater the height of the y-axis, the more samples were distributed. We calculated and visualized the SHAP values of the features for all boxes (**Fig. 5a**), inner city (**Fig. 5b**), and outer city (**Fig. 5c**) boxes to analyze their impact on LST by comparing and sorting the absolute SHAP values (**Table 2**). Overall, the mean value of DEM (DEM_MEAN, 44.19%), ENN (ENN_MEAN, 17.27%), NDVI (NDVI_MEAN, 11.12%), the proportion of IMP (IMP_P, 8.04%), and the mean value of TH (TH_MEAN, 3.83%) were the most important features affecting LST (**Fig. 5a**). Undoubtedly, the LST changes were mainly impacted by the local landscape and closely related to the compactness of urban buildings. The impact of IMP_P and BH_MEAN on LST was greater in inner cities (**Fig. 5b**) compared to all boxes (**Fig. 5a**), while the impact of TH_MEAN on LST was greater in outer cities (**Fig. 5c**).

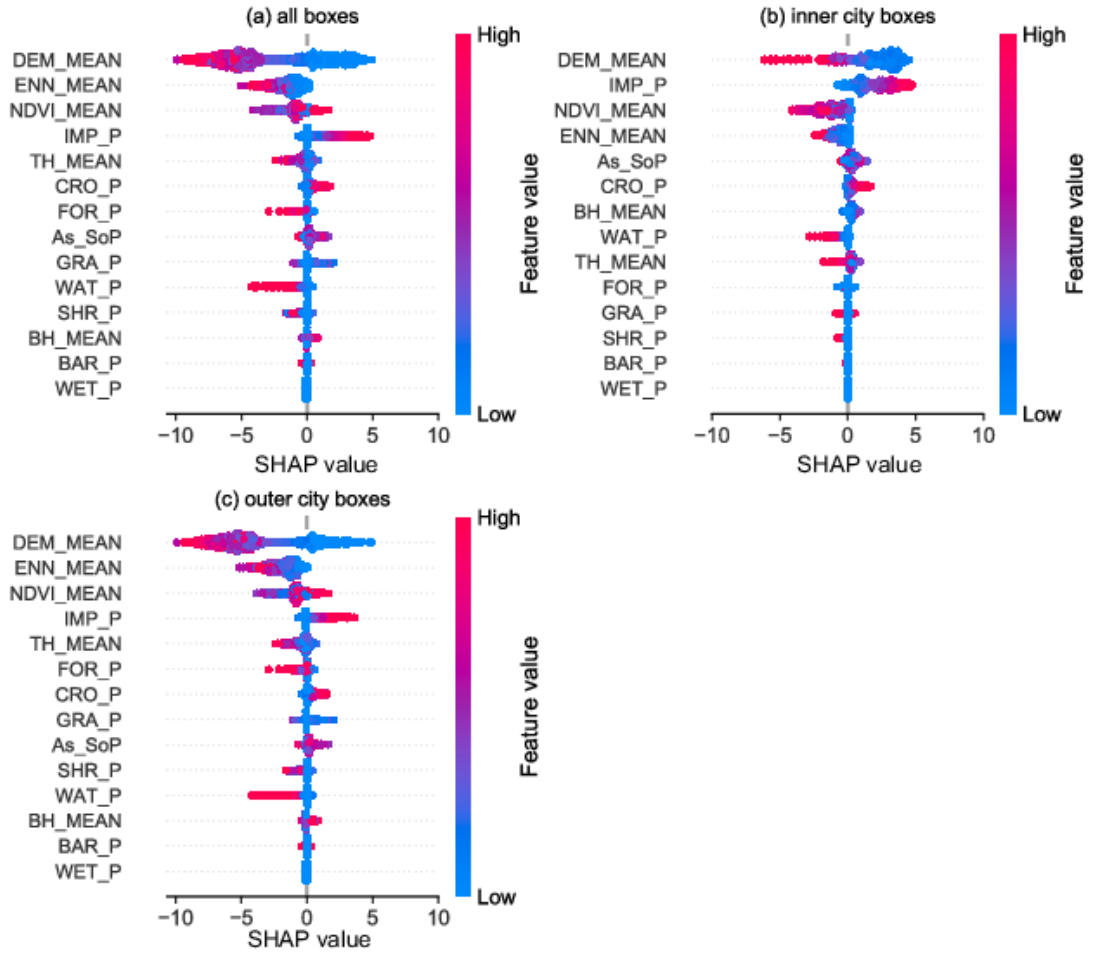

Fig 5. Contribution of features of the random forest model for (a) all boxes, (b) inner city boxes and (c) outer city boxes. The SHAP value expresses the specific impact of different features on land surface temperature. DEM, digital elevation model; ENN, Euclidean nearest-neighbor; NDVI, Normalized Difference Vegetation Index; TH, tree height; BH, building height; IMP, impervious surface area; CRO, cropland area; FOR, forest area; As_SoP, proportion of area facing south on the slope; GRA, grassland area; WAT, water bodies; SHR, shrubland; BAR, barren land; and WET, wetland.

Table 2. The net impact of urban features on land surface temperature.

Features	All boxes	Inner city boxes	Outer city boxes
DEM_MEAN	44.19	29.76	47.30
ENN_MEAN	17.27	8.90	19.07
NDVI_MEAN	11.12	14.75	10.33
IMP_P	8.04	26.44	4.07
TH_MEAN	3.83	2.85	4.04
BH_MEAN	1.38	3.34	0.95
CRO_P	3.19	4.27	2.95
FOR_P	3.06	1.55	3.38
As_SoP	2.61	4.86	2.13
GRA_P	1.99	0.30	2.36
WAT_P	1.90	2.86	1.69
SHR_P	1.41	0.09	1.70
BAR_P	0.02	0.02	0.02
WET_P	0.00	0.00	0.00

* The net impact of each feature is determined by its average SHAP value.
** For acronym definitions the reader is referred to **Figure 2**.

3.3 Non-linear interactions of impact features with LST and other features

3.3.1 Interactions of IMP_P, ENN, and BH with LST and other features

Anthropogenic features, including IMP_P, ENN_MEAN, and BH_MEAN, were selected to analyze their interactions with LST and other features across all sample boxes (**Fig. 6**). These impact features were closely related to the composition and configuration of the urban landscape. IMP_P generally showed a warming effect on LST, and as IMP_P increased the warming effect also increased in an almost linear pattern. In addition, we observed interactions between IMP_P and environmental features that influence LST, including NDVI_MEAN, TH_MEAN, FOR_P, and WAT_P. Specifically, when IMP_P was low and the impacts of these environmental features were large, then the warming effect of IMP_P was mitigated (**Fig. 6b-e**). This suggests that the presence of vegetation, forests, and water bodies can counteract the heat-retaining capacity of impervious surfaces, consistent with findings from other studies (Beaumont et al., 2022; Norton et al., 2015). As IMP_P increased, BH_MEAN also increased (**Fig. 6d**); this led to a stronger warming effect on LST.

ENN_MEAN, a measure of the spatial compactness of impervious surfaces, generally showed a negative (cooling) effect on LST. When the ENN_MEAN increased, environmental features such as NDVI_MEAN and TH_MEAN increased as well and the cooling effect became stronger (**Fig. 6g, h**), indicating a synergistic relationship between urban greenery and surface cooling. Similar results were also found in the study by Zhao et al. (Zhao et al., 2020). As ENN_MEAN gradually increased, the cooling effect rate of ENN_MEAN gradually slowed down.

BH_MEAN, categorized as an urban structural feature, showed the opposite warming patterns on LST. When BH_MEAN was low, the warming effect rate rapidly increased as BH_MEAN increased. However, when the BH_MEAN was high (e.g., exceeded 5 m), the warming effect rate weakened and maintained a relatively high SHAP value ranging from 0.25 to 0.75 (**Fig. 6l-o**). This previous study also noted a plateau in the warming effect of BH on LST beyond a certain threshold (Wang and Xu, 2021). It is also worth noting the boundaries with SHAP values of 0. For example, in

Fig. 4 (m), SHAP values are negative in areas with low BH_MEAN and high TH_MEAN. This suggests that the driving effect on LST values is negative in these areas, implying that low building height and high tree height contribute to mitigating UHI effect.

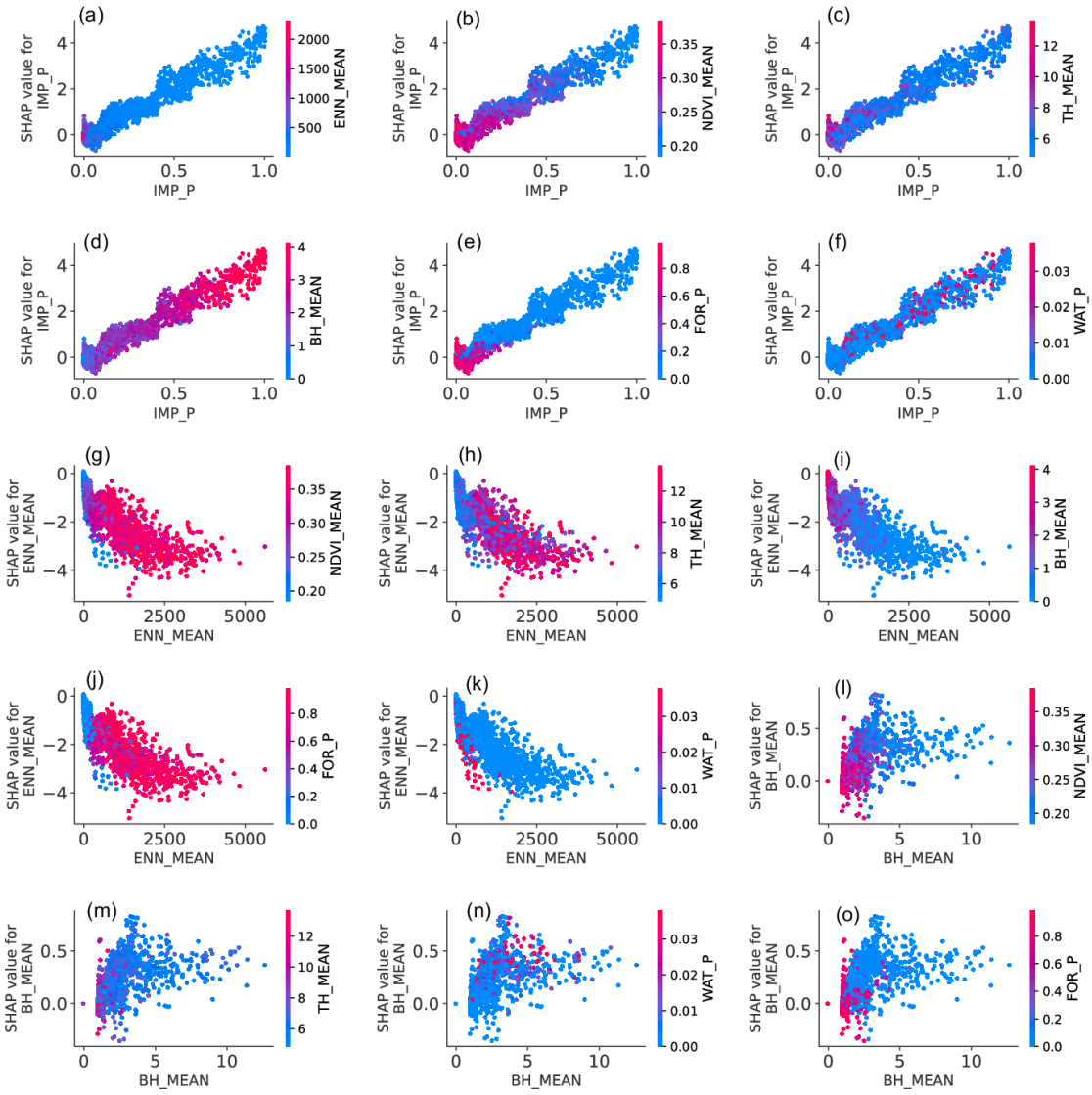

Fig 6. Dependence plot for interactions of IMP_P, ENN, and BH with land surface temperature and other features. The SHAP value expresses the specific impact of different features. The color of the dots from red to blue represent the value of the features, as shown by the bars on the right. (See **Fig. 2** and **Table 1** for acronym definitions)

3.3.2 Interactions of IMP_P, ENN, and BH with LST and other features across all samples, inner city and outer city samples

We further analyzed the interaction between different features across all samples, inner city samples, and outer city samples. For anthropogenic features, shown in **Figure 7**, when IMP_P increased, NDVI_MEAN showed a gradually decreasing trend (**Fig. 7a0-a2**). This suggests that a

higher IMP_P might have a negative impact on green space cover and vegetation growth, which are essential for temperature regulation through evapotranspiration and shading effects (Obiakor et al., 2012). In both the inner city and outer city samples, the interaction pattern between IMP_P and NDVI_MEAN appeared to be similar.

ENN_MEAN, which reflects the spatial distribution of impervious surfaces, influenced the urban cooling effect in a non-linear manner. For ENN_MEAN, as compactness increased, the cooling effect increased as well, but as compactness further increased (> 400 m for inner city boxes, > 2000 m for other boxes), the increase of the cooling effect tended to flatten out. As ENN_MEAN increased, NDVI_MEAN showed a gradually increasing trend. It is also worth noting that in the inner city samples (**Fig. 7c1**), ENN_MEAN was mainly concentrated in the range of <200 m, indicating that the layout of buildings in inner city areas was relatively compact.

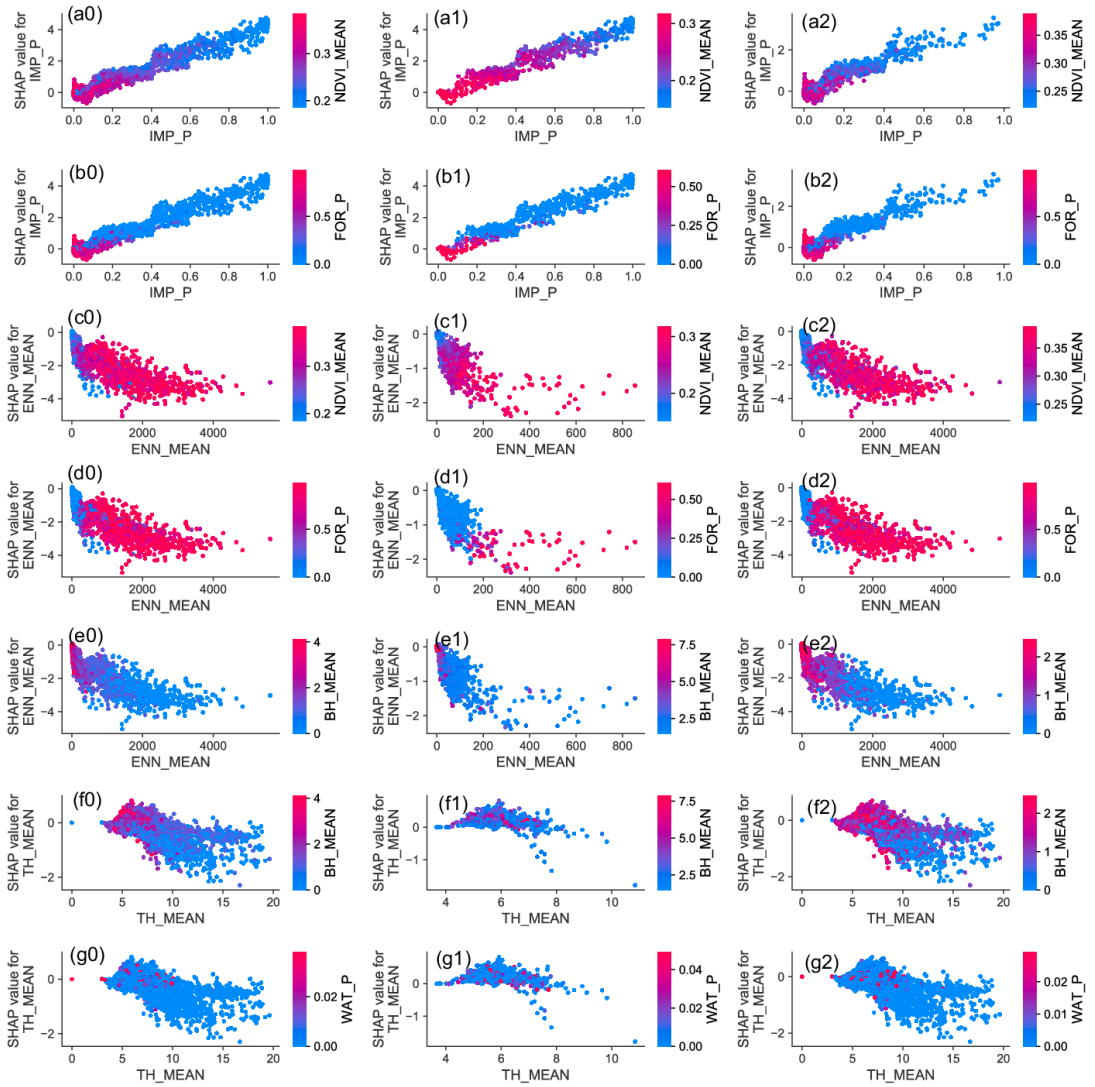

Fig. 7. Dependence plot for interactions of IMP_P, ENN, and BH with land surface temperature and other features across all samples, inner city samples, and outer city samples. The SHAP value expresses the specific impact of different features. The color of the dots from red to blue represent the value of the features, as shown by the bars on the right. (See **Fig. 2** and **Table 1** for acronym definitions)

3.4 Contribution of the most important features impacting LST in different thermal contexts

To compare and specifically explore the relationship between LST and impact features in different thermal contexts, fishnet box samples with LST of the 1st and 99th percentiles in the entire study area and 1st and 99th percentiles in the inner city area were counted and analyzed as four case studies, respectively. For the entire study area, **Fig. 8a** displays the features (i.e., IMP_P, DEM, and As_SoP) contributing the most positive effects (warming) to LST in hot samples (LST of the 99th percentile). Correspondingly, **Fig. 8b** illustrates the features (i.e., DEM_MEAN, ENN_MEAN, TH_MEAN, and FOR_P) contributing the most negative effects (cooling) to LST in cold samples

(LST of the 1st percentile). These findings suggest that elevation (DEM), the proportion (IMP_P) and compactness (ENN) of impervious surface area exerted a significant impact on LST from all data, including both cold and hot samples. The case studies of inner cities showed similar results. Notably, compared with the result of the entire study area where TH and FOR_P contributed to the cooling effect on LST (**Fig. 8b**), **Fig. 8d** shows that NDVI and WAT_P played a role in impacting the LST of inner cities.

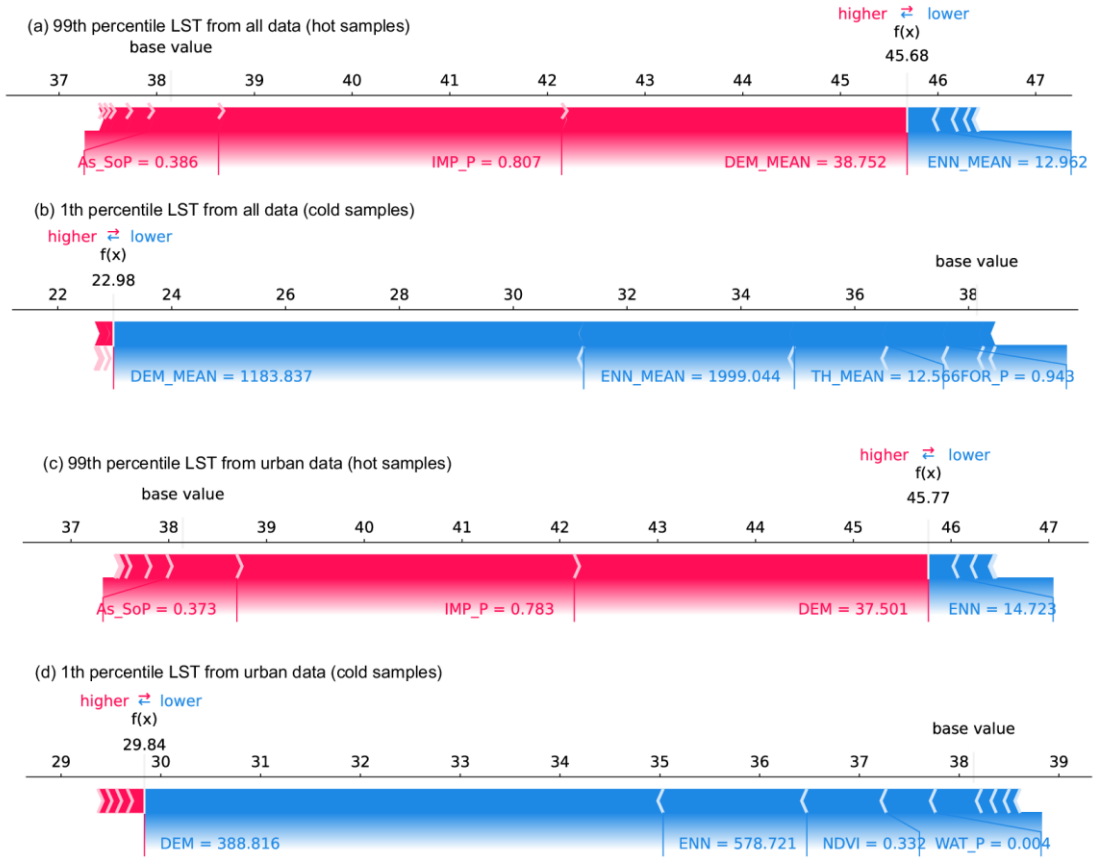

Fig. 8. Force plot of features that contributed the most to impacting LST in four case studies. The subplots (a) and (c) show the hot samples (LST of the 99th percentile) from all data and inner city data. The subplots (b) and (d) show the cold samples (LST of the 1st percentile) from all data and inner city data. The red bars represent the warming effect and blue bars the cooling effect. The length of the bar indicates impact intensity.

4. Discussion

4.1 Advantages of the XAI machine learning model

Linear regression models have been commonly applied to investigate the relationship between LST and its impact features (Aghazadeh et al., 2023; Zhang et al., 2021; D. Zhou et al., 2022a). For

example, five patch-level landscape metrics of green cover classes showed a significant relationship with LST based on the stepwise linear regression model (Asgarian et al., 2015). However, we found that the RF model outperformed the MLR model in predicting LST, demonstrating complex non-linear relationships between LST and impact features (Section 3.1). Although Wang et al. (2023) found that urban landscape components are strong explainers of LST in Beijing using linear spatial autocorrelation analysis, our results are consistent with those of Oukawa et al. (2022). These authors also compared the MLR model with the RF model and showed that MLR is only able to explain a modest percentage of variance in urban heat island intensity (64% and 34% for daytime and nighttime, respectively), while the RF model exhibited a superior performance with explanatory power over 96% of the variance for both daytime and nighttime conditions.

Moreover, the XAI machine learning model coupled with the RF model used in this study not only surpasses the traditional linear regression model, but also solves the transparency problem associated with machine learning methods. The XAI method employed in this study assigns a SHAP value to the features of each fishnet box, representing their contribution to LST in the RF model.

4.2 Relationship between LST and impact features

In this study, we explored the relationship between LST and its impact features in the study area of Beijing, China. Previous studies have shown that LST is closely influenced by urban landscape configurations, such as patch size, shape and land use type (Arnfield, 2003; Zhou et al., 2011; Jung et al., 2021). Our results show that DEM_MEAN, ENN_MEAN, NDVI_MEAN, and TH_MEAN were the most important features regulating LST in Beijing. An increase in DEM_MEAN had the greatest impact on the LST of the entire region and displayed a stronger cooling trend. The IMP_P and BH_MEAN contributed the most to increasing LST, while the ENN, NDVI and WAT_P were key features in reducing LST in urban areas. For all samples, including inner and outer cities, TH_MEAN and FOR_P were effective in decreasing LST. The study findings suggest that increasing green spaces and water bodies while reducing the compactness of buildings and properly controlling building

density and height could effectively decrease temperatures in urban areas.

Our results are consistent with those of previous studies demonstrating that water and vegetation contribute negatively to LST, whereas built-up areas contribute positively to LST (Zhang and Sun, 2019; Liu et al., 2021; Bala et al., 2021; Chen et al., 2022). Furthermore, we quantified the interactive effects and intensity of positive and negative contributions of these features. The interaction of features impacting LST revealed an inverse relationship between IMP_P and vegetation characteristics (TH, FOR_P), with a linear trend impact of IMP_P on LST. In comparison with previous studies that provide general patterns of landscape configurations(Zhang and Sun, 2019; L. Zhou et al., 2022b), our research more thoroughly demonstrates the non-linear interactions of impact features with LST and other features. For example, urban areas with low ENN were more likely to exhibit low TH and a weak cooling effect. Contrarily, urban areas with high ENN generally showed low BH and elevated TH with a strong cooling effect. The case studies further revealed that ENN plays a crucial role in regulating LST in both hot and cold samples.

4.3 Study implications and policy recommendations

Our study highlights the important cooling effect of environmental features such as vegetation and water bodies on LST. Therefore, urban planning policies should prioritize the preservation and expansion of existing green and blue spaces. With regard to anthropogenic features, our study reveals that building height positively correlates with LST, especially up to a height of 5 m, which suggests that tall buildings can provide shading effects in densely built areas. Consequently, it behooves policy-makers to promote the design of buildings that facilitate air circulation and reduce heat retention. By integrating these recommendations into urban planning and policy-making, cities can become more sustainable and thermally resilient environments.

4.4 Uncertainties and limitations

Uncertainties may arise from analyzing LST using satellite data. Considering the close relationship between solar radiation and daytime temperatures, Huang et al. (2016) reported that the sampling error within a 5×5-km^2 region was 1.4% for solar radiation in monthly time scales, which

suggests that uncertainties could be smaller for the LST results derived from the 3×3-km box used in this study. We also noticed that the feature data collected might contain uncertainties due to factors such as instrumentation, processing methods, misclassification and calibration (Schiavina et al., 2022; Yang and Huang, 2021). In this study we applied a SHAP method (based on fishnet boxes) to account for these potential uncertainties.

Variance inflation factor (VIF) is a standard metric for assessing multicollinearity in linear models. We calculated VIF values for each impact feature (**Appendix A, Table**), However, tree-based models like the RF model have low sensitivity to multicollinearity. The random sampling of features at each node creation helps reduce the effect of multicollinearity (Kurniati et al., 2023). All impact features were used due to the ability of the random forest model to effectively manage multicollinearity. Furthermore, we used the SHAP model by employing the Tree Explainer, and SHAP values do not assume feature independence (Aas et al., 2021).

Despite the presence of limitations, this study provides insight into the complex relationship between LST and various impact features. Future research endeavors could further investigate additional features that may contribute to variations in LST. In general, the findings from this research can help inform efforts to mitigate hot urban environments (e.g., urban heat islands).

5. Conclusions

The utilization of Explainable Artificial Intelligence (XAI) coupled with the RF model in this study provides a profound leap in understanding the non-linear relationships that govern LST. This capability not only surpasses that of traditional linear regression models but also addresses the transparency issues typically associated with machine learning methodologies, making our study results more interpretable and actionable. Our detailed analysis highlights the relevance of the compactness of impervious surfaces in mitigating urban LST, with decreasing compactness leading to a greater cooling effect when the Euclidean nearest-neighbor distance for impervious surface areas

ranges from 0 to 2000 m. These findings can equip policy-makers and urban planners with the data needed to implement strategies that effectively reduce LST, such as optimizing green space distribution and adjusting urban layout, ultimately contributing to the creation of thermally comfortable urban environments.

This study provides a more comprehensive understanding of how urban planning elements can modulate temperature. The complex non-linear interactions between LST and urban impact features emphasize the need for mitigating hot urban environments by designing new green space and water bodies while reducing impervious surfaces. From a practical standpoint, this work offers valuable insights and guidance to urban planners and policy-makers in their quest to build more sustainable and livable urban environments.

Acknowledgments

This study was funded by the Fundamental Research Funds for the Central Universities (BLX 202201) and carried out under the research project “CLEARING HOUSE - Collaborative Learning in Research, Information-sharing and Governance on How Urban tree-based solutions support Sino-European urban futures”, funded by the European Union’s Horizon 2020 Research and Innovation Program (Grant Agreement No. 821242). We would like to thank Yole DeBellis for revising the manuscript.

References

Aas, K., Jullum, M., Løland, A., 2021. Explaining individual predictions when features are dependent: More accurate approximations to Shapley values. Artif. Intell. 298, 103502. https://doi.org/10.1016/j.artint.2021.103502

Aghazadeh, F., Bageri, S., Garajeh, M.K., Ghasemi, M., Mahmodi, S., Khodadadi, E., Feizizadeh, B., 2023. Spatial-temporal analysis of day-night time SUHI and its relationship between urban land use, NDVI, and air pollutants in Tehran metropolis. Appl. Geomat. 15, 697–718. https://doi.org/10.1007/s12518-023-00515-w

Arnfield, A.J., 2003. Two decades of urban climate research: A review of turbulence, exchanges of energy and water, and the urban heat island. Int. J. Climatol. 23, 1–26. https://doi.org/10.1002/joc.859

Asgarian, A., Amiri, B.J., Sakieh, Y., 2015. Assessing the effect of green cover spatial patterns on

urban land surface temperature using landscape metrics approach. Urban Ecosyst. 18, 209–222. https://doi.org/10.1007/s11252-014-0387-7
Bala, R., Prasad, R., Yadav, V.P., 2021. Quantification of urban heat intensity with land use/land cover changes using Landsat satellite data over urban landscapes. Theor. Appl. Climatol. 145, 1–12. https://doi.org/10.1007/s00704-021-03610-3
Beaumont, B., Loozen, Y., Castin, T., Radoux, J., Wyard, C., Lauwaet, D., Lefebre, F., Halford, T., Haid, M., Defourny, P., Hallot, E., 2022. Green infrastructure planning through eo and gis analysis: The canopy plan of liège, belgium, to mitigate its urban heat island, in: ISPRS Annals of the Photogrammetry, Remote Sensing and Spatial Information Sciences. pp. 243–250. https://doi.org/10.5194/isprs-Annals-V-4-2022-243-2022
Cai, Z., Liu, Q., Cao, S., 2020. Real estate supports rapid development of China's urbanization. Land Use Policy 95, 104582. https://doi.org/10.1016/j.landusepol.2020.104582
Chen, J., Zhan, W., Jin, S., Han, W., Du, P., Xia, J., Lai, J., Li, J., Liu, Z., Li, L., Huang, F., Ding, H., 2021. Separate and combined impacts of building and tree on urban thermal environment from two- and three-dimensional perspectives. Build. Environ. 194, 107650. https://doi.org/10.1016/j.buildenv.2021.107650
Chen, S., Haase, D., Qureshi, S., Firozjaei, M.K., 2022. Integrated Land Use and Urban Function Impacts on Land Surface Temperature: Implications on Urban Heat Mitigation in Berlin with Eight-Type Spaces. Sustain. Cities Soc. 83, 103944. https://doi.org/10.1016/j.scs.2022.103944
Cook, M., 2014. Atmospheric Compensation for a Landsat Land Surface Temperature Product. Theses.
Dadashpoor, H., Azizi, P., Moghadasi, M., 2019. Land use change, urbanization, and change in landscape pattern in a metropolitan area. Sci. Total Environ. 655, 707–719. https://doi.org/10.1016/j.scitotenv.2018.11.267
Ding, H., Shi, W., 2013. Land-use/land-cover change and its influence on surface temperature: a case study in Beijing City. Int. J. Remote Sens. 34, 5503–5517. https://doi.org/10.1080/01431161.2013.792966
Ebrahimi, A., Motamedvaziri, B., Nazemosadat, S.M.J., Ahmadi, H., 2022. Investigating the land surface temperature reaction to the land cover patterns during three decades using landsat data. Int. J. Environ. Sci. Technol. 19, 159–172. https://doi.org/10.1007/s13762-021-03294-2
Estoque, R.C., Murayama, Y., Myint, S.W., 2017. Effects of landscape composition and pattern on land surface temperature: An urban heat island study in the megacities of Southeast Asia. Sci. Total Environ. 577, 349–359. https://doi.org/10.1016/j.scitotenv.2016.10.195
Fleming, S.W., Watson, J.R., Ellenson, A., Cannon, A.J., Vesselinov, V.C., 2021. Machine learning in Earth and environmental science requires education and research policy reforms. Nat. Geosci. 14, 878–880. https://doi.org/10.1038/s41561-021-00865-3
Fu, C., Huang, Z., Scheuer, B., Lin, J., Zhang, Y., 2023. Integration of dockless bike-sharing and metro: Prediction and explanation at origin-destination level. Sustain. Cities Soc. 99, 104906. https://doi.org/10.1016/j.scs.2023.104906
Gevaert, C.M., 2022. Explainable AI for earth observation: A review including societal and regulatory perspectives. Int. J. Appl. Earth Obs. Geoinformation 112, 102869. https://doi.org/10.1016/j.jag.2022.102869
Gunning, D., Stefik, M., Choi, J., Miller, T., Stumpf, S., Yang, G.-Z., 2019. XAI-Explainable artificial intelligence. Sci. Robot. 4, eaay7120. https://doi.org/10.1126/scirobotics.aay7120
Hamed Fahmy, A., Amin Abdelfatah, M., El-Fiky, G., 2023. Investigating land use land cover changes and their effects on land surface temperature and urban heat islands in Sharqiyah Governorate, Egypt. Egypt. J. Remote Sens. Space Sci. 26, 293–306. https://doi.org/10.1016/j.ejrs.2023.04.001
Han, L., Lu, L., Fu, P., Ren, C., Cai, M., Li, Q., 2023. Exploring the seasonality of surface urban heat islands using enhanced land surface temperature in a semi-arid city. Urban Clim. 49, 101455. https://doi.org/10.1016/j.uclim.2023.101455

Hawker, L., Uhe, P., Paulo, L., Sosa, J., Savage, J., Sampson, C., Neal, J., 2022. A 30 m global map of elevation with forests and buildings removed. Environ. Res. Lett. 17, 024016. https://doi.org/10.1088/1748-9326/ac4d4f

He, W., Cao, S., Du, M., Hu, D., Mo, Y., Liu, M., Zhao, J., Cao, Y., 2021. How Do Two- and Three-Dimensional Urban Structures Impact Seasonal Land Surface Temperatures at Various Spatial Scales? A Case Study for the Northern Part of Brooklyn, New York, USA. Remote Sens. 13, 3283. https://doi.org/10.3390/rs13163283

Hong, S., Lakshmi, V., Small, E.E., 2007. Relationship between Vegetation Biophysical Properties and Surface Temperature Using Multisensor Satellite Data. J. Clim. 20, 5593–5606. https://doi.org/10.1175/2007JCLI1294.1

Huang, F., Zhang, Yongkun, Zhang, Ye, Nourani, V., Li, Q., Li, L., Shangguan, W., 2023. Towards interpreting machine learning models for predicting soil moisture droughts. Environ. Res. Lett. 18, 074002. https://doi.org/10.1088/1748-9326/acdbe0

Huang, G., Li, X., Huang, C., Liu, S., Ma, Y., Chen, H., 2016. Representativeness errors of point-scale ground-based solar radiation measurements in the validation of remote sensing products. Remote Sens. Environ. 181, 198–206. https://doi.org/10.1016/j.rse.2016.04.001

Jung, M.C., Dyson, K., Alberti, M., 2021. Urban Landscape Heterogeneity Influences the Relationship between Tree Canopy and Land Surface Temperature. Urban For. Urban Green. 57, 126930. https://doi.org/10.1016/j.ufug.2020.126930

Kalnay, E., Cai, M., 2003. Impact of urbanization and land-use change on climate. Nature 423, 528–531. https://doi.org/10.1038/nature01675

Karami, P., Tavakoli, S., Esmaeili, M., 2023. Monitoring spatiotemporal impacts of changes in land surface temperature on near eastern fire salamander (Salamandra infraimmaculata) in the Middle East. Heliyon 9, e17241. https://doi.org/10.1016/j.heliyon.2023.e17241

Kim, M., Kim, D., Jin, D., Kim, G., 2023. Application of Explainable Artificial Intelligence (XAI) in Urban Growth Modeling: A Case Study of Seoul Metropolitan Area, Korea. Land 12, 420. https://doi.org/10.3390/land12020420

Kim, S.W., Brown, R.D., 2021. Urban heat island (UHI) intensity and magnitude estimations: A systematic literature review. Sci. Total Environ. 779, 146389. https://doi.org/10.1016/j.scitotenv.2021.146389

Kolevatova, A., Riegler, M.A., Cherubini, F., Hu, X., Hammer, H.L., 2021. Unraveling the Impact of Land Cover Changes on Climate Using Machine Learning and Explainable Artificial Intelligence. Big Data Cogn. Comput. 5, 55. https://doi.org/10.3390/bdcc5040055

Kurniati, B., Dewi, Y., Hadi, A., 2023. Handling Multicollinearity on Social Spatial Data Using Geographically Weighted Random Forest. SAR J. - Sci. Res. 149–153. https://doi.org/10.18421/SAR63-02

Li, F., Yigitcanlar, T., Nepal, M., Nguyen, K., Dur, F., 2023. Machine learning and remote sensing integration for leveraging urban sustainability: A review and framework. Sustain. Cities Soc. 96, 104653. https://doi.org/10.1016/j.scs.2023.104653

Liu, F., Hou, H., Murayama, Y., 2021. Spatial Interconnections of Land Surface Temperatures with Land Cover/Use: A Case Study of Tokyo. Remote Sens. 13, 610. https://doi.org/10.3390/rs13040610

Logan, T.M., Zaitchik, B., Guikema, S., Nisbet, A., 2020. Night and day: The influence and relative importance of urban characteristics on remotely sensed land surface temperature. Remote Sens. Environ. 247, 111861. https://doi.org/10.1016/j.rse.2020.111861

Lu, L., Fu, P., Dewan, A., Li, Q., 2023. Contrasting determinants of land surface temperature in three megacities: Implications to cool tropical metropolitan regions. Sustain. Cities Soc. 92, 104505. https://doi.org/10.1016/j.scs.2023.104505

McGovern, A., Lagerquist, R., John Gagne, D., Jergensen, G.E., Elmore, K.L., Homeyer, C.R., Smith, T., 2019. Making the black box more transparent: Understanding the physical implications of machine learning. Bull. Am. Meteorol. Soc. 2175–2199.

https://doi.org/10.1175/BAMS-D-18-0195.1
Morrison, W., Grimmond, S., Kotthaus, S., 2023. Simulating satellite urban land surface temperatures: sensitivity to sensor view angle and assumed landscape complexity. Remote Sens. Environ. 293, 113579. https://doi.org/10.1016/j.rse.2023.113579
Norton, B.A., Coutts, A.M., Livesley, S.J., Harris, R.J., Hunter, A.M., Williams, N.S.G., 2015. Planning for cooler cities: A framework to prioritise green infrastructure to mitigate high temperatures in urban landscapes. Landsc. Urban Plan. 134, 127–138. https://doi.org/10.1016/j.landurbplan.2014.10.018
Obiakor, M.O., Ezeonyejiaku, C.D., Mogbo, T.C., 2012. Effects of Vegetated and Synthetic (Impervious) Surfaces on the Microclimate of Urban Area. J. Appl. Sci. Environ. Manag. 16, 85–94.
Oukawa, G.Y., Krecl, P., Targino, A.C., 2022. Fine-scale modeling of the urban heat island: A comparison of multiple linear regression and random forest approaches. Sci. Total Environ. 815. https://doi.org/10.1016/j.scitotenv.2021.152836
Pesaresi, M., Corbane, C., Ren, C., Edward, N., 2021. Generalized Vertical Components of built-up areas from global Digital Elevation Models by multi-scale linear regression modelling. PLOS ONE 16, e0244478. https://doi.org/10.1371/journal.pone.0244478
Potapov, P., Li, X., Hernandez-Serna, A., Tyukavina, A., Hansen, M.C., Kommareddy, A., Pickens, A., Turubanova, S., Tang, H., Silva, C.E., Armston, J., Dubayah, R., Blair, J.B., Hofton, M., 2021. Mapping global forest canopy height through integration of GEDI and Landsat data. Remote Sens. Environ. 253, 112165. https://doi.org/10.1016/j.rse.2020.112165
Schiavina, M., Melchiorri, M., Pesaresi, M., Panagiotis, P., Freire, S., Maffenini, L., Goch, K., Tommasi, P., Kemper, T., 2022. GHSL Data Package 2022. https://doi.org/10.2760/19817
Schwaab, J., 2022. Sprawl or compactness? How urban form influences urban surface temperatures in Europe. City Environ. Interact. 16, 100091. https://doi.org/10.1016/j.cacint.2022.100091
Shapley, L.S., 1952. A Value for N-Person Games. RAND Corporation.
Temenos, A., Temenos, N., Kaselimi, M., Doulamis, A., Doulamis, N., 2023. Interpretable Deep Learning Framework for Land Use and Land Cover Classification in Remote Sensing Using SHAP. IEEE Geosci. Remote Sens. Lett. 20, 1–5. https://doi.org/10.1109/LGRS.2023.3251652
Wang, M., Xu, H., 2021. The impact of building height on urban thermal environment in summer: A case study of Chinese megacities. PLOS ONE 16, e0247786. https://doi.org/10.1371/journal.pone.0247786
Wang, X., Zhang, Y., Yu, D., 2023. Exploring the Relationships between Land Surface Temperature and Its Influencing Factors Using Multisource Spatial Big Data: A Case Study in Beijing, China. Remote Sens. 15, 1783. https://doi.org/10.3390/rs15071783
Won, J., Jung, M.C., 2023. Does compact development mitigate urban thermal environments? Influences of smart growth principles on land surface temperatures in Los Angeles and Portland. Sustain. Cities Soc. 90, 104385. https://doi.org/10.1016/j.scs.2022.104385
Yang, J., Huang, X., 2021. The 30 m annual land cover dataset and its dynamics in China from 1990 to 2019. Earth Syst. Sci. Data 13, 3907–3925. https://doi.org/10.5194/essd-13-3907-2021
Zhang, Q., Wu, Z., Singh, V., Liu, C., 2021. Impacts of Spatial Configuration of Land Surface Features on Land Surface Temperature across Urban Agglomerations, China. Remote Sens. 13, 4008. https://doi.org/10.3390/rs13194008
Zhang, Y., Sun, L., 2019. Spatial-temporal impacts of urban land use land cover on land surface temperature: Case studies of two Canadian urban areas. Int. J. Appl. Earth Obs. Geoinformation 75, 171–181. https://doi.org/10.1016/j.jag.2018.10.005
Zhang, Z., Luan, W., Yang, J., Guo, A., Su, M., Tian, C., 2023. The influences of 2D/3D urban morphology on land surface temperature at the block scale in Chinese megacities. Urban Clim. 49, 101553. https://doi.org/10.1016/j.uclim.2023.101553
Zhao, J., Zhao, X., Liang, S., Zhou, T., Du, X., Xu, P., Wu, D., 2020. Assessing the thermal contributions of urban land cover types. Landsc. Urban Plan. 204, 103927.

https://doi.org/10.1016/j.landurbplan.2020.103927
Zhou, D., Xiao, J., Frolking, S., Zhang, L., Zhou, G., 2022. Urbanization Contributes Little to Global Warming but Substantially Intensifies Local and Regional Land Surface Warming. Earths Future 10, e2021EF002401. https://doi.org/10.1029/2021EF002401
Zhou, L., Yuan, B., Hu, F., Wei, C., Dang, X., Sun, D., 2022. Understanding the effects of 2D/3D urban morphology on land surface temperature based on local climate zones. Build. Environ. 208. https://doi.org/10.1016/j.buildenv.2021.108578
Zhou, W., Huang, G., Cadenasso, M.L., 2011. Does spatial configuration matter? Understanding the effects of land cover pattern on land surface temperature in urban landscapes. Landsc. Urban Plan. 102, 54–63. https://doi.org/10.1016/j.landurbplan.2011.03.009
Zhou, X., Huang, Z., Scheuer, B., Wang, H., Zhou, G., Liu, Y., 2023. High-resolution estimation of building energy consumption at the city level. Energy 275, 127476. https://doi.org/10.1016/j.energy.2023.127476

Understanding the coupling effect of multiple urban features on Land Surface Temperature in Europe

Yaxue Ren[1], Fei Feng[2], Mario Elia[1], Vincenzo Giannico[1], Giovanni Sanesi[1], Raffaele Lafortezza[1,2*]

1. Department of Soil, Plant and Food Sciences, University of Bari Aldo Moro, Via Amendola 165/A 70126 Bari, Italy

2. Research Centre of Urban Forestry, Key Laboratory for Silviculture and Forest Ecosystem of State Forestry and Grassland Administration, Beijing Forestry University, Beijing 100083, China

[*] Corresponding author:
Raffaele Lafortezza, PhD
Department of Soil, Plant and Food Sciences (Di.S.S.P.A.)
University of Bari Aldo Moro
Via Amendola 165/A 70126 Bari, Italy
E-mail: raffaele.lafortezza@uniba.it

Abstract

Cities in Europe are facing significant challenges as rising temperatures exacerbate health risks, energy consumption, and environmental degradation. This study investigates the multiple features affecting land surface temperature (LST) across 780 European cities, categorized into eight macro-regions. The methodology involved utilizing SHAP values to interpret the results of a Random Forest model that evaluated the impact of individual urban features on LST. Additionally, the Generalized Additive Model (GAM) was employed to explore non-linear relationships between key urban features and LST, offering a deeper understanding of how specific features influence urban temperatures. The results highlight the important cooling effects of ecological attributes like tree height and evapotranspiration, particularly in warmer regions (e.g., the Iberian Peninsula and Turkey). Conversely, urban structure elements like built-up volume were shown to increase LST. These results emphasize the complexity of urban climate regulation, where ecological and built environments interact in diverse ways across different regions. This study underscores the importance of region-specific urban planning strategies that integrate both ecological and urban structure features to effectively mitigate the effects of urban heat. The findings offer actionable insights for policymakers seeking to enhance urban climate resilience and manage the growing challenges posed by global warming in European cities.

Keywords: Shapley additive explanations, Generalized Additive Models, Land surface temperature, Urban structure, Urban landscape, Ecological attributes

1. Introduction

Urbanization has profoundly transformed the thermal environment of cities, creating significant challenges for sustainability and human well-being. As cities expand, the concentration of impervious surfaces, dense building structures, and anthropogenic heat emissions disrupts natural energy exchange processes (Grimm et al., 2008), leading to distinct thermal anomalies such as the urban heat island (UHI) effect (Chen et al., 2022; Han et al., 2022; Oke, 1973). Rising urban temperatures exacerbate public health risks (Tan et al., 2010), including heat-related illnesses, while also increasing energy demands for cooling (Donovan and Butry, 2009; Hirano and Fujita, 2012) and contributing to the degradation of air quality (Akbari et al., 2001; Tan et al., 2010). Moreover, urban areas in Europe often experience greater climate sensitivity due to the complex interplay between urbanization patterns and localized climatic conditions (Schwaab et al., 2021). Approximately 40% of the EU population lives in cities of at least 50,000 inhabitants (Dijkstra and Poelman, 2012) and the urban population experiences overall higher levels of temperature stress, particularly heat (Oleson et al., 2015). These factors highlight the urgency of understanding and mitigating the thermal impacts of urbanization in the European context.

The growing interest in land surface temperature (LST) has been aided by significant advancements in computing technology over the past two decades. Researchers have harnessed sophisticated techniques to gather LST and to delineate urban systems from a rich repository of historical satellite imagery that spans nearly half a century (Lafortezza and Giannico, 2019; Ren et al., 2023; Voogt and Oke, 2003). These technological strides have positioned LST replace air temperature as the focal point of research in the realm of large-scale UHI studies, encompassing continental or even global analyses. For this reason, we have chosen LST as the target feature of our investigation. The appeal of using remotely sensed data lies in its consistency across time and space, coupled with the advantage of accessing high-resolution satellite imagery at no cost (Li et al., 2019). These unique benefits have catalyzed the adoption of satellite data in comprehensive studies, enabling a deeper understanding of urban thermal dynamics on the continental scale (Angearu et al., 2022; Bird et al., 2022; Rehman et al., 2022).

Research on urban heat phenomena has increasingly explored the coupling effects of various urban features on the thermal environment (Fei et al., 2022; Ma and Peng, 2022). The impact of urbanization on the urban thermal environment is more dramatic than the impact of global climate change (Tam et al., 2015; Zhang et al., 2010). In particular, the extent of the built environment, population size and density, anthropogenic activities, and the socioeconomics of cities play a crucial role in leading to temperature increases in the urban area compared to the rural area (Han et al., 2022; Oke, 1976; Shahfahad et al., 2022). Conversely, vegetation can reduce urban temperatures through direct shade and evapotranspiration and create a localized island of coolness (Dong et al., 2022; Schwaab et al., 2021; Tyrväinen et al., 2005; Zhang et al., 2023). Therefore, increasing green and blue spaces in cities is widely recognized as an effective way to mitigate urban heat (Macháč et al., 2022; Shen et al., 2022).

Large-scale analyses have been instrumental in identifying general trends and drivers (Clinton and Gong, 2013; Mentaschi et al., 2022; Yang et al., 2023) of the urban thermal environment. For instance, Imhoff et al., (2010) investigated diurnal and seasonal variations in UHI intensity across major U.S. cities, while Zhou et al., (2018) examined satellite-based UHI patterns, globally, revealing the importance of vegetation and urban density. Despite these advancements, most studies focus on isolated drivers or regional patterns, neglecting the systemic nature of urban thermal dynamics. In Europe, where climatic, socioeconomic, and planning conditions vary significantly across regions, a more integrated approach is needed to address the spatial heterogeneity and coupling effects of urban features on LST.

Against this background, the overarching goal of the present study is to explain the coupling effect of multiple urban features in determining LST across Europe. The specific objectives are to: (1) investigate the combined effects of multiple features on LST; (2) determine which features contribute the most to warming and cooling effects; and (3) explore the non-linear impact of the most influencing features on LST.

The core hypothesis of our study hinges on the integrated design of urban environments, including strategic integration of vegetation and optimization of urban structure, and how these can significantly mitigate heat stress. Therefore, a detailed analysis of the coupling between LST and impact features can inform sustainable urban planning and policy development and encourage effective urban heat mitigation strategies in the face of climate change and increasing urban sprawl. Stakeholders will gain a more comprehensive perspective and deeper understanding of urban heat dynamics, equipping them with the knowledge necessary to address and mitigate the negative impacts of rising temperatures in the context of global warming and urban expansion. The study's findings are expected to underscore and demonstrate the importance of integrated urban structure, landscape and reduced heat stress in urban settings, thereby contributing to the creation of more livable and sustainable cities in Europe. The use of advanced machine learning techniques, combined with interpretable artificial intelligence tools, will enhance our understanding of the complex relationships between urban features and LST, paving the way for more effective urban climate resilience strategies.

2. Materials and Methods

The methodology used for the data analysis process comprises of three main phases: data collection and pre-processing, model development, and results interpretation, as shown in Figure 1. Initially, data on European cities were standardized to a 500-m resolution, encompassing variables of ecological attributes, urban structure, and landscape categories (Sections 2.2 and 2.3). In the phase of model development, a Random Forest (RF) model was trained to predict LST, with SHapley Additive exPlanation (SHAP) values providing insight on feature importance (Section 2.4), while a Generalized Additive Model (GAM) captured non-linear feature relationships (Section 2.5). Details

of each phase are provided in the following sections.

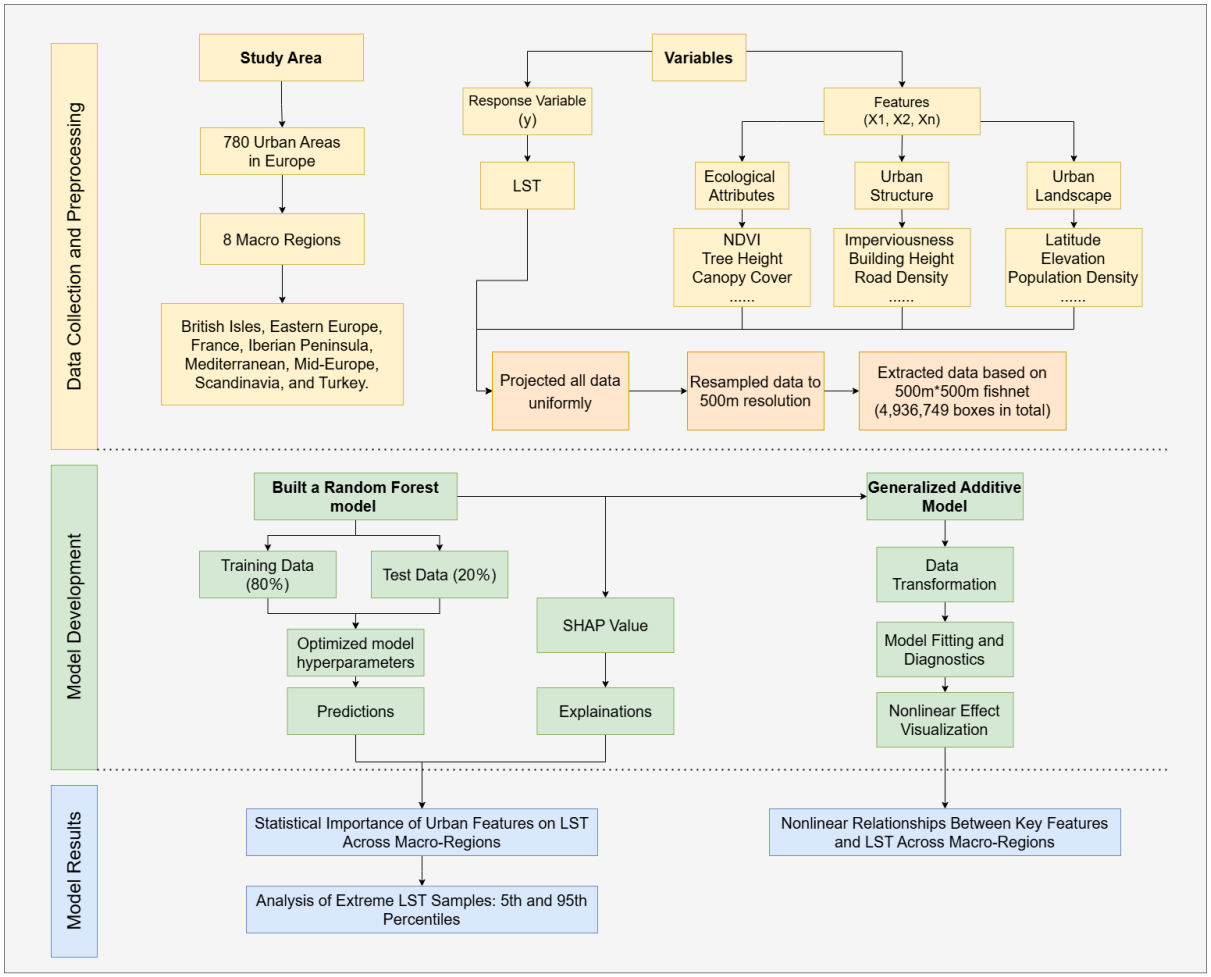

Fig. 1. Flowchart of the data analysis process. LST, land surface temperature; NDVI, Normalized Difference Vegetation Index.

2.1 Study Area

This study focuses on 780 cities across Europe (Figure 1), derived from the Urban Atlas dataset which provides comprehensive land cover and land use data. Initially, 788 Functional Urban Areas (FUAs) were included, but cities located on islands overseas were excluded, resulting in a final selection of 780 cities. These cities have been categorized into eight macro-regions based on geographical location which are the British Isles, Eastern Europe, France, the Iberian Peninsula, the Mediterranean, Mid-Europe, Scandinavia, and Turkey.

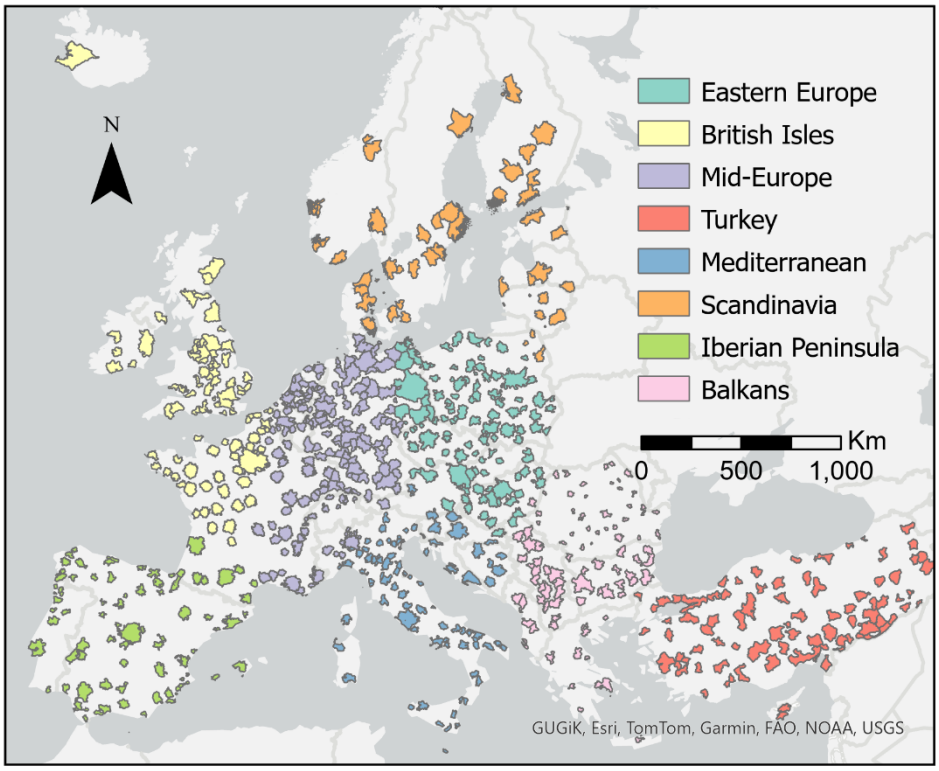

Fig. 2. Location map of the study area. European cities (N = 780) divided into eight macro-regions.

2.2 Data Collection

Multiple datasets from 2018 were used to comprehensively analyze the features affecting LST (Table 1). The data were extracted based on a 500-m x 500-m grid system to ensure spatial precision across all cities in the analysis. The features were categorized into three groups: Urban Landscape, Urban Structure, and Ecological Attributes.

The Urban Landscape group focuses on the geographic, topographic, and spatial characteristics that influence LST. In addition to latitude (Lat), longitude (Long), and elevation (DEM), this category includes distance to the sea (SEA_DIST), which accounts for the cooling effects of proximity to large bodies of water. Urban area (Area) was also included, as the size of a city impacts its capacity for heat absorption and dissipation.

The Urban Structure group represents man-made structures and socioeconomic factors. Built-up Height (BH) represents the vertical development of cities, which affects heat retention and dissipation, while Built-up Volume (BV) quantifies the total volume of urban structures, impacting

how cities trap and release heat. Population Density (PD) accounts for the concentration of people, which correlates with energy use and heat production. Electricity Consumption (EC) reflects the level of human activity and its associated heat emissions. Imperviousness Density (IMD) captures the extent of surfaces like concrete and asphalt, which retain more heat than natural landscapes. Road Density (RD) reflects the compactness of the urban layout, influencing heat distribution. Gross Domestic Product (GDP) is included as an economic indicator that reflects the wealth and development of the urban area, potentially influencing infrastructure and energy usage.

Ecological Attributes encompass both vegetation and water-related features that reflect the natural components of the urban environment. The Normalized Difference Vegetation Index (NDVI) represents the density and health of vegetation, while Tree Height (TH) provides a measure of vertical vegetation structure. Biomass (BIO) is included as a measure of total plant material. Water and Wetlands (WT) indicates the spatial extent of water bodies and wetlands. Tree Cover Density (TCD) quantifies the extent of tree cover in urban areas, whereas Small Woody Features (SWF) represents small patches of woodland areas. Additionally, Evapotranspiration (ET) accounts for the combined water loss from plants and soil.

Table 1. Summary of land surface temperature (LST) and impact feature datasets.

	Abbreviation	Feature	Resolution (m)
T1	LST_MEAN	Summer Mean Land Surface Temperature	30
UL1	Lat	Latitude	-
UL2	Long	Longitude	-
UL3	DEM	Elevation	30
UL4	SEA_DIST	Sea Distance	-
UL5	Area	Urban Area	10
US1	BH	Built-up Height	100
US2	BV	Built-up Volume	100
US3	PD	Population Density	100
US4	EC	Electricity Consumption	1000
US5	IMD	Imperviousness Density	10
US6	RD	Road Density	100
US7	GDP	Gross Domestic Product	1000
EA1	NDVI	Normalized Difference Vegetation Index	30
EA2	TH	Tree Height	10
EA3	BIO	Biomass	100
EA4	WT	Water and Wetlands	10
EA5	TCD	Tree Cover Density	10
EA6	SWF	Small Woody Features	10
EA7	ET	Evapotranspiration	30

T, Target features; UL, Urban Landscape; US, Urban Structure; EA, Ecological Attributes.

2.3 Data Processing

After downloading the datasets, all data were resampled to ensure consistency across the study, using a 500-m x 500-m grid. This ensured that all features were extracted at the same spatial scale for analysis. LST and NDVI data were obtained from the Collection 2 Landsat 8 products on Google Earth Engine. These datasets underwent preprocessing to remove cloud-contaminated pixels and were corrected for atmospheric and geometric inconsistencies, as outlined by Cook (2014). DEM data were sourced from the FABDEM (Forest And Buildings removed Copernicus DEM), which provides a global elevation map free from building and tree height biases (Hawker et al., 2022). The data were available at a 30-m resolution and licensed under a Creative Commons "CC BY-NC-SA 4.0" license. Built-up Height (BH), Built-up Volume (BV), and Population Density (PD) were sourced from the Global Human Settlement Layer (GHSL). The GHSL project (Schiavina et

al., 2022) provides global spatial information on human presence, using automated data analytics to extract information from diverse geospatial sources, including satellite imagery and census data. Electricity consumption (EC) and Gross Domestic Product (GDP) (Chen and Gao, 2021) were calculated using a top-down method based on nighttime light data. The nighttime light data were unified from DMSP/OLS and NPP/VIIRS images using a particle swarm optimization-back propagation (PSO-BP) algorithm, yielding continuous 1-km x 1-km gridded data for the 1992–2019 time period. These data served as proxies for economic growth and Electricity consumption. Tree Height (TH) data (Lang et al., 2023) were sourced from the ETH Global Sentinel-2 10-m Canopy Height dataset (2020). This dataset fuses GEDI and Sentinel-2 images to generate a global map of canopy height at 10-m resolution, reducing the saturation effect commonly encountered in canopy height estimation from satellite images. Evapotranspiration (ET) data were derived using the MOD16 approach (Hu et al., 2012), which estimates latent heat flux and converts it to equivalent evaporation using high-resolution meteorological data from TerraClimate (Abatzoglou et al., 2018), provided by the University of Idaho, USA. The latent heat flux, initially in W/m^2, was converted to mm/day for ET analysis.

The following datasets were provided by the Copernicus High-Resolution Layers and Urban Atlas projects, coordinated by the European Environment Agency (EEA) under the EU Copernicus program:

- Urban Atlas (EEA, 2020a): The source for city boundaries and urban areas (Area). Urban Atlas 2018 offers high-resolution, inter-comparable land use and land cover data for 788 FUAs with populations over 50,000, covering EEA38 countries and the United Kingdom.
- Water and Wetlands (WT) (EEA, 2020b): The Water and Wetness layer (WAW) shows the occurrence of water and wet surfaces from 2012 to 2018, with products defining classes of permanent/temporary water and wetness.

- Imperviousness Density (IMD) (EEA, 2020c): The Imperviousness Density product captures the percentage of sealed, artificial surfaces for the year 2018, with values ranging from 0% to 100% across the EEA38 countries and the United Kingdom.
- Small Woody Features (SWF) (EEA, 2023): The Small Woody Features layer detects small patches of linear and isolated woody elements, which are important for biodiversity and landscape fragmentation analysis.
- Tree Cover Density (TCD) (EEA, 2020d): The Tree Cover Density product provides proportional crown coverage per pixel at 10-m resolution, ranging from 0% to 100%, representing the vertical projection of tree crowns.

2.4 Random Forest and SHAP Value Analysis

The Random Forest (RF) model was employed to analyze the impact of various features on LST. RF is an ensemble learning technique that constructs multiple decision trees during training, and it outputs the average prediction from these trees for regression tasks. This model was chosen due to its ability to handle large datasets and capture complex interactions between features, making it suitable for spatial analysis across multiple urban and natural attributes. The RF model was trained on the dataset, using features grouped into Ecological Attributes, Urban Landscape, and Urban Structure, as described in the Data Collection section. By using this model, the influence of each feature on LST predictions could be analyzed across the cities included in the study.

To interpret the RF model's predictions, SHAP (SHapley Additive exPlanations) values were applied. SHAP provides a consistent and robust method for explaining individual predictions made by machine learning models. Specifically, SHAP deconstructs a prediction into the contributions made by each input feature. For every instance (i.e., grid cell in this study), SHAP quantifies how much each feature contributed to the final prediction of LST.

In the case of regression models, such as the RF model employed here, the output is a continuous prediction, such as LST values. SHAP assigns a value to each feature based on its contribution to that prediction. By summing the SHAP values of all features for a given instance, we can

reconstruct the predicted LST value and understand the relative importance of each feature in influencing temperature outcomes. SHAP was utilized to rank the importance of different features across all regions and to provide visual insights into how specific variables influenced LST at different scales. This approach allows for a more nuanced understanding of the spatial variation in temperature impacts across the dataset.

2.5 Generalized Additive Model Analysis

To further explore the impact of key features on LST across different regions, a Generalized Additive Model (GAM) was applied. GAM is a flexible extension of generalized linear models, allowing for the modeling of nonlinear relationships between the dependent variable (LST) and independent features while maintaining the interpretability of the model. This method is particularly useful in capturing complex, smooth relationships between the features and LST that may not be fully captured by linear models.

The key features selected for the GAM analysis were those identified as significant from the previous RF and SHAP value analyses. These included variables from Ecological Attributes, Urban Landscape, and Urban Structure categories. The GAM approach allowed to assess the nonlinear effects of variables such as Tree Height (TH), Imperviousness Density (IMD), Built-up Volume (BV), and Evapotranspiration (ET) on LST.

The model was fitted for each of the eight geographic regions separately to account for regional variations in the impact of these features. The flexibility of GAM enabled the analysis to capture the smooth interactions and variations in feature importance across different regions, providing a more nuanced understanding of how ecological and urban characteristics contribute to LST variations.

3. Results

3.1 Combined effects of urban features on LST across macro-regions in Europe

In Figure 3, the urban features influencing LST are ranked by importance in descending order from top to bottom. The x-axis displays SHAP values expressing the specific impact of different features on LST prediction. In all eight macro-regions across Europe (Fig. 3), the features in the Ecological

Attributes category, such as TH, ET, and TCD, consistently showed high importance ranking in regulating LST. In particular, TH and ET emerged as key features in the Mediterranean and Turkey macro-regions, where the presence of vegetation plays a critical role in cooling the environment. In contrast, features from the Urban Landscape category, such as Sea Distance (SEA_DIST), showed high importance ranking on LST in macro-regions like the Mediterranean and British Isles. Proximity to large bodies of water provided localized cooling effects, highlighting the influence of natural geographic factors on urban temperature dynamics. Lastly, features from the Urban Structure category, including IMD and BV, had the most pronounced influence on LST in Mid-Europe and the British Isles. These artificial surfaces contribute to elevated LST due to their heat-retention properties, which are particularly prominent in areas with high population densities and extensive urban infrastructure. Although features like PD and BH exerted more localized effects on LST, their influence varied depending on the specific urban layout and density in each macro-region. In essence, the distribution of feature importance across the macro-regions demonstrates that while Ecological Attributes features play a vital role in reducing LST, the Urban Structure and Landscape features also significantly modulate temperature dynamics.

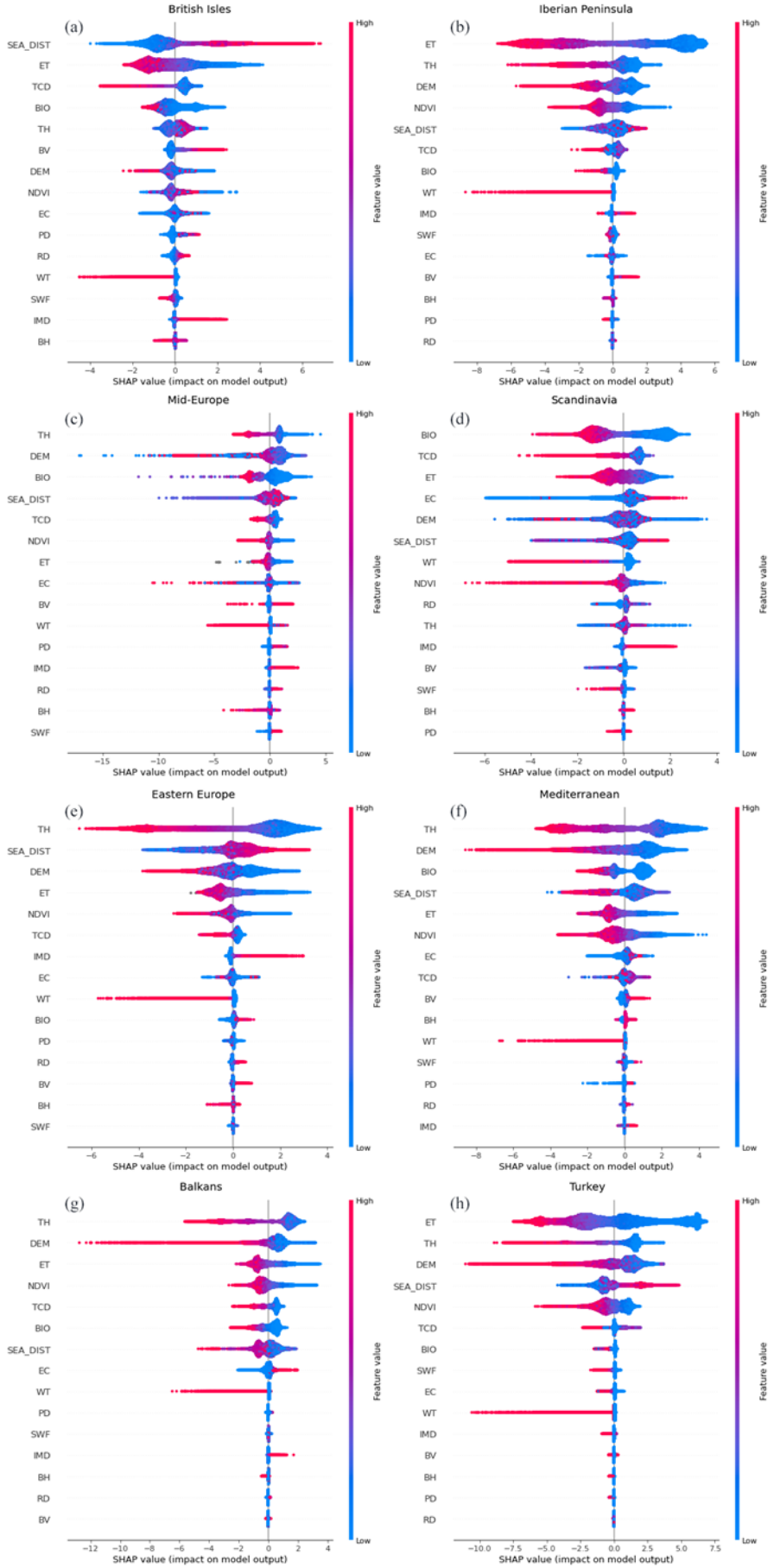
British Isles
(a)
SEA_DIST
ET
TCD
BIO
TH
BV
DEM
NDVI
EC
PD
RD
WT
SWF
IMD
BH
SHAP value (impact on model output)
High
Feature value
Low
Iberian Peninsula
(b)
ET
TH
DEM
NDVI
SEA_DIST
TCD
BIO
WT
IMD
SWF
EC
BV
BH
PD
RD
SHAP value (impact on model output)
High
Feature value
Low
Mid-Europe
(c)
TH
DEM
BIO
SEA_DIST
TCD
NDVI
ET
EC
BV
WT
PD
IMD
RD
BH
SWF
SHAP value (impact on model output)
High
Feature value
Low
Scandinavia
(d)
BIO
TCD
ET
EC
DEM
SEA_DIST
WT
NDVI
RD
TH
IMD
BV
SWF
BH
PD
SHAP value (impact on model output)
High
Feature value
Low
Eastern Europe
(e)
TH
SEA_DIST
DEM
ET
NDVI
TCD
IMD
EC
WT
BIO
PD
RD
BV
BH
SWF
SHAP value (impact on model output)
High
Feature value
Low
Mediterranean
(f)
TH
DEM
BIO
SEA_DIST
ET
NDVI
EC
TCD
BV
BH
WT
SWF
PD
RD
IMD
SHAP value (impact on model output)
High
Feature value
Low
Balkans
(g)
TH
DEM
ET
NDVI
TCD
BIO
SEA_DIST
EC
WT
PD
SWF
IMD
BH
RD
BV
SHAP value (impact on model output)
High
Feature value
Low
Turkey
(h)
ET
TH
DEM
SEA_DIST
NDVI
TCD
BIO
SWF
EC
WT
IMD
BV
BH
PD
RD
SHAP value (impact on model output)
High
Feature value
Low

Fig. 3. SHAP value-based feature importance ranking for individual macro-regions. The *y*-axis lists urban features, red points represent high feature values, and blue points represent low feature values. The *x*-axis represents the SHAP values, indicating the contribution of each feature to the model prediction. A positive SHAP value suggests a warming effect, while a negative SHAP value implies a cooling effect. The vertical spread of points for each feature corresponds to the density of samples at different SHAP values. (a) British Isles, (b) Iberian Peninsula, (c) Mid-Europe, (d) Scandinavia, (e) Eastern Europe, (f) Mediterranean, (g) Balkans, and (h) Turkey. (See Table 1 for acronym definitions)

3.2 Urban features contributing the most to warming and cooling effects

For the purpose of comparing and specifically exploring the relationship between LST and urban features in different thermal environments, samples of grids with LST at the 5th and 95th percentiles in eight macro-regions were selected and extracted as cooler (LST at the 5th percentile) and warmer areas (LST at the 95th percentile) for analysis. In the cooler areas across the European macro-regions of this study, features such as TH, ET, and BIO contributed significantly to lower LST values (Fig. 4). For instance, in regions like Mid-Europe, the Mediterranean, the Balkans, and Eastern Europe, TH played a major role in cooling. Similarly, ET and BIO reduced temperatures in the British Isles, the Iberian Peninsula, Scandinavia and Turkey, further indicating the influence of

Ecological Attributes features in moderating urban temperatures.

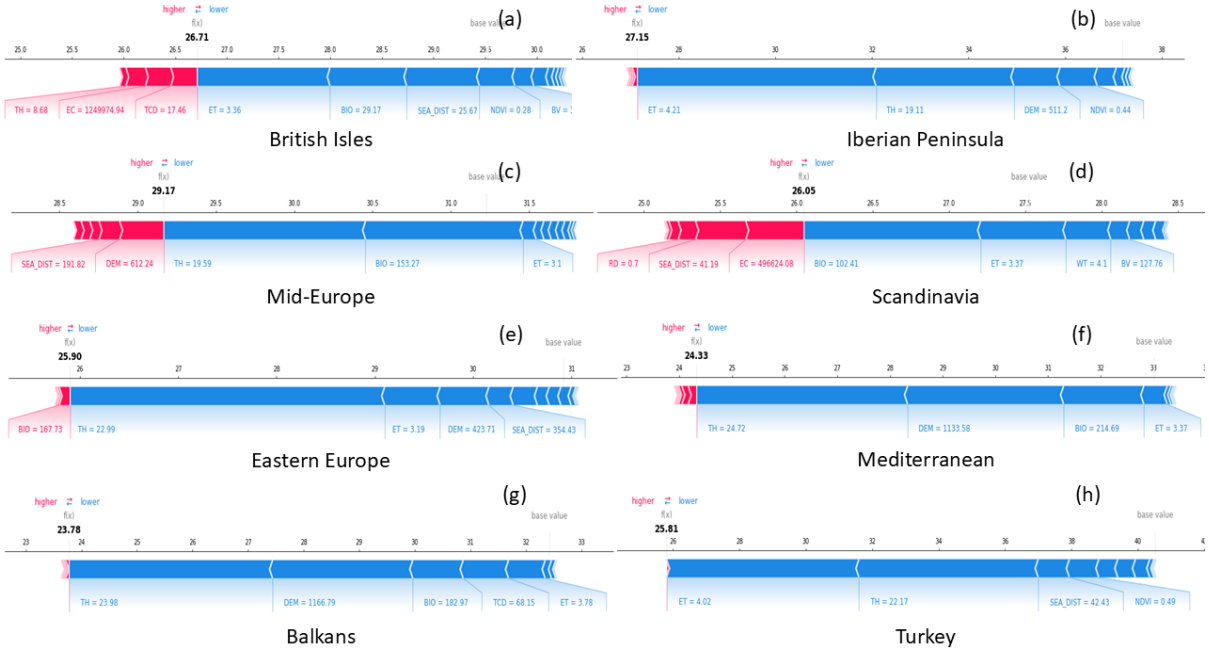

Fig. 4. SHAP force plots showing urban feature contributions to the 5th percentile LST predictions (cooler areas) for each macro-region. Features with SHAP values that 'push' LST towards a higher value appear on the left in red, whereas those that 'push' LST towards a lower value appear on the right in blue. The actual values of the features are shown alongside the feature names. Features with larger SHAP values (i.e. indicating greater impact) have larger arrows.

Figure 5 illustrates the contributions of urban features to LST in warmer areas, represented by the 95th percentile of LST across eight macro-regions in Europe. A key finding is the significant contribution of lower ET and TH to increased LST in these regions. For example, in the Mediterranean, ET with a value of 1.24 and TH with a value of 2.0 both strongly "push" LST higher, as represented by prominent red arrows. This pattern is similarly observed in the Iberian Peninsula, where ET = 0.54 and TH = 0.42 exacerbate warming effects. These findings highlight the critical role of reduced vegetation-driven cooling in amplifying urban heat. Similarly, BV has substantial impacts in the British Isles (Fig. 5a) and the Balkans (Fig. 5g), emphasizing the role of

urbanization in driving higher LST.

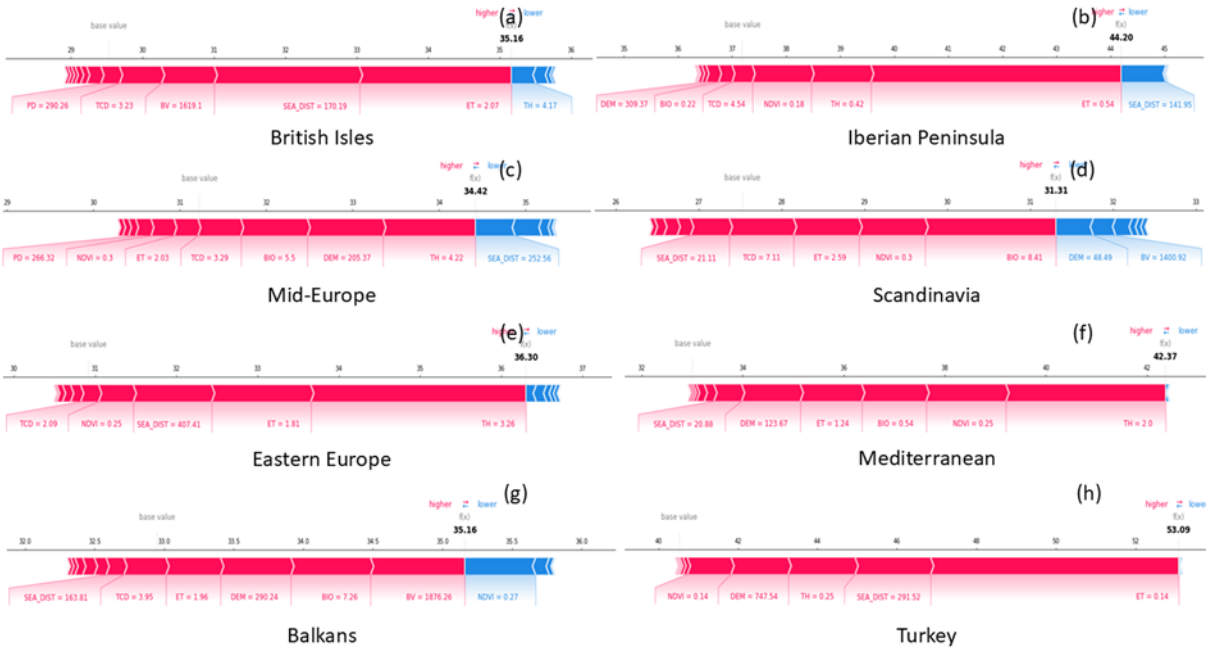

Fig. 5. SHAP force plots showing urban feature contributions to the 95th percentile LST predictions (warmer areas) for each macro-region. Features with SHAP values that 'push' LST towards a higher value appear on the left in red, whereas those that 'push' LST towards a lower value appear on the right in blue. The actual values of the features are shown alongside the feature names. Features with larger SHAP values (i.e. indicating greater impact) have larger arrows.

3.3 Non-linear impact of the most influencing features on LST

The selected features for the GAM analysis—TH, ET, NDVI, and IMD—were identified as dominant features in the previous SHAP analyses. These features demonstrated the strongest influence on LST across the eight macro-regions and thus were chosen for further analysis using the GAM. Figure 6 illustrates the relationship between TH and predicted LST. In all macro-regions, the analysis reveals a clear negative correlation between TH and LST, with taller trees consistently contributing to lower temperatures. This trend is most pronounced in Turkey (Fig. 6h), the Iberian Peninsula (Fig. 6b), and the Balkans (Fig. 6g), where the correlations are the strongest (R = 0.74, 0.72, and 0.71, respectively). In these macro-regions, LST decreased sharply with increasing TH,

showing the substantial cooling impact of mature tree cover. In macro-regions such as Mid-Europe (Fig. 6c), Eastern Europe (Fig. 6e), and the Mediterranean (Fig. 6f), the relationship remained significant (R values between 0.66 and 0.68), but the cooling effect was more gradual. This suggests that while TH contributes to reducing temperatures, the impact may be modulated by other environmental factors. The weakest correlations were observed in the British Isles (Fig. 6a) and Scandinavia (Fig. 6d) (R = 0.58 and 0.46, respectively), where the cooling effect of TH was minimal. In these cooler, wetter regions, TH had less of an influence on LST, and other factors or overall climate conditions likely dominated temperature regulation.

Overall, the results (Fig. 6) highlight the non-linear effect of TH on LST, with diminishing returns beyond a certain TH (typically about 20-30 m) in most macro-regions. Nonetheless, the cooling impact of mature tree cover is clear across all macro-regions, reinforcing the importance of maintaining and enhancing urban TH to mitigate urban heat.

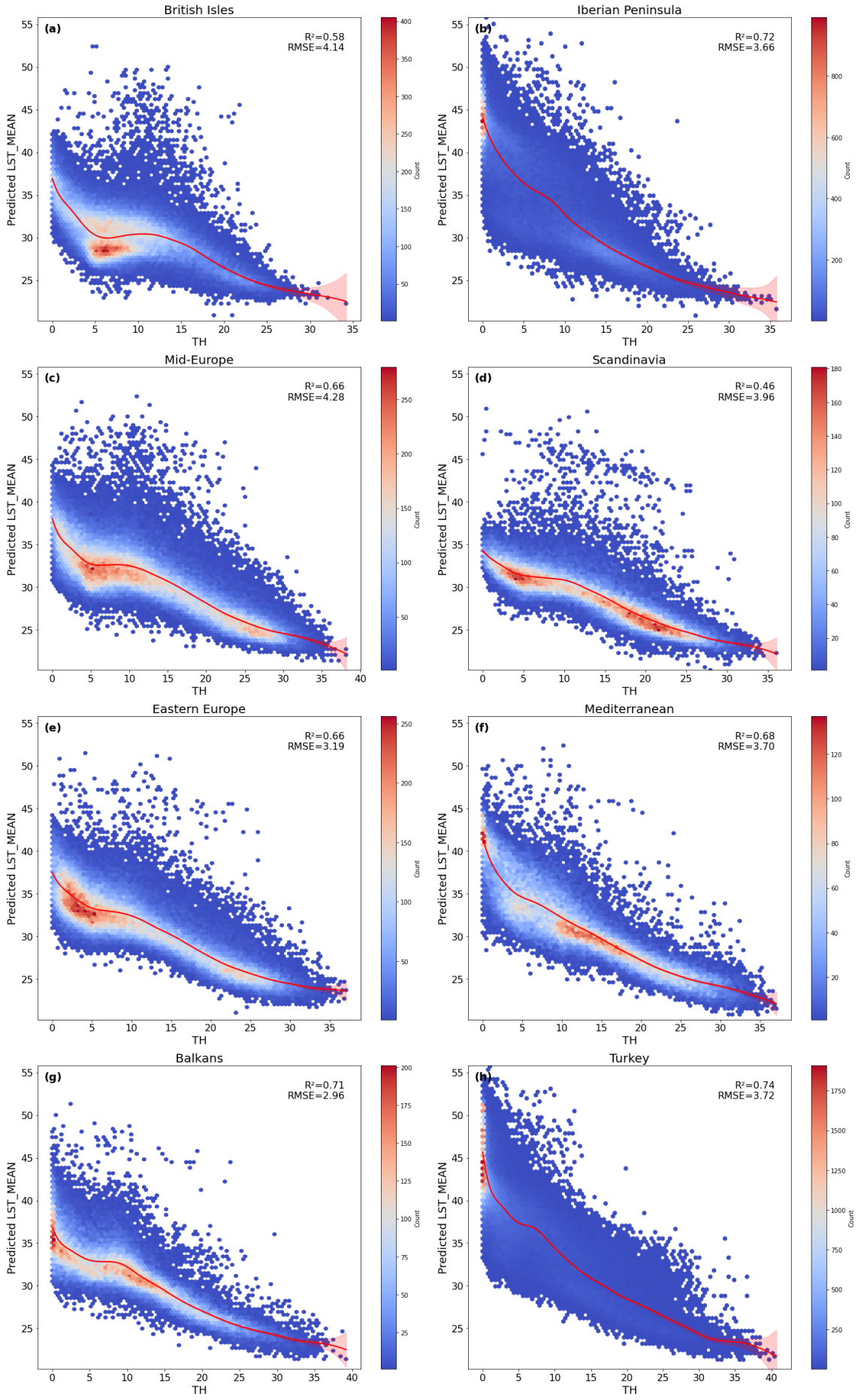
British Isles
(a)
R²=0.58
RMSE=4.14
Iberian Peninsula
(b)
R²=0.72
RMSE=3.66
Mid-Europe
(c)
R²=0.66
RMSE=4.28
Scandinavia
(d)
R²=0.46
RMSE=3.96
Eastern Europe
(e)
R²=0.66
RMSE=3.19
Mediterranean
(f)
R²=0.68
RMSE=3.70
Balkans
(g)
R²=0.71
RMSE=2.96
Turkey
(h)
R²=0.74
RMSE=3.72
Predicted LST_MEAN
TH
Count

Fig. 6. Non-linear relationship between Tree Height (TH) and Land Surface Temperature (LST) across eight European macro-regions. Root Mean Square Error (RMSE). (a) British Isles, (b) Iberian Peninsula, (c) Mid-Europe, (d) Scandinavia, (e) Eastern Europe, (f) Mediterranean, (g) Balkans, and (h) Turkey.

Figure 7 showed a clear negative correlation between ET and LST similarly to Figure 6, with higher ET values leading to lower temperatures in all areas. This trend was particularly prominent in macro-regions like Turkey (Fig. 7h) and the Iberian Peninsula (Fig. 7b) (R = 0.75 and 0.74, respectively). In these macro-regions, ET increased from 0 to approximately 3-4.5 mm/d. A sharp decline in LST was found, emphasizing the cooling role that ET plays in mitigating urban heat, especially in hotter climates. An important observation from the figure is the variation in ET concentration across macro-regions. In Turkey and the Iberian Peninsula, the majority of the data points were clustered around lower ET values, typically between 0 and 2 mm/d. Despite this lower range of ET values, these macro-regions exhibited strong correlations with LST (R values of 0.75 and 0.74, respectively). This finding suggests that in these areas, even modest increases in ET can significantly reduce LST, likely due to the pronounced impact of water vapor and vegetation in these typically drier climates.

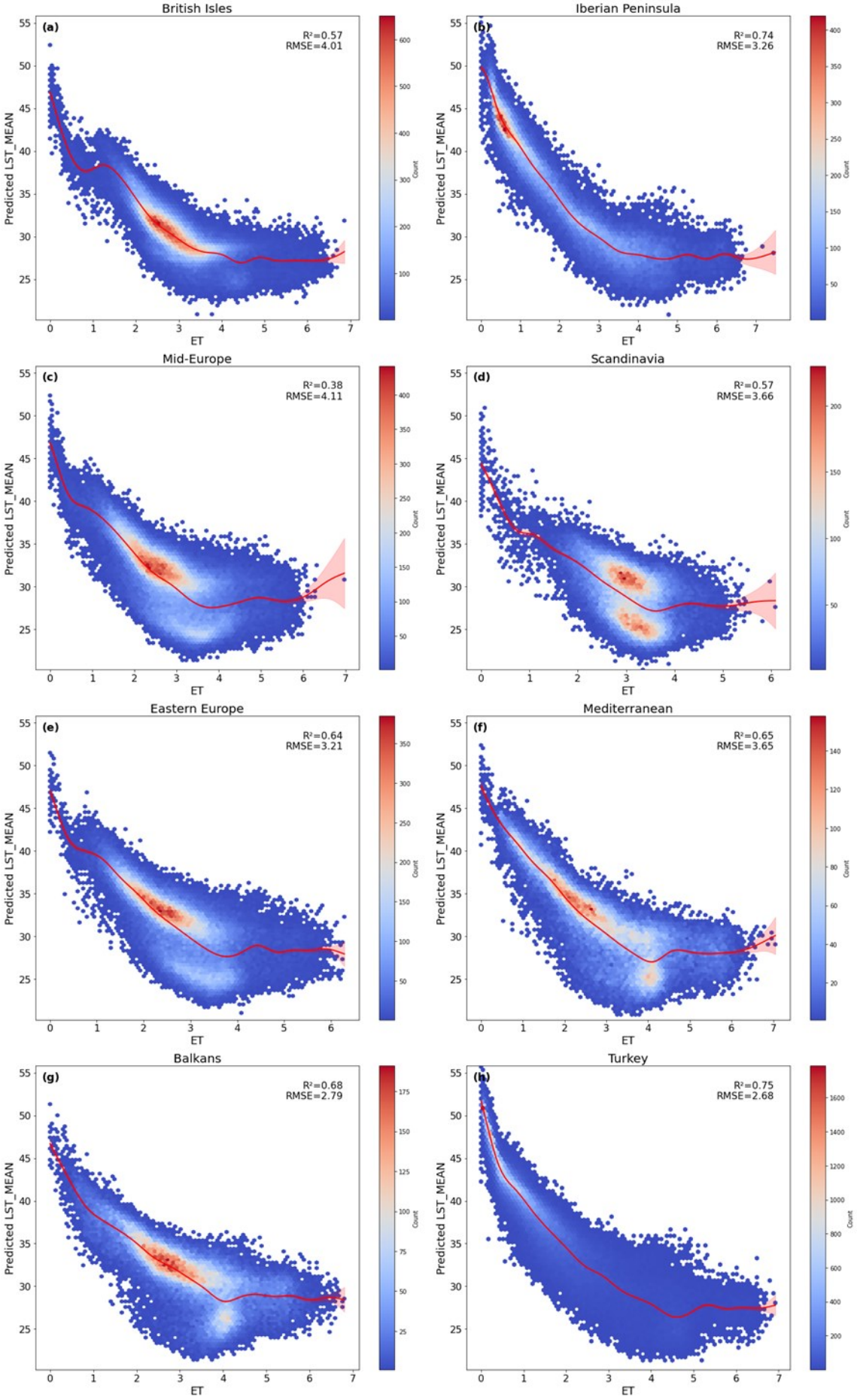
British Isles
(a)
R²=0.57
RMSE=4.01
Iberian Peninsula
(b)
R²=0.74
RMSE=3.26
Mid-Europe
(c)
R²=0.38
RMSE=4.11
Scandinavia
(d)
R²=0.57
RMSE=3.66
Eastern Europe
(e)
R²=0.64
RMSE=3.21
Mediterranean
(f)
R²=0.65
RMSE=3.65
Balkans
(g)
R²=0.68
RMSE=2.79
Turkey
(h)
R²=0.75
RMSE=2.68
Predicted LST_MEAN
ET
Count

Fig. 7. Non-linear relationship between Evapotranspiration (ET) and Land Surface Temperature (LST) across eight European macro-regions. Root Mean Square Error (RMSE). (a) British Isles, (b) Iberian Peninsula, (c) Mid-Europe, (d) Scandinavia, (e) Eastern Europe, (f) Mediterranean, (g) Balkans, and (h) Turkey.

As shown in Figure 8, the cooling effect of NDVI was most pronounced in the Iberian Peninsula (Fig. 8b), Turkey (Fig. 8h), and the Balkans (Fig. 8g), with steep drops in LST as vegetation cover increased. In contrast, macro-regions like the British Isles (Fig. 8a) and Scandinavia (Fig. 8d) showed weaker correlations between NDVI and LST, mirroring the patterns observed in the previous figures for ET and TH. What stands out is the strong non-linear effect in macro-regions like the Iberian Peninsula and the Balkans, where LST decreased sharply at lower NDVI values (below 0.4), but the effect reached plateaus at higher NDVI values, indicating diminishing returns of vegetation on cooling once a certain threshold was attained.

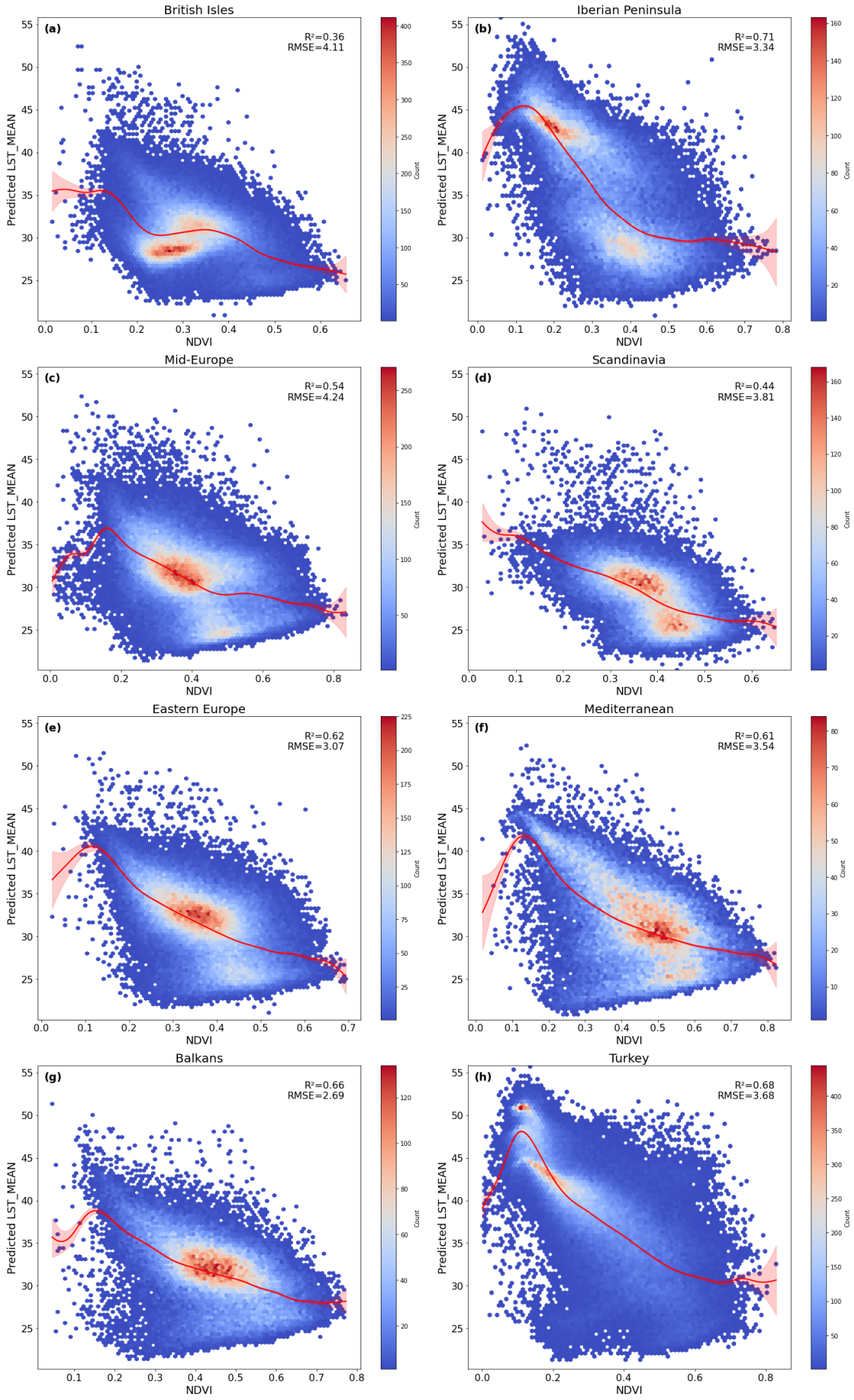
British Isles
(a)
R²=0.36
RMSE=4.11
Iberian Peninsula
(b)
R²=0.71
RMSE=3.34
Mid-Europe
(c)
R²=0.54
RMSE=4.24
Scandinavia
(d)
R²=0.44
RMSE=3.81
Eastern Europe
(e)
R²=0.62
RMSE=3.07
Mediterranean
(f)
R²=0.61
RMSE=3.54
Balkans
(g)
R²=0.66
RMSE=2.69
Turkey
(h)
R²=0.68
RMSE=3.68
Predicted LST_MEAN
NDVI
Count

Fig. 8. Non-linear relationship between Normalized Difference Vegetation Index (NDVI) and Land Surface Temperature (LST) across eight European macro-regions. Root Mean Square Error (RMSE). (a) British Isles, (b) Iberian Peninsula, (c) Mid-Europe, (d) Scandinavia, (e) Eastern Europe, (f) Mediterranean, (g) Balkans, and (h) Turkey.

Unlike the previous features such as TH (Fig. 6), ET (Fig. 7), and NDVI (Fig. 8) which exhibited a cooling effect with increasing values, IMD showed a strong positive correlation with LST (Fig. 9). In macro-regions such as Turkey (Fig. 9h) and the Iberian Peninsula (Fig. 9b) the correlations were the strongest (R = 0.74 and 0.67, respectively). As IMD increased LST rose sharply, particularly once IMD exceeded approximately 40%. This suggests that beyond a certain threshold, impervious surfaces dramatically amplify heat retention in urban areas, underscoring the importance of managing impervious surfaces to mitigate UHI effects.

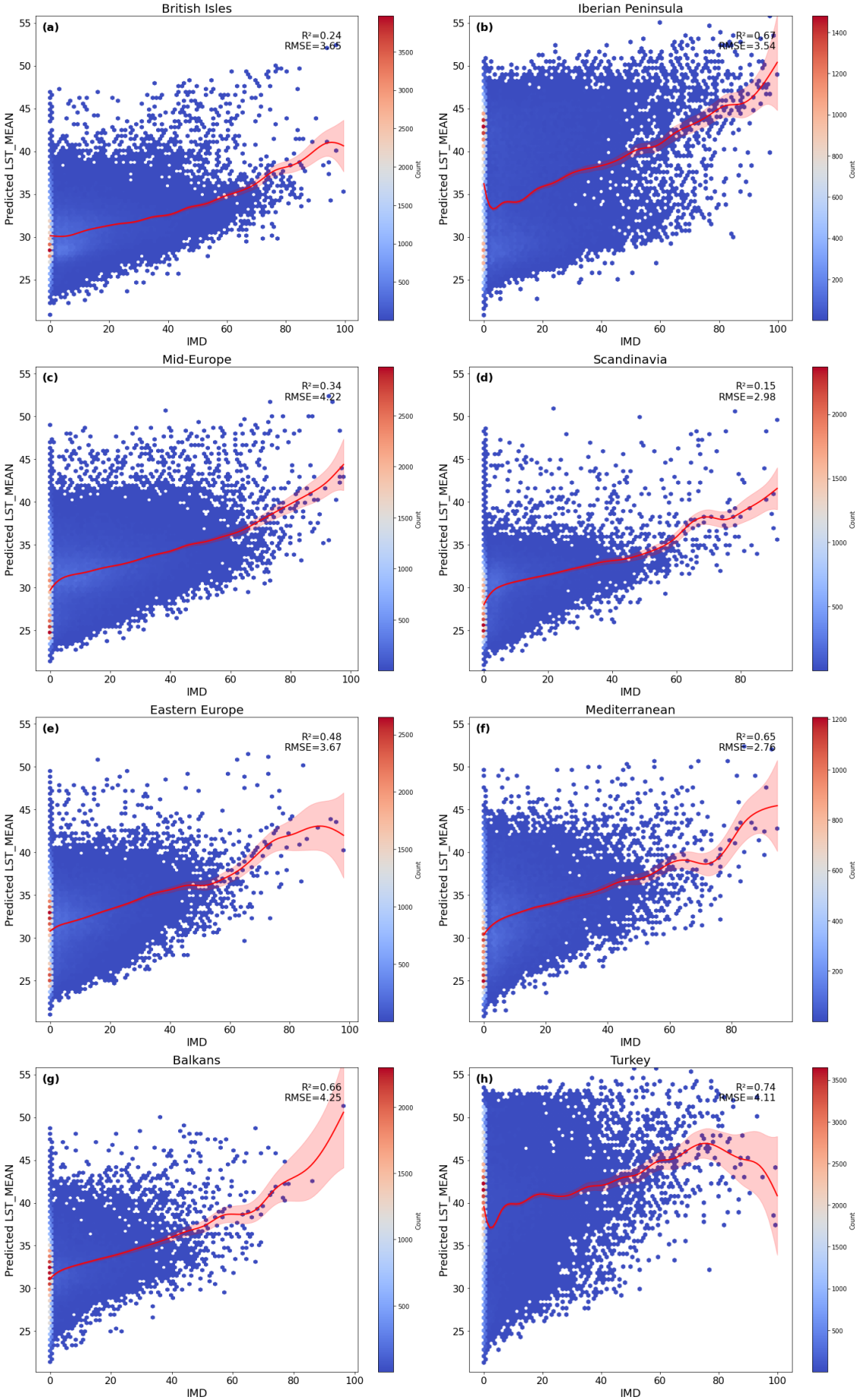
British Isles
(a)
R²=0.24
RMSE=3.65
Iberian Peninsula
(b)
R²=0.67
RMSE=3.54
Mid-Europe
(c)
R²=0.34
RMSE=4.22
Scandinavia
(d)
R²=0.15
RMSE=2.98
Eastern Europe
(e)
R²=0.48
RMSE=3.67
Mediterranean
(f)
R²=0.65
RMSE=2.76
Balkans
(g)
R²=0.66
RMSE=4.25
Turkey
(h)
R²=0.74
RMSE=4.11
Predicted LST_MEAN
IMD
Count

Fig. 9. Non-linear relationship between Imperviousness Density (IMD) and Land Surface Temperature (LST) across eight European macro-regions. Root Mean Square Error (RMSE). (a) British Isles, (b) Iberian Peninsula, (c) Mid-Europe, (d) Scandinavia, (e) Eastern Europe, (f) Mediterranean, (g) Balkans, and (h) Turkey.

4. Discussion

This study represents an initial investigation into the influence of various urban landscape, urban structure, and ecological attributes features on LST across different European macro-regions. SHAP, a tool deriving from the field of XAI, is particularly effective in highlighting the contribution of individual features to predictive models. For example, a recent study (Cilli et al., 2022) in the Mediterranean region applied a Random Forest model with SHAP values to estimate wildfire occurrence. Similarly, SHAP has also been employed to evaluate the cooling effects of urban blue-green infrastructures on urban thermal environment (Islam et al., 2024).

The key advantage of SHAP lies in its ability to quantify the marginal contribution of each feature, allowing scholars to understand both the magnitude and direction of their effects. In the context of this study, SHAP highlights the significant role that ecological attributes, such as TH, ET, and TCD, play in reducing LST, particularly in warmer macro-regions like the Iberian Peninsula and Turkey. A case study (Zeren Cetin et al., 2022) carried out in Turkey has also shown an increase in LST and a decrease in vegetation over the last 30 years. For this reason, the authors recommend encouraging green roof installations and creating a system of urban parks and green belts. Consistent with previous research (Algretawee, 2022; Dong and Shi, 2022; Kong et al., 2014; Schwaab et al., 2021), this study has revealed that these ecological attributes are critical for cooling, emphasizing the importance of ecological management in urban heat mitigation.

Conversely, urban structure features such as IMD and BV were shown to have the opposite effect driving up LST in densely populated and highly urbanized macro-regions like Mid-Europe and the British Isles. These findings confirm the well-known UHI effect, where impervious surfaces

and artificial infrastructure retain heat, generating higher temperatures in cities (Hou et al., 2022; Xiang et al., 2022; Zhou et al., 2022). The influence of these features was particularly evident in densely built areas, where the increase in LST was stark when IMD and BV values were high. Our study also highlights the urban landscape, such as SEA_DIST, as having a significant impact on macro-regions like the Mediterranean and British Isles where coastal proximity offers a buffer against urban heat (Fig. 3). Similar results were obtained in the study by Firozjaei et al. (2023), showing that distance from the sea has a significant effect on UHI intensity.

While urban tree cover is widely recognized as an environmentally friendly and effective method for urban cooling, the mechanisms behind it are not simply linear. The application of GAM in this study further reveals the non-linear relationship between these ecological factors and LST. In macro-regions such as the Iberian Peninsula and Turkey, the strong negative correlation between TH and LST suggests that mature tree cover provides significant cooling benefits, especially when TH exceeds 15-20 m (Fig. 5). A study of the cooling efficiency of urban trees in Africa also found a similar result on air temperature (Cheng et al., 2022). Interestingly, in the Iberian Peninsula and the Mediterranean, the cooling impact of NDVI stabilized at higher vegetation levels, indicating diminishing benefits of additional vegetation cover above a certain threshold. This non-linear relationship was also found between LST and NDVI in a study conducted in Shanghai, China (Li et al., 2011).

This study focuses on data extracted from the high-resolution satellite imagery available primarily for the year 2018. While this approach provides a robust snapshot of LST and urban feature interactions, it does not capture temporal dynamics or trends over multiple years. As a result, our findings may not fully reflect interannual variability or long-term shifts in urban thermal dynamics caused by factors such as climate change or evolving urbanization patterns. Future research should incorporate multi-year or longitudinal datasets to explore these dynamics and validate the temporal stability of the relationships identified in this study. Additionally, the reliance on satellite-based measurements, while advantageous for spatial consistency, may introduce

limitations in accurately capturing fine-scale urban variations or microclimatic conditions influenced by temporary phenomena.

5 Conclusion

This study provides a comprehensive examination of the key factors influencing LST across different European macro-regions, emphasizing the interplay between ecological attributes, urban landscape, and urban structural features. By applying the SHAP method, we were able not only to quantify the importance of individual urban features but also to uncover their nuanced effects in various geographical contexts. The study highlights the critical role that ecological attributes play in reducing LST, particularly in warmer macro-regions where mature trees and higher ET levels offer significant cooling benefits. In contrast, urban structure features, especially impervious surfaces, exacerbate urban heat most evidently in densely built macro-regions.

The SHAP-based analysis underscores the importance of using interpretable machine learning models to uncover complex non-linear relationships between urban features and LST. Furthermore, our study demonstrates that the effectiveness of natural cooling mechanisms varies significantly according to region, climate, and economic conditions, suggesting that region-specific strategies are essential for optimizing urban heat mitigation efforts. While ecological features offer substantial relief from urban heat, the study also points out the diminishing returns beyond certain thresholds. This indicates that although increasing vegetation cover is necessary, a strategic approach to balancing green and urban infrastructure is key.

Overall, this research offers actionable insights for policymakers and urban planners, particularly in regions where urban heat is becoming an increasingly pressing issue due to climate change. The findings emphasize the need for targeted, region-specific urban cooling strategies that optimize both ecological and urban features.

References

Abatzoglou, J.T., Dobrowski, S.Z., Parks, S.A., Hegewisch, K.C., 2018. TerraClimate, a high-

resolution global dataset of monthly climate and climatic water balance from 1958–2015. Sci. Data 5, 170191. https://doi.org/10.1038/sdata.2017.191
Akbari, H., Pomerantz, M., Taha, H., 2001. Cool surfaces and shade trees to reduce energy use and improve air quality in urban areas. Sol. Energy 70, 295–310. https://doi.org/10.1016/S0038-092X(00)00089-X
Algretawee, H., 2022. The effect of graduated urban park size on park cooling island and distance relative to land surface temperature (LST). Urban Clim. 45. https://doi.org/10.1016/j.uclim.2022.101255
Angearu, C.-V., Ontel, I., Irimescu, A., Sorin, B., Dodd, E., 2022. Remote sensing methods for detecting and mapping hailstorm damage: a case study from the 20 July 2020 hailstorm, Baragan Plain, Romania. Nat. Hazards. https://doi.org/10.1007/s11069-022-05457-x
Bird, D.N., Banzhaf, E., Knopp, J., Wu, W., Jones, L., 2022. Combining Spatial and Temporal Data to Create a Fine-Resolution Daily Urban Air Temperature Product from Remote Sensing Land Surface Temperature (LST) Data. Atmosphere 13. https://doi.org/10.3390/atmos13071152
Chen, J., Gao, M., 2021. Global 1 km × 1 km gridded revised real gross domestic product and electricity consumption during 1992-2019 based on calibrated nighttime light data. https://doi.org/10.6084/M9.FIGSHARE.17004523.V1
Chen, Y., Chen, W.Y., Giannico, V., Lafortezza, R., 2022. Modelling inter-pixel spatial variation of surface urban heat island intensity. Landsc. Ecol. 37, 2179–2194. https://doi.org/10.1007/s10980-022-01464-2
Cheng, X., Peng, J., Dong, J., Liu, Y., Wang, Y., 2022. Non-linear effects of meteorological variables on cooling efficiency of African urban trees. Environ. Int. 169, 107489. https://doi.org/10.1016/j.envint.2022.107489
Cilli, R., Elia, M., D'Este, M., Giannico, V., Amoroso, N., Lombardi, A., Pantaleo, E., Monaco, A., Sanesi, G., Tangaro, S., Bellotti, R., Lafortezza, R., 2022. Explainable artificial intelligence (XAI) detects wildfire occurrence in the Mediterranean countries of Southern Europe. Sci. Rep. 12, 16349. https://doi.org/10.1038/s41598-022-20347-9
Clinton, N., Gong, P., 2013. MODIS detected surface urban heat islands and sinks: Global locations and controls. Remote Sens. Environ. 134, 294–304. https://doi.org/10.1016/j.rse.2013.03.008
Cook, M., 2014. Atmospheric Compensation for a Landsat Land Surface Temperature Product. Theses.
Dijkstra, L., Poelman, H., n.d. CITIES IN EUROPE THE NEW OECD-EC DEFINITION.
Dong, N., Luo, M., Liu, Z., Sun, J., Wu, K., Lin, H., 2022. The roles of leaf area index and albedo in vegetation induced temperature changes across China using modelling and observations. Clim. Dyn. 58, 2557–2573. https://doi.org/10.1007/s00382-021-06028-9
Dong, S., Shi, Y., 2022. Impact of the dynamic vegetation on climate extremes during the wheat growing period over China. Sci. Total Environ. 819. https://doi.org/10.1016/j.scitotenv.2022.153079
Donovan, G.H., Butry, D.T., 2009. The value of shade: Estimating the effect of urban trees on summertime electricity use. Energy Build. 41, 662–668. https://doi.org/10.1016/j.enbuild.2009.01.002
European Environment Agency, 2023. Small Woody Features 2018 (raster 100 m), Europe, 3-yearly, May 2023. https://doi.org/10.2909/89EEB6C1-EE72-44B3-B0E3-83C74F2C306D
European Environment Agency, 2020a. Urban Atlas Land Cover/Land Use 2018 (vector), Europe, 6-yearly, Jul. 2021. https://doi.org/10.2909/FB4DFFA1-6CEB-4CC0-8372-1ED354C285E6
European Environment Agency, 2020b. Water and Wetness 2018 (raster 10 m), Europe, 3-yearly - version 2, Nov. 2020. https://doi.org/10.2909/7992F641-BF77-47B7-B0C1-74FC832B78B1
European Environment Agency, 2020c. Imperviousness Density 2018 (raster 10 m), Europe, 3-yearly, Aug. 2020. https://doi.org/10.2909/3BF542BD-EEBD-4D73-B53C-A0243F2ED862
European Environment Agency, 2020d. Tree Cover Density 2018 (raster 10 m), Europe, 3-yearly, Sep. 2020. https://doi.org/10.2909/486F77DA-D605-423E-93A9-680760AB6791

Fei, F., Wang, Y., Yao, W., Gao, W., Wang, L., 2022. Coupling mechanism of water and greenery on summer thermal environment of waterfront space in China's cold regions. Build. Environ. 214. https://doi.org/10.1016/j.buildenv.2022.108912
Firozjaei, M.K., Sedighi, A., Mijani, N., Kazemi, Y., Amiraslani, F., 2023. Seasonal and daily effects of the sea on the surface urban heat island intensity: A case study of cities in the Caspian Sea Plain. Urban Clim. 51, 101603. https://doi.org/10.1016/j.uclim.2023.101603
Grimm, N.B., Faeth, S.H., Golubiewski, N.E., Redman, C.L., Wu, J., Bai, X., Briggs, J.M., 2008. Global Change and the Ecology of Cities. Science 319, 756–760. https://doi.org/10.1126/science.1150195
Han, D., Zhang, T., Qin, Y., Tan, Y., Liu, J., 2022. A comparative review on the mitigation strategies of urban heat island (UHI): a pathway for sustainable urban development. Clim. Dev. https://doi.org/10.1080/17565529.2022.2092051
Hawker, L., Uhe, P., Paulo, L., Sosa, J., Savage, J., Sampson, C., Neal, J., 2022. A 30 m global map of elevation with forests and buildings removed. Environ. Res. Lett. 17, 024016. https://doi.org/10.1088/1748-9326/ac4d4f
Hirano, Y., Fujita, T., 2012. Evaluation of the impact of the urban heat island on residential and commercial energy consumption in Tokyo. Energy 37, 371–383. https://doi.org/10.1016/j.energy.2011.11.018
Hou, H., Su, H., Liu, K., Li, X., Chen, S., Wang, W., Lin, J., 2022. Driving forces of UHI changes in China's major cities from the perspective of land surface energy balance. Sci. Total Environ. 829. https://doi.org/10.1016/j.scitotenv.2022.154710
Hu, D., Yang, L., Zhou, J., Deng, L., 2012. Estimation of urban energy heat flux and anthropogenic heat discharge using aster image and meteorological data: case study in Beijing metropolitan area. J. Appl. Remote Sens. 6, 3559. https://doi.org/10.1117/1.JRS.6.063559
Imhoff, M.L., Zhang, P., Wolfe, R.E., Bounoua, L., 2010. Remote sensing of the urban heat island effect across biomes in the continental USA. Remote Sens. Environ. 114, 504–513. https://doi.org/10.1016/j.rse.2009.10.008
Islam, M.R., Shahfahad, Talukdar, S., Rihan, M., Rahman, A., 2024. Evaluating cooling effect of blue-green infrastructure on urban thermal environment in a metropolitan city: Using geospatial and machine learning techniques. Sustain. Cities Soc. 113, 105666. https://doi.org/10.1016/j.scs.2024.105666
Kong, F., Yin, H., James, P., Hutyra, L.R., He, H.S., 2014. Effects of spatial pattern of greenspace on urban cooling in a large metropolitan area of eastern China. Landsc. Urban Plan. 128, 35–47. https://doi.org/10.1016/j.landurbplan.2014.04.018
Lafortezza, R., Giannico, V., 2019. Combining high-resolution images and LiDAR data to model ecosystem services perception in compact urban systems. Ecol. Indic. 96, 87–98. https://doi.org/10.1016/j.ecolind.2017.05.014
Lang, N., Jetz, W., Schindler, K., Wegner, J.D., 2023. A high-resolution canopy height model of the Earth. Nat. Ecol. Evol. 7, 1778–1789. https://doi.org/10.1038/s41559-023-02206-6
Li, J., Song, C., Cao, L., Zhu, F., Meng, X., Wu, J., 2011. Impacts of landscape structure on surface urban heat islands: A case study of Shanghai, China. Remote Sens. Environ. 15.
Li, X., Chen, W.Y., Sanesi, G., Lafortezza, R., 2019. Remote Sensing in Urban Forestry: Recent Applications and Future Directions. Remote Sens. 11, 1144. https://doi.org/10.3390/rs11101144
Ma, X., Peng, S., 2022. Research on the spatiotemporal coupling relationships between land use/land cover compositions or patterns and the surface urban heat island effect. Environ. Sci. Pollut. Res. 29, 39723–39742. https://doi.org/10.1007/s11356-022-18838-3
Macháč, J., Brabec, J., Arnberger, A., 2022. Exploring public preferences and preference heterogeneity for green and blue infrastructure in urban green spaces. Urban For. Urban Green. 75. https://doi.org/10.1016/j.ufug.2022.127695
Mentaschi, L., Duveiller, G., Zulian, G., Corbane, C., Pesaresi, M., Maes, J., Stocchino, A., Feyen,

L., 2022. Global long-term mapping of surface temperature shows intensified intra-city urban heat island extremes. Glob. Environ. Change 72, 102441. https://doi.org/10.1016/j.gloenvcha.2021.102441
Oke, T.R., 1976. The distinction between canopy and boundary-layer urban heat Islands. Atmosphere 14, 268–277. https://doi.org/10.1080/00046973.1976.9648422
Oke, T.R., 1973. City size and the urban heat island. Atmospheric Environ. 1967 7, 769–779. https://doi.org/10.1016/0004-6981(73)90140-6
Oleson, K.W., Monaghan, A., Wilhelmi, O., Barlage, M., Brunsell, N., Feddema, J., Hu, L., Steinhoff, D.F., 2015. Interactions between urbanization, heat stress, and climate change. Clim. Change 129, 525–541. https://doi.org/10.1007/s10584-013-0936-8
Rehman, A., Qin, J., Shafi, S., Khan, M.S., Ullah, S., Ahmad, K., Rehman, N.U., Faheem, M., 2022. Modelling of Land Use/Cover and LST Variations by Using GIS and Remote Sensing: A Case Study of the Northern Pakhtunkhwa Mountainous Region, Pakistan. Sensors 22. https://doi.org/10.3390/s22134965
Ren, Y., Lafortezza, R., Giannico, V., Sanesi, G., Zhang, X., Xu, C., 2023. The unrelenting global expansion of the urban heat island over the last century. Sci. Total Environ. 880, 163276. https://doi.org/10.1016/j.scitotenv.2023.163276
Schiavina, M., Melchiorri, M., Pesaresi, M., Panagiotis, P., Freire, S., Maffenini, L., Goch, K., Tommasi, P., Kemper, T., 2022. GHSL Data Package 2022. https://doi.org/10.2760/19817
Schwaab, J., Meier, R., Mussetti, G., Seneviratne, S., Bürgi, C., Davin, E.L., 2021. The role of urban trees in reducing land surface temperatures in European cities. Nat. Commun. 12, 6763. https://doi.org/10.1038/s41467-021-26768-w
Shahfahad, Talukdar, S., Rihan, M., Hang, H.T., Bhaskaran, S., Rahman, A., 2022. Modelling urban heat island (UHI) and thermal field variation and their relationship with land use indices over Delhi and Mumbai metro cities. Environ. Dev. Sustain. 24, 3762–3790. https://doi.org/10.1007/s10668-021-01587-7
Shen, Z.-J., Zhang, B.-H., Xin, R.-H., Liu, J.-Y., 2022. Examining supply and demand of cooling effect of blue and green spaces in mitigating urban heat island effects: A case study of the Fujian Delta urban agglomeration (FDUA), China. Ecol. Indic. 142. https://doi.org/10.1016/j.ecolind.2022.109187
Tam, B.Y., Gough, W.A., Mohsin, T., 2015. The impact of urbanization and the urban heat island effect on day to day temperature variation. Urban Clim. 12, 1–10. https://doi.org/10.1016/j.uclim.2014.12.004
Tan, J., Zheng, Y., Tang, X., Guo, C., Li, L., Song, G., Zhen, X., Yuan, D., Kalkstein, A.J., Li, F., Chen, H., 2010. The urban heat island and its impact on heat waves and human health in Shanghai. Int. J. Biometeorol. 54, 75–84. https://doi.org/10.1007/s00484-009-0256-x
Tyrväinen, L., Pauleit, S., Seeland, K., Vries, S. de, 2005. Benefits and use of urban forests and trees, in: Urban Forests and Trees; a Reference Book. Springer, pp. 81–114.
Voogt, J.A., Oke, T.R., 2003. Thermal remote sensing of urban climates. Remote Sens. Environ. 86, 370–384. https://doi.org/10.1016/S0034-4257(03)00079-8
Xiang, Y., Ye, Y., Peng, C., Teng, M., Zhou, Z., 2022. Seasonal variations for combined effects of landscape metrics on land surface temperature (LST) and aerosol optical depth (AOD). Ecol. Indic. 138. https://doi.org/10.1016/j.ecolind.2022.108810
Yang, Q., Xu, Y., Tong, X., Hu, T., Liu, Y., Chakraborty, T.C., Yao, R., Xiao, C., Chen, S., Ma, Z., 2023. Influence of urban extent discrepancy on the estimation of surface urban heat island intensity: A global-scale assessment in 892 cities. J. Clean. Prod. 426, 139032. https://doi.org/10.1016/j.jclepro.2023.139032
Zeren Cetin, I., Varol, T., Ozel, H.B., Sevik, H., 2022. The effects of climate on land use/cover: a case study in Turkey by using remote sensing data. Environ. Sci. Pollut. Res. https://doi.org/10.1007/s11356-022-22566-z
Zhang, C., Su, Y., Liu, L., Wu, J., Huang, G., Li, X., Bi, C., Yan, W., Lafortezza, R., 2023. Seasonal

and long-term dynamics in forest microclimate effects: global pattern and mechanism. Npj Clim. Atmospheric Sci. 6, 1–12. https://doi.org/10.1038/s41612-023-00442-y
Zhang, K., Wang, R., Shen, C., Da, L., 2010. Temporal and spatial characteristics of the urban heat island during rapid urbanization in Shanghai, China. Environ. Monit. Assess. 169, 101–112. https://doi.org/10.1007/s10661-009-1154-8
Zhou, X., Li, Z., Zheng, T., Yan, Y., Li, P., Odey, E.A., Mang, H.P., Uddin, S.M.N., 2018. Review of global sanitation development. Environ. Int. 120, 246–261. https://doi.org/10.1016/j.envint.2018.07.047
Zhou, Y., Zhao, H., Mao, S., Zhang, G., Jin, Y., Luo, Y., Huo, W., Pan, Z., An, P., Lun, F., 2022. Exploring surface urban heat island (SUHI) intensity and its implications based on urban 3D neighborhood metrics: An investigation of 57 Chinese cities. Sci. Total Environ. 847. https://doi.org/10.1016/j.scitotenv.2022.157662

Conclusion

This thesis integrates three comprehensive studies to explore the urban heat island (UHI) effect, focusing on its spread, dynamics, and contributing factors at multiple scales. Together, these studies emphasize the importance of understanding UHI as a multifaceted phenomenon influenced by urbanization, ecological features, and local climate conditions. By analyzing UHI from global, city-specific, and regional perspectives, this research provides a nuanced understanding of how urban features drive land surface temperature (LST) and how cities might effectively mitigate urban heat.

The first study investigates the global expansion of UHI over the past century, highlighting a clear and accelerating trend of cities experiencing elevated temperatures compared to rural areas. This research reveals that the impacts of UHI are not confined to specific climatic zones but rather have spread across diverse geographic and climatic contexts. As urbanization continues to transform natural landscapes worldwide, the study shows that even cities at higher latitudes and altitudes are increasingly affected by rising temperatures. The global-scale analysis draws attention to the vast and growing footprint of UHI, underscoring the role of urban expansion and land-use changes in intensifying this effect. The study suggests that as urbanization progresses, a coordinated international approach is essential to understand UHI drivers, share mitigation strategies, and address the consequences of urban-induced warming.

The second study takes a city-specific approach, delving into the complex, nonlinear impacts of various urban features—such as vegetation, building density, and impervious surfaces—on LST. Using explainable artificial intelligence (XAI), this research goes beyond traditional linear models to capture the subtleties of how urban design elements interact with temperature in diverse urban contexts. For instance, the cooling effect of tree cover and vegetation density was found to vary not only by amount but also by type and distribution, highlighting the importance of strategic green space planning to maximize cooling. Similarly, impervious surfaces and dense building areas are shown to have nonlinear warming effects, where certain thresholds exacerbate heat retention. By using XAI, this study demonstrates the value of sophisticated modeling techniques that reveal more accurate

insights into urban temperature dynamics. This approach provides policymakers and urban planners with actionable recommendations to design urban landscapes that minimize heat retention while considering the unique characteristics of each city.

The third study expands the focus to regional analysis, examining UHI effects across 780 cities in eight macro-regions of Europe. This research investigates the combined influence of ecological, structural, and geographic factors on LST within distinct macro-regions, such as the Mediterranean, Scandinavia, and the British Isles. The study finds that different regions respond uniquely to the presence of natural and built environments. In warmer regions, such as the Mediterranean and Turkey, ecological attributes like tree height and evapotranspiration show strong cooling effects, particularly when vegetation cover reaches specific maturity levels. Conversely, densely built and highly urbanized areas, especially in regions like Mid-Europe and the British Isles, are more sensitive to impervious surface density and building volume, both of which contribute to elevated LST. This regional analysis underscores the need for region-specific urban planning strategies that consider the local climate, geography, and socioeconomic conditions, as different strategies may be required to optimize cooling in different environmental settings.

Taken together, this thesis contributes to the understanding of UHI by highlighting the complex interplay between urban design, natural features, and climate in shaping urban temperature patterns. By demonstrating the varied impacts of urbanization across different contexts, it advocates for a more integrative approach that balances natural and built environments to achieve sustainable urban cooling. It also highlights the importance of advanced modeling techniques, such as XAI, in revealing the complex, nonlinear interactions within urban climates—insights that traditional models might overlook.

Ultimately, the research presented here offers critical insights for policymakers, urban planners, and climate scientists seeking to develop resilient urban environments. As climate change continues to exacerbate heat in urban areas, targeted, adaptive urban cooling strategies that consider local conditions and leverage both natural and built infrastructure will be essential. This thesis suggests

that future research and policy should focus on promoting green infrastructure, controlling urban density, and considering regional variability to foster sustainable urban development. The findings underscore the urgent need for climate-sensitive urban planning that can mitigate UHI impacts and enhance the resilience of cities in the face of global warming.